State of Oregon
Oregon Department of Geology and Mineral Industries
Brad Avy, State Geologist

GEOLOGIC MAP 123

GEOLOGIC MAP OF THE POISON CREEK AND BURNS 7.5' QUADRANGLES, HARNEY COUNTY, OREGON

Jason D. McClaughry[1], Carlie J. M. Duda[2], and Mark L. Ferns[3]

2019

[1] Jason.McClaughry@oregon.gov; Oregon Department of Geology and Mineral Industries, Baker City Field Office, Baker County Courthouse, 1995 3rd Street, Suite 130, Baker City, OR 97814
[2] Oregon Department of Geology and Mineral Industries, 800 NE Oregon Street, Suite 965, Portland, OR 97232
[3] Oregon Department of Geology and Mineral Industries, Baker City Field Office; retired.

NOTICE

Cover photograph: A view looking northeast into the Silvies River valley in the southwestern part of the Poison Creek 7.5' quadrangle, Harney County, Oregon (43.66616, −119.11520 WGS84 geographic coordinates; 4836764mN, 329547mE WGS84 UTM Zone 11 coordinates*). The outcrops here expose a sequence of 8.41 Ma Prater Creek Ash-flow Tuff (Tmtp) overlain by a trachyandesite lava flow (Tmat; middle outcrop) and the 7.093 Ma Rattlesnake Tuff. Photo credit: Jason D. McClaughry, 2018.*

Expires: 12/1/2019

Oregon Department of Geology and Mineral Industries Geologic Map 123
Published in conformance with ORS 516.030.

For additional information:
Administrative Offices
800 NE Oregon Street, Suite 965
Portland, OR 97232
Telephone (971) 673-1555
Fax (971) 673-1562
https://www.oregongeology.org
https://www.oregon.gov/dogami

TABLE OF CONTENTS

LIST OF FIGURES

LIST OF TABLES

GEODATABASE

PCB2019_GeMS_v10.6.gdb

See the appendix for geodatabase description.
Geodatabase is Esri® version 10.6 format.

SHAPEFILES AND SPREADSHEETS

Shapefiles

Bedding: PCB2019_Bedding.shp
Geochemistry: PCB2019_Geochemistry.shp
Geochronology: PCB2019_Geochronology.shp
Reference map: PCB2019_RefMap.shp
Water Wells: PCB2019_WaterWells.shp
Cross Section Lines: PCB2019_XSectionLines.shp

Spreadsheets (Microsoft® Excel®)

PCB2019_DATA.xlsx master file contains sheets:
Bedding: PCB2019_Bedding
Geochemistry: PCB2019_Geochemistry
Geochronology: PCB2019_Geochronology
Water Wells: PCB2019_WaterWells

See the digital publication folder for files.
Metadata is embedded in the geodatabase and shapefiles and is also provided as separate .xml format files.

MAP PLATES

Plate 1. Geologic map of the Poison Creek 7.5' quadrangle, Harney County, Oregon, scale 1:24,000
Plate 2. Geologic map of the Burns 7.5' quadrangle, Harney County, Oregon, scale 1:24,000

1.0 INTRODUCTION

The geology of the Poison Creek and Burns 7.5' quadrangles was mapped by the Oregon Department of Geology and Mineral Industries (DOGAMI) during 2018 and 2019. This mapping is part of a multi-year geologic study of the Harney Basin, designated a high priority by the Oregon Geologic Mapping Advisory Committee (OGMAC; **Figure 1-1**; Plate 1). Key objectives of this project are to 1) provide an updated and spatially accurate geologic framework for those quadrangles, referred to as the map area in the following report; 2) correlate lithologic units to surrounding areas; 3) improve the understanding of the structural and lithologic controls on groundwater aquifers; and 4) describe the occurrence of geologic resources (aggregate, industrial, mineral, and energy) and geologic hazards within the map area. This study was supported in part by a grant from the STATEMAP component of the National Cooperative Geologic Mapping Program (G18AC00136). Additional funds were provided by the State of Oregon.

The core products of this study are this report, an accompanying set of digital geologic maps and cross sections (Plates 1 and 2), and an Esri ArcGIS™ ArcMap™ geodatabase. The geodatabase presents the new geologic mapping in a digital format consistent with the Geologic Map Schema (GeMS), version 2.7 (USGS National Cooperative Geologic Mapping Program, 2010, 2018). This geodatabase contains spatial information, including geologic polygons, contacts, structures, geochemistry, geochronology, bedding, and water well data, as well as data about each geologic unit such as age, lithology, mineralogy, and structure. Digitization at scales of 1:8,000 or better was accomplished using a combination of 1-m lidar digital elevation models (DEMs) and 1-m 2016 National Agriculture Imagery Program (NAIP) digital orthophotos. Surficial and bedrock geologic units contained in the geodatabase are depicted on the map plates at a scale of 1:24,000. Both the geodatabase and digital geologic maps are supported by this report describing the geology in detail.

Collectively, this report, digital geologic maps, and cross sections refine our understanding of geologic conditions that control the distribution, quantity, and quality of groundwater resources, the distribution of terrain susceptible to landslides, the nature of seismic hazards, and the distribution of potential aggregate sources and other mineral resources in the Poison Creek and Burns 7.5′ quadrangles. New detailed geologic data presented here also provide a basis for future geologic, geohydrologic, and geohazard studies in the greater Harney Basin.

Figure 1-1. Location map of the Poison Creek and Burns 7.5′ quadrangles (next page), showing a status map of geologic mapping completed, in progress, and planned in the Harney Basin. Deep pink area encompasses 2018 to 2019 geologic mapping in the Poison Creek and Burns 7.5′ quadrangles (this study). Blue quadrangles were mapped by DOGAMI with funding from STATEMAP between 2015 and 2018 (R.A. Houston, unpub. mapping, 2015; Niewendorp and others, 2018; Houston and others, 2018). Yellow quadrangles include geologic maps completed by the USGS (Johnson, 1994, 1996; Sherrod and Johnson, 1994). Orange quadrangles include geologic mapping completed or in progress by Portland State University (EdMap). Green Burns Butte 7.5′ quadrangle will be mapped for STATEMAP 2019. Light pink quadrangles include targets of future geologic mapping by DOGAMI. Blue line is the Harney Basin hydrologic boundary. Asterisks are landmarks and labeled as follows: GB – Glass Buttes; JR – Juniper Ridge; SM – Sheep Mountain; WM – Wagontire Mountain; DM – Dry Mountain; LJ – Little Juniper Mountain; HM – Horsehead Mountain; IM – Iron Mountain; CH – Capehart Lake; SL – Silver Lake; LA – Lake Abert; GL – Goose Lake; CL – Crump Lake; AL – Alkali Lake; DC – Diamond Craters; MNWR – Malheur National Wildlife Refuge; HL – Harney Lake; ML – Malheur Lake; WRP – Wright Point; LW – Lawen; CN – Crane; BC – Buchanan; LV – Logan Valley; BV – Bear Valley; IR – Ingle Mountain; CG – Cougar Mountain; CM – Cottonwood Mountain; CR – Castle Rock; BR – Beulah Reservoir; WR – Warm Springs Reservoir; NHS – Neil Hot Springs; LO – Lake Owyhee; JC – Jordan Craters; CW – Cow Lakes; AR – Antelope Reservoir; BB – Burns Butte.

Figure 1-1. (Location map of the Poison Creek and Burns 7.5′ quadrangles – caption on previous page)

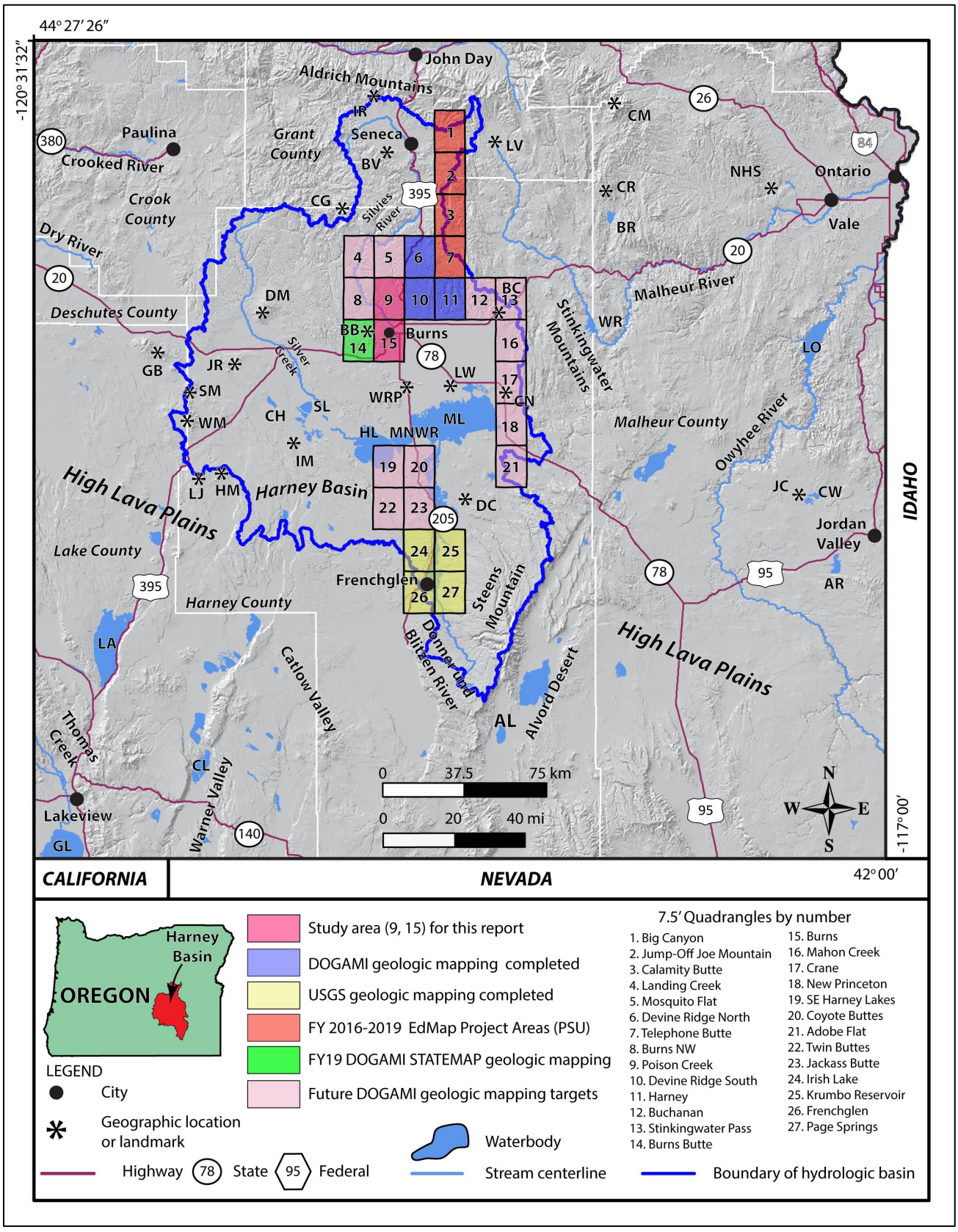

2.0 GEOGRAPHIC AND GEOLOGIC SETTING

The Poison Creek and Burns 7.5′ quadrangles are located in the north-central part of the Harney Basin of southeastern Oregon. The Harney Basin encompasses an area of approximately 13,566 km^2 (5,247 mi^2) in southeastern Oregon (**Figure 1-1**). The basin is a hydraulically closed basin fed by several creeks and rivers, including Silver Creek, Silvies River, and the Donner und Blitzen River (**Figure 1-1**; Dugas, 1998). These waterways drain into numerous plains, marshes, and seasonal to permanent lakes, including Harney and Malheur lakes, which lie near the geographic center of the basin. Topographic relief is substantial, ranging from a high of 2,967 m (9,733 ft) at the summit of Steens Mountain to a low of 1,248 m (4,093 ft) at Harney Lake in the center of the basin. Climate in this region is semi-arid, and precipitation amounts (rainfall and snow) vary greatly from year to year.

The low-relief, flat-lying depression that forms the Harney Basin is a major physiographic feature in southeastern Oregon lying at the east end of the High Lava Plains (HLP) and along the southern margin of the Blue Mountains Province (BMP; Walker and MacLeod, 1991; **Figure 2-1**). The basin is separated by the Brothers fault zone (BFZ) from the Basin and Range Province (BRP) to the south and borders the Owyhee Uplands on the east (**Figure 2-1**).

Rocks of the BMP, composed of four distinct pre-Cenozoic terranes, the Baker, Wallowa, Olds Ferry, and Izee terranes, are present in the northern part of the Harney Basin, along the core and flanks of the east-west trending Aldrich and Strawberry Mountain ranges (**Figure 1-1**, **Figure 2-1**, **Figure 2-2**). Pre-Cenozoic terranes (Olds Ferry-Izee terrane in this area) form an extensive, south-southeast-dipping block that plunges beneath the Harney Basin (Plate 1, cross section A-A′). Deeply eroded pre-Cenozoic rocks in the northern part of the Harney Basin are variably covered by late Oligocene to early Miocene (ca. 24 to 22 Ma) calc-alkaline lavas (Niewendorp and others, 2018; Houston and others, 2018), early to middle Miocene tholeiitic Columbia River flood basalt, and middle Miocene calc-alkaline lavas of the Strawberry Volcanics. The ca. 16 Ma Picture Gorge Basalt of the Columbia River Basalt Group occurs over a large area of north-central Oregon, extending south into the northern part of the Harney Basin (Cahoon and Streck, 2017).

The northern extent of the BRP, forming the southern part of the Harney Basin, comprises a series of north-dipping regional fault blocks that include north-trending Steens Mountain (**Figure 1-1**, **Figure 2-1**, **Figure 2-2**). The volcanic sequence in the southern Harney Basin includes late Oligocene and early Miocene calc-alkaline volcanic rocks (ca. 26 to 22 Ma; Langer, 1991; Scarberry and others, 2009), early to middle Miocene tholeiitic Columbia River flood basalts, intercalated middle Miocene ash-flow tuffs, and overlying olivine basalt flows. Flows of the 16.75 to 16.54 Ma Steens Basalt (Camp and others, 2013; Kasbohm and Schoene, 2018), forming part of this southern volcanic sequence, are the earliest lavas to erupt as part of the Columbia River Basalt Group. Steens flows cover much of southeastern Oregon and parts of southwestern Idaho to northern Nevada, and likely underlie a significant portion of the southern to central part of the Harney Basin (**Figure 2-2**). Large-displacement (>150 m [>500 feet]), north-northeast to northwest-trending normal faults (e.g., Winter Rim fault, Abert Rim fault, Hart Mountain fault, Steens Mountain fault) characterize the northern part of the Basin and Range Province. Basin and Range Province deformation began during the Miocene (~17 Ma; Donath, 1962; Thompson and Burke, 1974).

The HLP transects the central part of the Harney Basin, forming an Oligocene to late Cenozoic volcanic upland, continuous and gradational into the BRP. Volcanic rocks exposed in the HLP younger than 12 Ma are strongly bimodal, including relatively equal volumes of thin primitive basalt flows and rhyolitic tuffs and domes (MacLeod and others, 1976; Jordan and others, 2004; Scarberry and others, 2009; Ford and

others, 2013). Rhyolitic rocks, in general, successively young to the northwest, toward Newberry Volcano (MacLeod and others, 1976). Basaltic flows of the HLP, as young as latest Holocene, are present in the southern part of the Harney Basin (e.g., Diamond Craters) (**Figure 1-1**, **Figure 2-2**). The BFZ lies across the southern part of the Harney Basin as a wide diffuse zone interpreted as an intracontinental transform fault separating the extended crust of the BRP from comparatively un-extended BM crust to the north (Lawrence, 1976; **Figure 2-1**). The Steens fault extends across the eastern end of the BFZ, while the western end is obscured by Holocene ash deposits (Lawrence, 1976). Lawrence describes the BFZ as a series of longer (as much as 20 km [12.4 miles]), discontinuous en echelon faults (Reidel shears) trending ~N 50° W and less abundant shorter (5 km [3.1 miles]) N 30° E faults expressed as horst and graben structures (Lawrence, 1976). Faults in the BFZ largely dip steeply northeast, with a down-on-the northeast sense of offset. Iademarco (2009) and Trench (2008) suggested en echelon faults in the BFZ formed from ~7 Ma to 5 Ma. Trench (2008) suggested east-west extension in the BRP is transitioned to the BFZ by way of dextral oblique strike-slip horsetail fractures and structural clockwise rotation about a pole located in northeastern Oregon.

Three voluminous late Miocene ash-flow tuffs are widely exposed across the Harney Basin, above the Columbia River Basalt Group (**Figure 2-2**; **Figure 2-3**; Plates 1 and 2). These units include the 9.63/9.74 Ma Devine Canyon Ash-flow Tuff (**Tmtd**), 8.41 Ma Prater Creek Ash-flow Tuff (**Tmtp**), and 7.093 Ma Rattlesnake Tuff (**Tmtr**) (Walker, 1979; Streck, 1994; Streck and Grunder, 1995, 2008; Jordan and others, 2004; Ford and others, 2013; Isom, 2017). These successive cliff- and bench-forming ash-flow tuffs are locally separated from one another by intervening, poorly exposed tuff beds and tuffaceous sedimentary rocks (**Tmst**). The Rattlesnake Tuff (**Tmtr**) is the youngest and largest of the three late Miocene Harney Basin tuffs, having an estimated eruptive volume >280 km^3 (>67 mi^3) and outcrops covering an area >35,000 km^2 (>13,500 mi^2) (Streck and Grunder, 1995; **Figure 2-3**). The Devine Canyon Ash-flow Tuff (**Tmtd**) is the oldest and second most widespread of the late Miocene tuffs with an eruptive volume estimated at 250 to 300 km^3 (60 to 72 mi^3) and outcrops covering an area >30,800 km^2 (>11,891 mi^2) (Isom, 2017). The intermediate age Prater Creek Ash-flow Tuff (**Tmtp**) is the smallest of the three late Miocene tuffs, having an eruptive volume of ~200 km^3 (~48 mi^3) and outcrops covering an area of ~9,615 km^2 (~3,713 mi^2) (Greene, 1973; Parker, 1974; Streck and Ferns, 2004). The type sections for these ash-flow tuffs are in Devine Canyon, located along the eastern edge of the Poison Creek 7.5′ quadrangle (Plate 1).

Caldera sources for the three late Miocene Harney Basin ash-flow tuffs (**Tmtd, Tmtp, Tmtr**) have no surface expression (**Figure 2-2**; **Figure 2-3**). Their locations are inferred by a number of workers to be in the Harney Basin (Parker, 1974; Walker, 1974, 1979; Walker and Nolf, 1981; Streck and Grunder, 1995, 2008; Cox, 2011; Cox and others, 2013; Ford and others, 2013; Khatiwada and Keller, 2015). Varying ideas about possible caldera locations have been made on the basis of mapped outcrop distribution, thickness changes, welding characteristics, and distance correlations with pumice-lithic size or shape (**Figure 2-3**). Additional suggestions about the locations of source calderas beneath the Harney Basin have come from geophysical studies by Cox (2011), Cox and others (2013), and Khatiwada and Keller (2015). Possible Devine Canyon Ash-flow Tuff (**Tmtd**) caldera or vent sources may underlie the north-central Harney Basin, between Burns and Wright Point (Greene, 1973; Walker, 1974, 1979; Isom, 2017; **Figure 2-3**). Meigs and others (2009) and Ford and others (2013) showed a possible Devine Canyon Ash-flow Tuff eruptive center location lying along the southeastern edge of Malheur Lake. Khatiwada and Keller (2015), on the basis of geophysical imaging, inferred a possible eruptive source area for the Devine Canyon (**Tmtd**) in a similar location centered between Malheur Lake and Diamond Craters. The Prater Creek Ash-flow Tuff (**Tmtp**) eruptive center was suggested by Parker (1974) to be at Double O Ranch, ~25 km (~15.6 mi)

south of the mapped area. Parker (1974) argued that the rhyolite of Double O Ranch (unit Trr of Greene and others, 1972) is a dome-flow complex mineralogically and chemically similar to the Prater Creek Ash-flow Tuff (**Tmtp**). Meigs and others (2009) and Ford (2013) suggested an eruptive center for the Prater Creek Ash-flow Tuff (**Tmtp**) lying along the northern edge of Wright Point, in the central part of the Harney Basin. Khatiwada and Keller (2015), on the basis of geophysical imaging, inferred a possible eruptive source area for the Prater Creek Ash-flow Tuff (**Tmtp**) in a similar location centered on Malheur Lake and Wright Point (their "northern caldera"). Streck (1994) and Streck and Grunder (1995) proposed a vent for the Rattlesnake Tuff (**Tmtr**) located at Capehart Lake in the western part of the Harney Basin on the basis of degree of welding, pumice size and distance correlations, and thickness.

Rattlesnake Tuff (**Tmtr**) outflow deposits originating from the Capehart Lake area completely inundated and largely buried evidence for late Miocene caldera structures across the Harney Basin (**Figure 2-2**; **Figure 2-3**). Detailed geologic mapping, augmented by lithologic description and geochemical characterization of numerous intervals from two deep exploration wells (Federal 1-10, CTI; **Table 2-1**) penetrating through the extensive Rattlesnake Tuff (**Tmtr**) cover in the Poison Creek and Burns 7.5′ quadrangles, now reveals the location of at least one of the source calderas for the three late Miocene ash-flow tuffs (**Tmtd, Tmtp, Tmtr**). No previous investigations, outside of Cox and others (2013), have incorporated deep well lithologic data and no studies have physically examined or analyzed existing cuttings from historic Harney Basin exploration wells. Geologic information obtained for this study from the Harney Basin exploration wells listed in **Table 2-1** demonstrates that the source caldera for the 8.41 Ma Prater Creek Ash-flow Tuff (**Tmtp**) lies buried at depth beneath the city of Burns, extending west into the Burns Butte 7.5′ quadrangle. In this report, we formally name and refer to the eruptive center for the Prater Creek Ash-flow Tuff (**Tmtp**) as the Silvies River caldera (**Figure 2-3**, Plates 1 and 2).

The Silvies River caldera contains a >427 m (>1,400 ft) thick, monotonous section of granophyric rhyolitic intracaldera tuff (**Tmtpi**) geochemically indistinguishable from the equivalent outflow Prater Creek Ash-flow Tuff (**Tmtp**). Stratigraphic discontinuity between the CTI and the Weed and Poteet #1 wells indicates the eastern margin of the Silvies River caldera runs north through the Burns 7.5′ quadrangle (Plate 2) and then parallels the Silvies River before it exits the west side of the Poison Creek 7.5′ quadrangle (Plate 1). South of Burns, the caldera margin may extend to Double O Ranch, where Parker (1974) inferred a Prater Creek Ash-flow Tuff (**Tmtp**) source area associated with the 8.28 Ma rhyolite of Double O Ranch (red star in **Figure 2-3**; age date by Jordan and others, 2004). West and northwest of the city of Burns (Plates 1 and 2), in the northwest part of the Harney Basin, thick **Tmtpi** deposits are spatially associated with a bimodal suite of late Miocene (ca. 8.4 to 7.68 Ma) rhyolitic tuffs (tuff of Wheeler Springs, **Tmtw**, **Tmtwh**), exogenous rhyolite domes and flows (rhyolite of Golden Ranch **Tmrg**, rhyolite of Burns Butte **Tmrb**), and (7.68 to 7.1 Ma) basaltic trachyandesite and trachyandesite flows, dikes, and vent deposits (**Tmat**, **Tmvt**). These rocks define a narrow volcanic field of silicic domes and mafic shield volcanoes lying above caldera-filling tuffs (**Tmtpi**) along the eastern ring fracture zone of the Silvies River caldera (Plates 1 and 2, cross sections).

Late Miocene rocks in the Poison Creek and Burns 7.5′ quadrangles are locally covered by late Pliocene to Quaternary sedimentary rocks (**QTst**), and younger surficial units, including older fan deposits (**Qoaf**), colluvium (**Qc**), fan deposits (**Qaf**), stream channel alluvium (**Qa**), marsh and alluvial deposits (**Qma**), fan delta deposits (**Qfd**), and modern fill (**Qf**). Landslide deposits (**Qls**) are also present in some areas. Mima mounds, observed in 1-m lidar DEMs, are a conspicuous surficial feature across most bedrock surfaces, exclusive of unit **Tmat**.

Table 2-1. List of oil and gas exploration wells, geothermal test wells, and groundwater observation wells drilled in and adjacent to Poison Creek and Burns 7.5' quadrangles. See Section 6 for detailed well information.

Well Name	Year Drilled	Total Depth (m)	Total Depth (ft)	Type	Cuttings	LAT_NAD83	LONG_NAD83
Dog Mountain	1912	>1,147	>3,763	oil and gas exploration	no	unknown#	
United Company of Oregon, Inc., #1 Fay*	1945	1,166	3,826	oil and gas exploration	yes	43.50400	−118.77003
United Company of Oregon, Inc., Weed and Poteet #1 (HARN 52707) *^	1949	1,976	6,480	oil and gas exploration	no	43.59358	−119.01930
H.C. Voglar No. 1	1949	1,387	4,550	oil and gas exploration	no	43.45563	−118.94754
Michael T. Halbouty Federal 1-10*	1977	2,343	7,684	oil and gas exploration	yes	43.59260	−119.22004
HARN 50087 CTI geothermal test well^	1996	596	1,956	geothermal exploration	yes	43.55013	−119.08158
HARN 52747 EOARC Observation Well^	2018	171	560	groundwater observation	yes	43.52580	−119.02042

*Additional information is available for these wells from the DOGAMI Oil and Gas Well Log Index — https://www.oregongeology.org/mlrr/oilgas-logs.htm

^Additional information available for these wells from the OWRD Groundwater Information System — https://apps.wrd.state.or.us/apps/gw/gw_info/gw_info_report/gw_details.aspx?gw_site_id=30497 (HARN 52707 Weed and Poteet);
https://apps.wrd.state.or.us/apps/gw/gw_info/gw_info_report/gw_details.aspx?gw_site_id=12735 (HARN 50087);
https://apps.wrd.state.or.us/apps/gw/gw_info/gw_info_report/gw_details.aspx?gw_site_id=31110 (HARN 52747).

#Buwalda (1921) reported a location 19 km (12 mi) south of Burns near Dog Mountain.

Figure 2-1. Physiographic province map of Oregon, showing location of the Brothers fault zone, selected Basin and Range faults, and the study area. Abbreviations: CR – Coast Range; HC – High Cascades; KM – Klamath Mountains; WC – Western Cascades; WV – Willamette Valley. Solid black lines demarcate physiographic provinces (after Walker, 1977). Blue lines are selected major Basin and Range type normal faults, showing normal displacement direction (ball and bar on downdropped block). White line marks the location of the Harney hydrologic basin. Basemap: 10-m hillshade DEM.

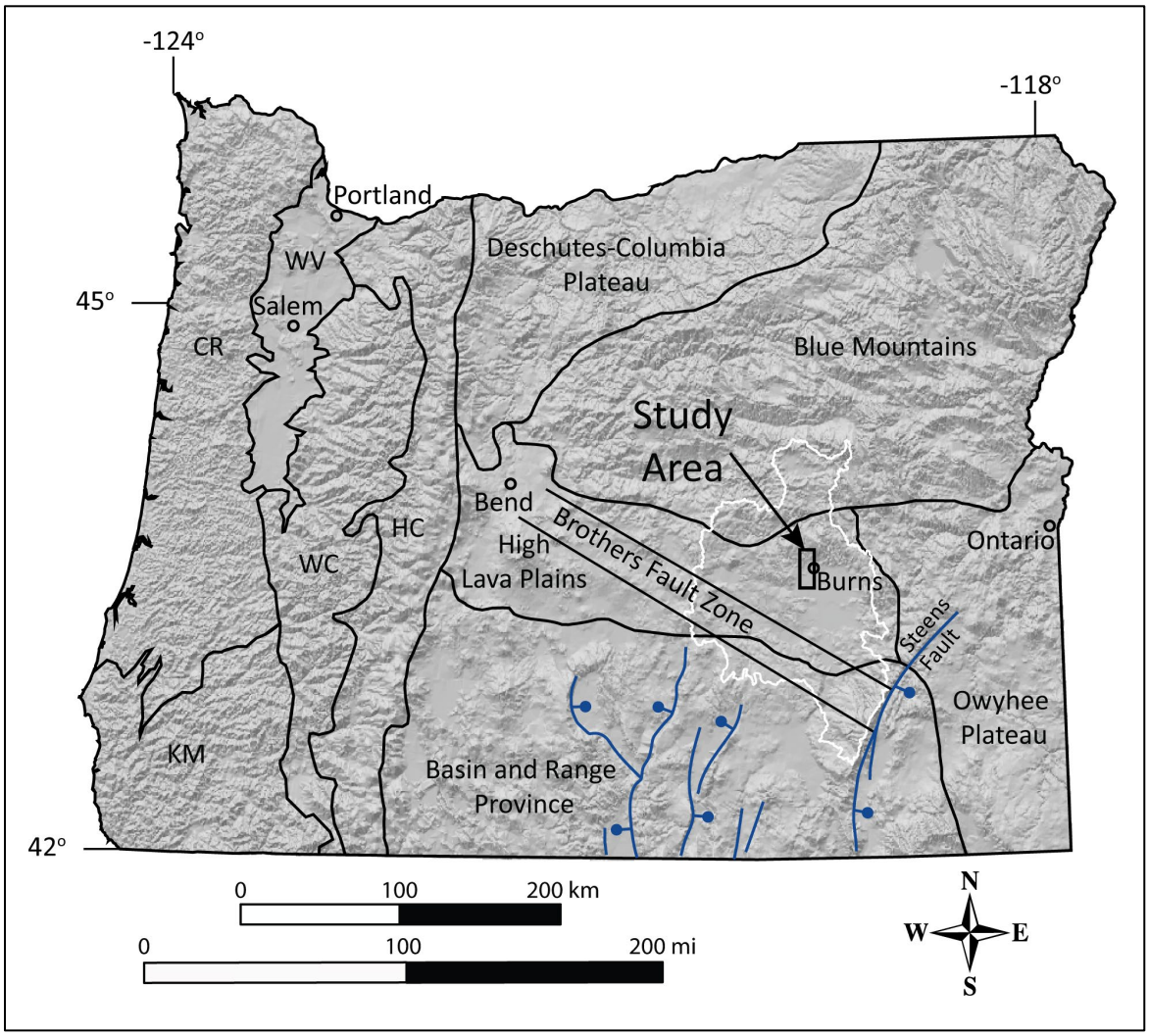

Figure 2-2. Generalized geologic map of southeastern Oregon, after Smith and Roe (2015). Red-outlined quadrangles are the map area. The blue line marks the location of the Harney hydrologic basin.

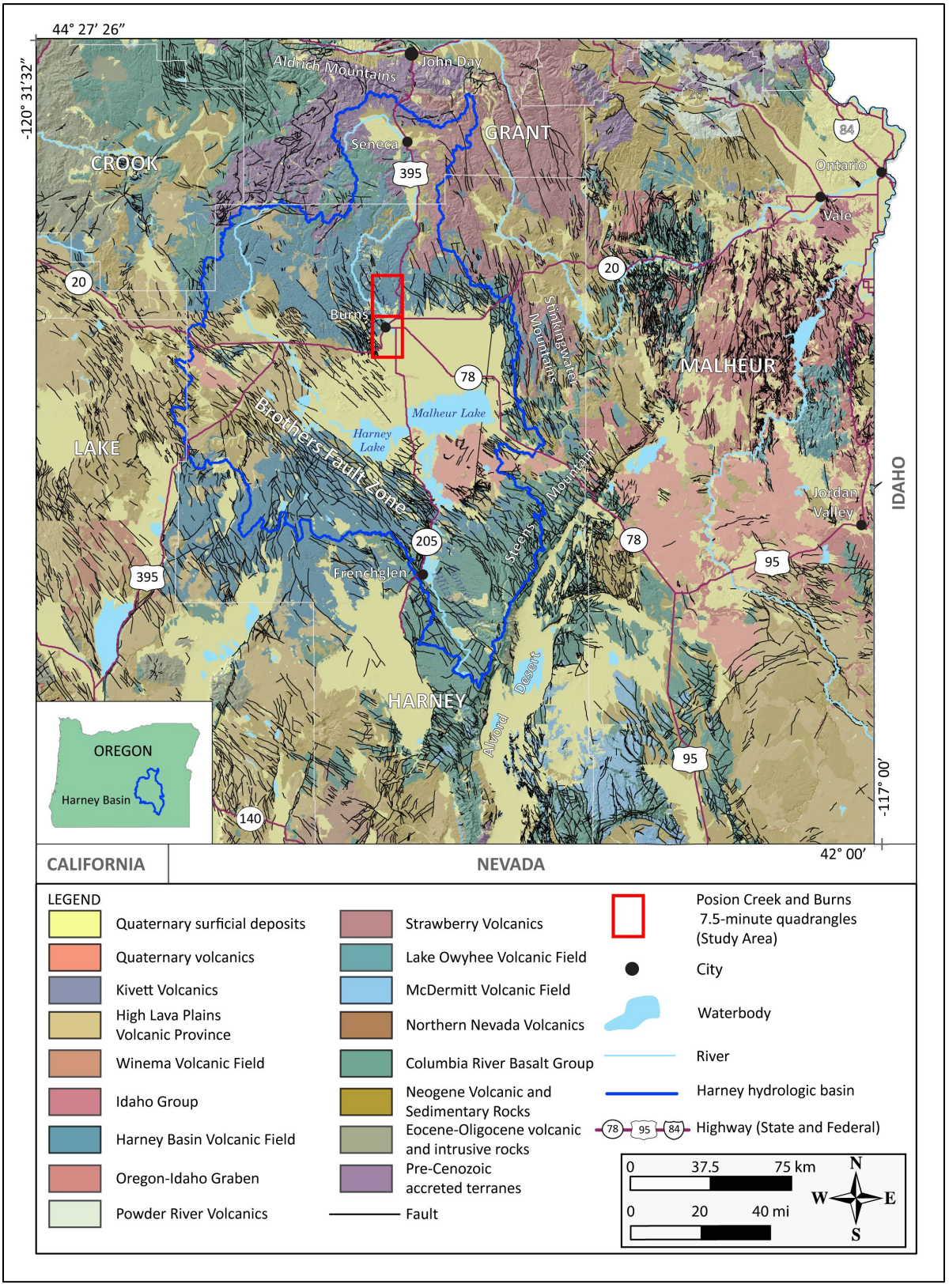

Figure 2-3. Outcrop distribution and possible source areas for late Miocene tuffs in the Harney Basin (next page). RT – Rattlesnake Tuff (Tmtr), PCT – Prater Creek Ash-flow Tuff (Tmtp), DCT – Devine Canyon Ash-flow Tuff (Tmtd). Estimated distribution outline for RT is from Streck and Grunder (1995) and Streck and Ferns (2004). Estimated unit distribution outlines for the DCT and PCT are from Streck and Ferns (2004) and Isom (2017), modified from Greene (1973) and Walker (1979), respectively. Red-dashed outline representing the outline of the Silvies River caldera as defined by this study (see Structure section for further discussion).

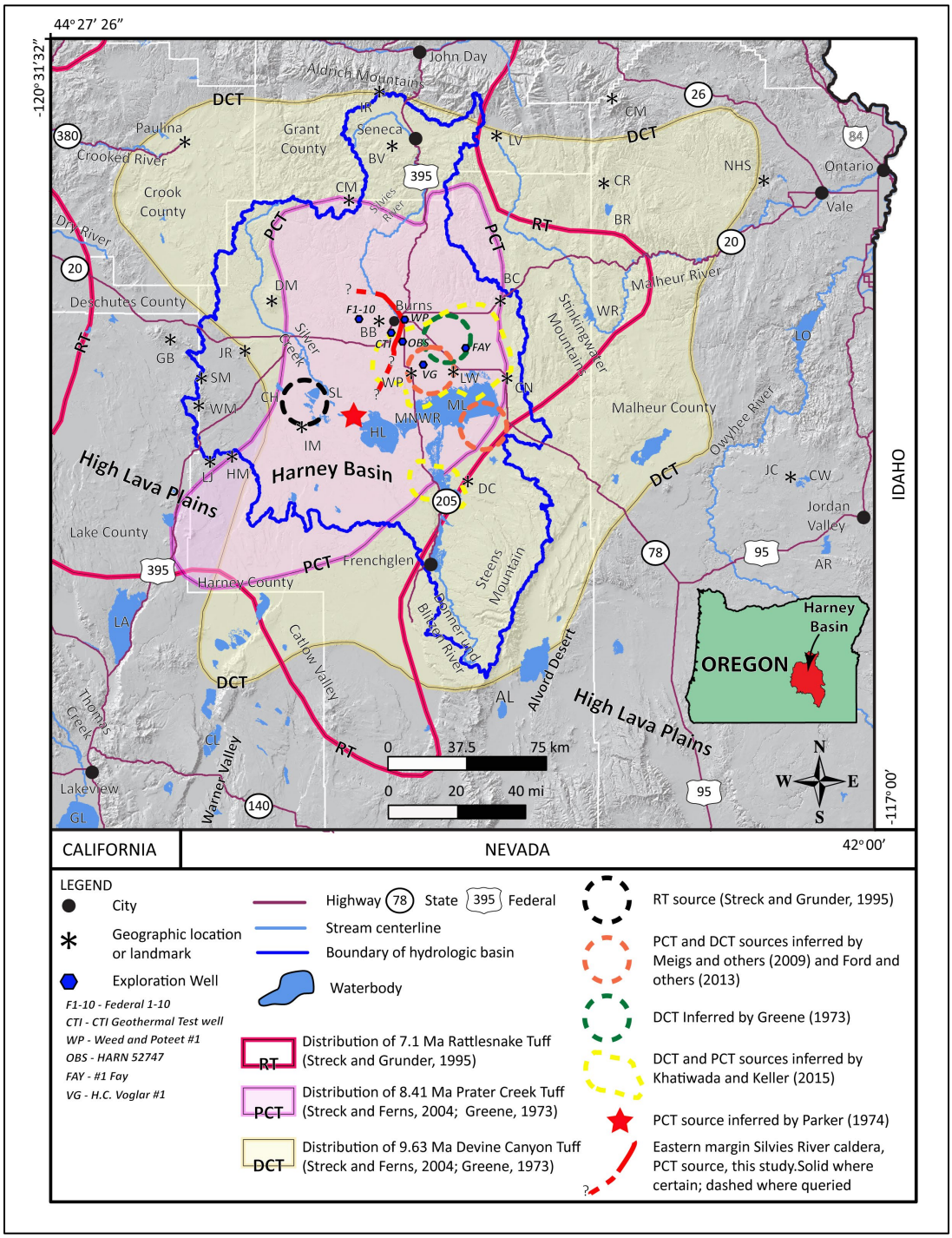

3.0 PREVIOUS WORK

Table 3-1 shows a list of previous regional geologic investigations consulted for work in the Poison Creek and Burns 7.5′ quadrangles. Reports and maps listed in **Table 3-1** are organized in chronological order; those shown in bold are geologic maps that lie within the study area. The index map shown in **Figure 3-1** summarizes the sources of previous geologic mapping consulted during this project. Earlier geologic maps and reports displaying the bedrock geology in and adjacent to the study area include those by Piper and others (1939), Greene (1972), Greene and others (1972), Brown and others (1980a,b), Brown (1982), McGrane (1985), Walker and MacLeod (1991), Smith and Roe (2015), S. L. Isom and M. J. Streck (unpub. data, 2017), Niewendorp and others (2018), Houston and others (2018), R. Houston and others (unpub. data, 2016), and M. Cruz and M. J. Streck (unpub. data, 2018). Additional scientific investigations consulted during this study include Russell (1884), Leonard (1970), Walker (1970), Greene (1973), Niem (1974), Lawrence (1976), Walker (1979), Sherrod and Johnson (1994), Sheppard (1994), MacLean (1994), Streck (1994), Streck and Grunder (1995), Johnson (1994, 1996), Jordan (2001), Jordan and others (2002), Camp and others (2003), Jordan and others (2004), Streck and Ferns (2004), Trench (2008), Meigs and others (2009), Milliard (2010), Ford (2012), Boschmann (2012), Ferns and McClaughry (2013), Camp and others (2013), Ford and others (2013), Streck and others (2015), and Khatiwada and Keller (2015).

Table 3-1. Partial chronological list of maps and reports on which this study builds. Maps shown in bold lie within or adjacent to the study are. Unpub. is unpublished geologic mapping.

Author	Year	Subject	Scale
Piper and others	**1939**	**Geology and groundwater resources of the Harney Basin**	**1:125,000**
Leonard	1970	Ground-water resources in Harney Valley	na
Walker	1970	Cenozoic ash-flow tuffs of Oregon	na
Greene	**1972**	**Geologic map Burns and West Myrtle-Butte 15' quadrangles**	**1:62,500**
Greene and others	**1972**	**Geologic map of the Burns quadrangle**	**1:250,000**
Greene	1973	Petrology of the welded tuff of Devine Canyon	na
Niem	1974	Wright's Point, Harney County, Oregon	na
Walker	1979	Revisions to the Cenozoic stratigraphy of Harney Basin	na
Brown and others	**1980a**	**Geothermal resource potential northern Harney Basin**	**1:62,500**
Brown and others	**1980b**	**Geothermal resource potential southern Harney Basin**	**1:62,500**
Brown	**1982**	**Geology/geothermal resources south half Burns 15' quad.**	**1:24,000**
McGrane	1985	Geology of the Idol City area	1:24,000
Walker and MacLeod	1991	Geologic map of Oregon	1:500,00
MacLean	1994	Geochem. Juniper Ridge, Horsehead Mtn., Burns Butte	na
Streck	1994	Volcanology and petrology of the Rattlesnake Tuff	na
Streck and Grunder	1995	Crystallization and welding variations Rattlesnake Tuff	na
Jordan	2001	Basaltic volcanism and tectonism of the High Lava Plains	na
Jordan and others	2002	Bimodal volcanism and tectonism of the High Lava Plains	na
Jordan and others	2004	Geochronology of the High Lava Plains	na
Streck and Ferns	2004	The Rattlesnake Tuff and silicic volcanism	na
Meigs and others	2009	Magmatic and tectonic development of High Lava Plains	na
Cox	2011	controlled-source seismic/gravity study High Lava Plains	na
Ford	2012	Rhyolitic magmatism of the High Lava Plains	na
Ford and others	2013	Bimodal volcanism of the High Lava Plains	na
Cox and others	2013	controlled-source seismic/gravity study High Lava Plains	na
Smith and Roe	2015	Oregon geologic data compilation [OGDC], release 6	variable
Khatiwada and Keller	2015	Geophysical imaging of upper crust Harney Basin	na
Isom	2017	Composition of the Devine Canyon Tuff	na
Isom and Streck	unpub.	Geologic map of the Telephone Butte 7.5' quadrangle	1:24,000
Cruz and Streck	unpub.	Geologic map of the Calamity Butte 7.5' quadrangle	1:24,000
Niewendorp and others	**2018**	**Geologic map of the Devine Ridge South 7.5' quadrangle**	**1:24,000**
Houston and others	**2018**	**Geologic map of the Devine Ridge North 7.5' quadrangle**	**1:24,000**
R. Houston and others	unpub.	Geologic map of the Harney 7.5' quadrangle	1:24,000

Figure 3-1. Sources of geologic mapsused during the project. See DataSourcePolys feature class in the geodatabase. Blue line marks the location of the Harney hydrologic basin. Basemap: 10-m shaded relief DEM.

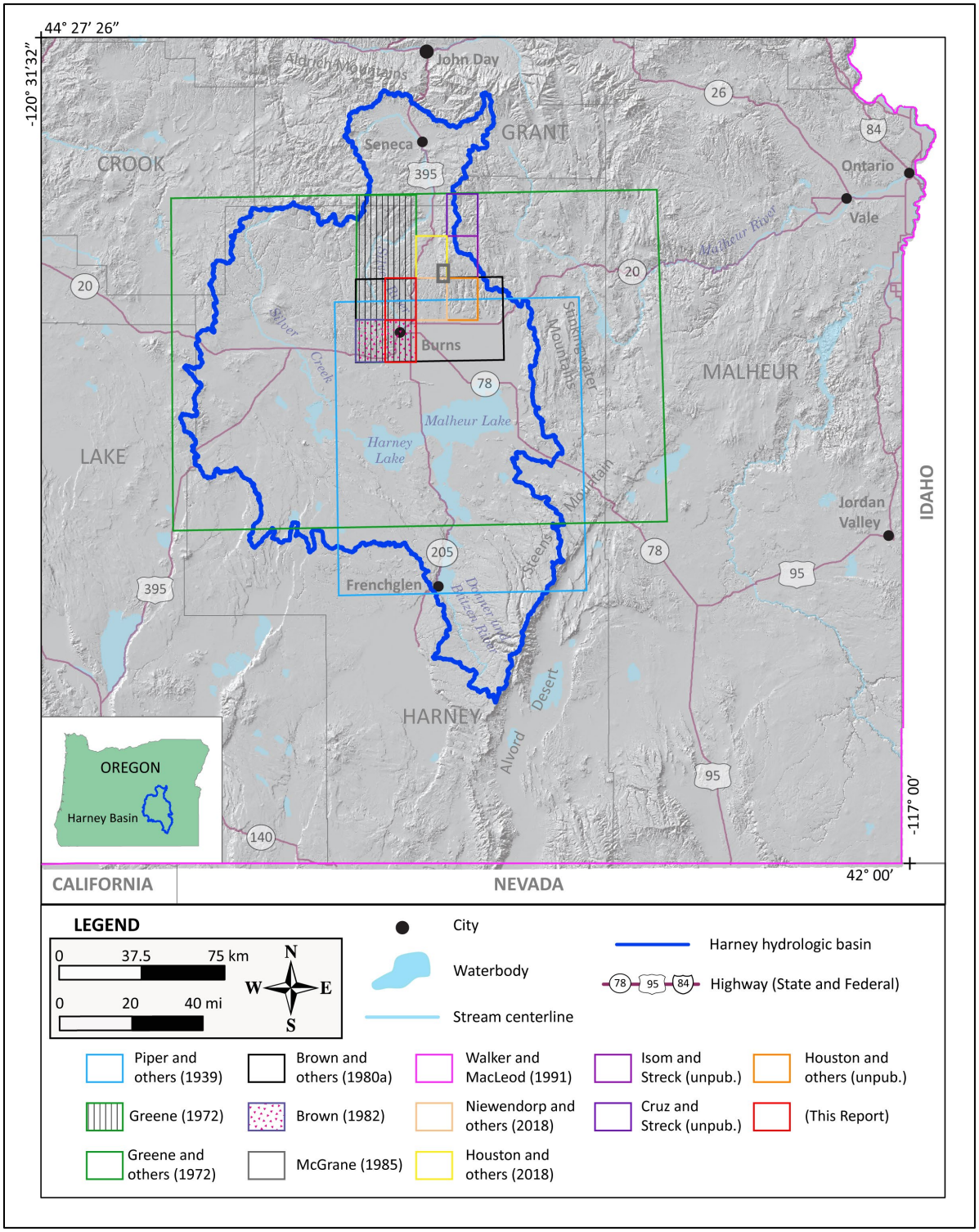

4.0 METHODOLOGY

Geologic data were collected digitally using a GPS-enabled Apple® iPad® 4, loaded with Geometry Pty Ltd iGIS Pro, a geographic information system software package compatible with Esri ArcGIS. Geologic mapping used 1-m lidar DEMs, USGS digital raster graphics (DRGs), and digital orthophoto imagery (2016) obtained from Google Earth™ as basemaps. Fieldwork conducted during this study consisted of data collection along roads, combined with transects following lithologic contacts and faults across public and private rangelands. Standard geologic methods for collecting samples and measuring attitudes of inclined bedding, geologic features, and faults were employed. Digitization and the final digital Esri ArcGIS ArcMap format geologic database was completed at a minimum scale of 1:8,000.

Mapping was supported by new and compiled X-ray fluorescence (XRF) geochemical analyses of whole-rock samples, thin-section petrography, measurements of natural remanent magnetization (magnetic polarity), and field and remotely collected strike and dip measurements of inclined bedding (Plates 1 and 2). Whole-rock geochemical samples were prepared and analyzed by XRF at the Washington State University GeoAnalytical Lab, Pullman, Washington, under the direction of Dr. Ashley Steiner. In addition to outcrop samples, cuttings were obtained from two oil exploration holes (Federal 1-10, #1 Fay) and one geothermal hole (CTI). Picked cuttings were examined under a binocular microscope, and altered and foreign chips were removed prior to XRF analysis. Analytical procedures for the Washington State University GeoAnalytical Lab are described by Johnson and others (1999) and can be obtained online at https://s3.wp.wsu.edu/uploads/sites/2191/2017/06/Johnson-Hooper-and-Conrey.pdf. Major element determinations are normalized to a 100-percent total on a volatile-free basis and recalculated with total iron expressed as FeO*. Whole-rock geochemical data are useful in classifying volcanic rocks, as many lavas are too fine grained and glassy to be adequately characterized by mineralogical criteria alone. Descriptive rock unit names for volcanic rocks are based in part on the online British Geological Survey classification schemes (Gillespie and Styles, 1999; Robertson, 1999; Hallsworth and Knox, 1999), and normalized major element analyses plotted on the total alkali ($Na_2O + K_2O$) versus silica (SiO_2) diagram (TAS) of Le Bas and others (1986), Le Bas and Streckeisen (1991), and Le Maitre and others (1989, 2004). The magnetic polarity of strongly magnetized lavas was determined at numerous outcrops using a handheld digital magnetometer. Strike and dip measurements of geological planes (e.g., inclined bedding) were obtained in the field area by traditional compass and clinometer methods and were compiled from data published by previous workers. Additional bedding measurements were generated from lidar imagery by using a routine and model DOGAMI developed in Esri ArcGIS™ Model Builder to calculate three-point solutions from lidar bare-earth DEMs. Further details of this process are described in the appendix under the heading "Bedding (strike and dip)." Microsoft Excel® spreadsheets tabulating geochemical and geochronological analyses, and strike and dip measurements are provided as part of this publication. The appendix contains a summary of data collection methods and the field list for the spreadsheets mentioned above.

In this report, volcanic rocks with fine-grained (<1 mm [0.04 in]; Mackenzie and others, 1997; Le Maitre and others, 2004), average crystal or particle size in the groundmass are characterized in the following manner:

- A "coarse groundmass" if the average crystal or particle size is <1 mm (0.04 in) and can be determined using the naked eye (>~0.5 mm [0.02 in]).
- A "medium groundmass" if crystals of average size cannot be determined by eye but can be distinguished by using a hand lens (>~0.05 mm [0.02 in]).

- A “fine groundmass” if crystals or grains of average size can be determined only by using a microscope (or by hand lens recognition of phyllite-like sparkle or sheen in reflected light, indicating the presence of crystalline groundmass).
- A “glassy groundmass” if the groundmass has (fresh), or originally had (altered), groundmass with the characteristics of glass (conchoidal fracture; sharp, transparent edges; vitreous luster; etc.).
- Mixtures of crystalline and glassy groundmass are described as intersertal; ratios of glass to crystalline materials may be indicated by textural terms including holocrystalline, hypocrystalline, hyalophitic, and hyalopilitic.
- Microphenocrysts are defined as crystals larger than the overall groundmass and < 1 mm across (0.04 in).

Grain size of clastic sedimentary rocks is described following the Wentworth (1922) scale. Hand samples of unconsolidated sediments and clastic sedimentary rocks were compared in the field and/or in the laboratory to graphical representations (comparator) of the Wentworth scale to determine average representative grain size in various parts of a respective sedimentary geologic unit. Colors given for hand-sample descriptions are from the Geological Society of America Rock-Color Chart Committee (1991).

Subsurface geology shown in the geologic cross sections on Plates 1 and 2 incorporates lithologic descriptions, analyses, and geologic interpretations from 1) oil and gas exploration well logs (Federal 1-10, United Co. Weed and Poteet #1, #1 Fay), 2) geothermal exploration well logs (CTI well), and 3) water-well drill records (appendix). Records of historical oil and gas and geothermal exploration are available online from the DOGAMI Oil and Gas Well Log Index (https://www.oregongeology.org/mlrr/oilgas-logs.htm) and Geothermal Information Layer for Oregon web portal (https://www.oregongeology.org/gtilo/index.htm). Water well logs are available through the Oregon Water Resources Department (OWRD) Groundwater Resource Information Distribution (GRID) system (https://apps.wrd.state.or.us/apps/gw/well_log/). Water wells were not physically located. However, an attempt was made remotely to locate water wells and other drill holes that have well logs archived by OWRD. Approximate locations were estimated by using a combination of sources, including internal OWRD databases of located wells, Google Earth™, tax lot maps, street addresses, and aerial photographs. The accuracy of the locations ranges widely, from errors of 1.1 km (0.7 mi) possible for wells located only by section and plotted at the section centroid, to a few tens of feet for wells located by address or tax lot number on a city lot with bearing and distance from a corner. A well log ID is queried in the database (e.g., HARN-51852) to retrieve an image of the well log from the OWRD website (https://apps.wrd.state.or.us/apps/gw/well_log/). A database of 213 well logs with interpreted subsurface geologic units for the Poison Creek and Burns 7.5′ quadrangle is provided with the geodatabase.

To allow the interested reader to visit these sites in the field or to visualize remotely the area by using Google Earth™, map coordinates are provided for outcrop photographs shown in report figures. Locations are provided in two coordinate systems: 1) Geographic (datum = WGS84, units = decimal degree); and 2) Universal Transverse Mercator (UTM) Zone 11 (datum = WGS84, units = meters). Decimal degree coordinates can be entered into the “Fly to” box (e.g., 45.66132, −121.47123) in the search toolbar, and Google Earth™ will automatically locate and “fly” to the specified site.

5.0 EXPLANATION OF MAP UNITS

The suite of terrestrial volcanic and sedimentary bedrock units in the Poison Creek and Burns 7.5′ quadrangles ranges in age from late Miocene to early Pleistocene (**Figure 5-1**; Plate 1). Bedrock geologic units are locally covered along drainages and on some slopes in the project area by Late Pleistocene and Holocene surficial deposits. Widely separated stratigraphic units were grouped on the basis of apparent stratigraphic position, lithology, and chemical composition. Unit names follow local stratigraphic nomenclature when available, but when formal rock names are lacking, informal names are given because of composition or sites of good exposure. **Figure 5-1** depicts a time-rock chart showing age ranges for late Cenozoic bedrock and surficial units.

5.1 Overview of map units

UPPER CENOZOIC SURFICIAL DEPOSITS

Qf modern fill and construction material (upper Holocene)
Qma marsh and alluvial deposits (Holocene and Upper Pleistocene[?])
Qfd fan delta deposits (Holocene and Upper Pleistocene[?])
Qa alluvium (Holocene and Upper Pleistocene[?])
Qaf fan deposits (Holocene and Upper Pleistocene[?])
Qls landslide deposits (Holocene and Upper Pleistocene[?])
Qc colluvium (Holocene and Upper Pleistocene[?])
Qoaf older fan deposits (Holocene and Pleistocene[?])

Angular unconformity to disconformity

UPPER CENOZOIC VOLCANIC AND SEDIMENTARY ROCKS

LOWER PLEISTOCENE TO UPPER MIOCENE SEDIMENTARY ROCKS

QTst sedimentary rocks (lower Pleistocene to upper Miocene [?])

UPPER MIOCENE VOLCANIC AND SEDIMENTARY ROCKS

Tmtr Rattlesnake Tuff (upper Miocene) 7.093 ± 0.015 Ma ($^{40}Ar/^{39}Ar$)
Tmat basaltic trachyandesite and trachyandesite flows and dikes (upper Miocene)
Tmvt basaltic trachyandesite and trachyandesite vent deposits (upper Miocene)
Tmrb rhyolite of Burns Butte (upper Miocene) 7.68 ± 0.04 Ma ($^{40}Ar/^{39}Ar$)
Tmrg rhyolite of Golden Ranch (upper Miocene) 8.03 ± 0.26 Ma (K/Ar)
Tmri rhyolite intrusive (upper Miocene)
Tmtwh tuff of Wheeler Springs, non-welded lapilli tuff (upper Miocene)
Tmtw tuff of Wheeler Springs, welded tuff (upper Miocene)
Tmtp Prater Creek Ash-flow Tuff (upper Miocene) 8.41 ± 0.16 Ma ($^{40}Ar/^{39}Ar$)
Tmtpi Prater Creek Ash-flow Tuff, intracaldera unit (upper Miocene) (cross section only)
Tmtd Devine Canyon Ash-flow Tuff (upper Miocene) 9.63 ± 0.05 Ma, 9.74 ± 0.02 Ma ($^{40}Ar/^{39}Ar$)
Tmst tuffaceous sedimentary rocks (upper Miocene)

Angular unconformity to disconformity

Figure 5-1. Time-rock chart for the Poison Creek and Burns 7.5' quadrangles showing the 21 geologic units displayed on the geologic maps and in cross sections on Plates 1 and 2.

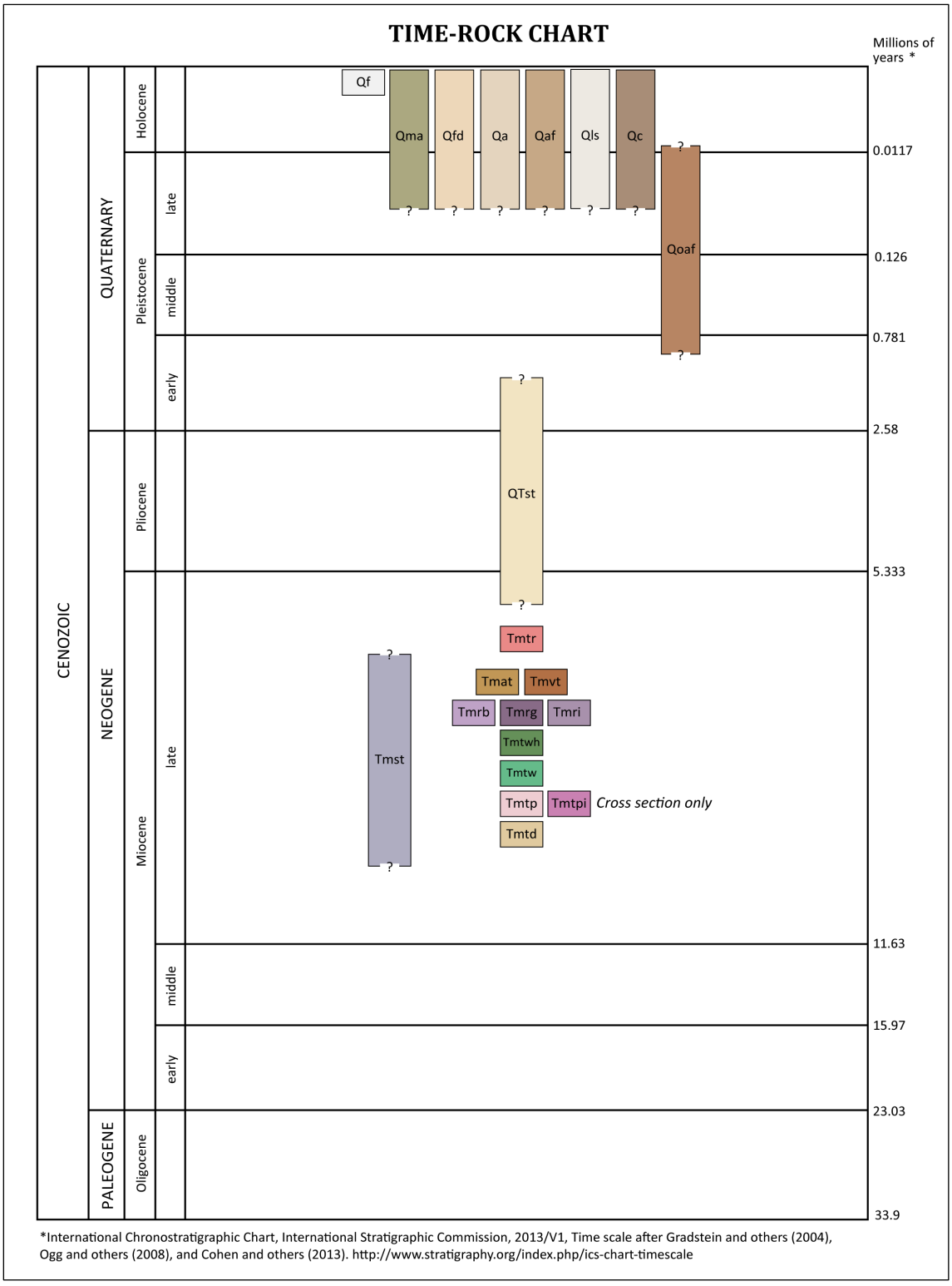

5.2 Upper Cenozoic surficial deposits

Upper Cenozoic sedimentary and volcanic rocks are locally covered by Upper Pleistocene and Holocene surficial deposits in the Poison Creek and Burns 7.5′ quadrangles, including alluvial, landslide, and fan deposits (**Figure 5-1**; Plates 1 and 2). Surficial units within the project area are delineated on the basis of geomorphology as interpreted from a combination of field observations, 1-m lidar DEMS, shaded relief raster images, USGS digital raster graphics (DRGs), and digital orthophoto imagery (2016).

Qf **modern fill and construction material (upper Holocene)**—Variable artificial or constructed fill deposits of poorly sorted and crudely layered mixed gravel, sand, clay, and other engineered fill (Plates 1 and 2). These deposits usually contain rounded to angular clasts ranging from small pebbles to boulders up to several meters across. The orientation of clasts is typically less uniform than is found in naturally occurring imbricated or bedding-parallel gravel. Deposits mapped as modern fill and construction material are generally associated with dams, road embankments, approaches to bridges, rail beds, culvert fills, mined land, and other low-lying areas (Plates 1 and 2). Major areas of continuous fill are shown on Plates 1 and 2 where extensive highway and road networks, and the abandoned Union Pacific Rail line, cross low-lying areas of the Silvies River Valley and Harney Valley. Additional artificial fills are present throughout the study area but are at too small a scale to digitize or portray on the map plates. The thickness of fill-deposits may locally exceed several meters.

Qma **marsh and alluvial deposits (Holocene and Upper Pleistocene[?])**—Peat and muck interbedded with unconsolidated clay and silt deposited across the broad, low relief and saturated alluvial plain of the Harney Valley (Plate 2). Includes some horizons of volcanic ash (Piper and others, 1939). Coarser alluvium composed of sand and gravel may occur along larger valley-traversing streams. The area covered by marsh and alluvial deposits prior to settlement was originally native meadow and swamp. The area is now extensively reclaimed as serviceable meadow-like ranch and agriculture land (Piper and others, 1939). The thickness of marsh and alluvial deposits may be 30 to 45 m (98 to 150 ft) in the Harney Valley. The unit is assigned a Holocene and Late Pleistocene age on the basis of stratigraphic position. Partly equivalent to Qal (valley fill) of Piper and others (1939), Qs (sedimentary deposits) of Greene (1972), Greene and others (1972), and Walker (1977), Qs/Qal (alluvium and Holocene sedimentary deposits, undifferentiated) of Brown and others (1980a), and Qal (recent alluvium and sedimentary deposits, undivided) of Brown (1982).

Qfd **fan delta deposits (Holocene and Upper Pleistocene[?])**—Unconsolidated gravel, sand, and silt, with interlayered clay deposited in a broad fan delta covering ~2,210 hectares (~5,462 acres) where the Silvies River and Poison Creek exit confined upland drainages and flow south onto the floor of the Harney Valley (**Figure 5-2**; Plate 2). Piper and others (1939) refer to this mapped area as the "Silvies River fan." At the apex of the fan delta, drainages branch into a loosely braided network of channels and sloughs that traverse the broad alluvial plain from northwest to southeast (Piper and others, 1939). Distal portions of the delta have intricate branching networks of distributary channels, displaying a "dichotomic" drainage pattern where streams radiate from a common point in a branching or tree-shaped fashion (**Figure 5-2**; Deffontaines and Chorowicz, 1991). Dichotomic drainage networks form on alluvial fans and deltas in coarse granular material and have been associated with recent tectonic uplift and development of drainages parallel to

tilted strata forming an inclined surface (Deffontaines and Chorowicz, 1991, p. 256). The delta may have prograded south into areas of shallow standing water during Late Pleistocene high-stands of paleo-Lake Malheur Lake documented by Dugas (1998).

The approximate mapped boundary between units **Qa**, **Qfd**, and **Qma** is determined on the basis of the farthest reaches of the dichotomic drainage networks of the Silvies River. Partly equivalent to Qal (valley fill) of Piper and others (1939), Qs (sedimentary deposits) of Greene (1972), Greene and others (1972), and Walker (1977), Qs/Qal (alluvium and Holocene sedimentary deposits, undifferentiated) of Brown and others (1980a), and Qal (recent alluvium and sedimentary deposits, undivided) of Brown (1982).

Qa **alluvium (Holocene and Upper Pleistocene[?])**—Unconsolidated gravel, sand, silt, and clay deposited along active stream channels and on adjacent floodplains of the Silvies River, Poison Creek, Foley Creek, and smaller tributaries (Plates 1 and 2). Gravels deposited as imbricated, massive to cross-stratified accumulations on smaller mid-channel islands and bars are the most common type of near-channel alluvium along major tributaries. Composed completely of locally derived volcanic detritus. Thickness of alluvial deposits is generally less than 5 m (16 ft) in smaller upland tributary streams; thickness of alluvial deposits underlying the Silvies River locally ranges between 15 and 90 m (50 and 300 ft). Bedrock units may be locally exposed in the bottoms of stream channels within areas mapped as unit **Qa**. The unit is assigned a Holocene and Late Pleistocene age on the basis of stratigraphic position and a lack of more precise age indicators. Partly equivalent to Qal (valley fill) of Piper and others (1939), Qal (alluvium) and Qs (sedimentary deposits) of Greene (1972), Greene and others (1972), and Walker (1977), Qs/Qal (alluvium and Holocene sedimentary deposits, undifferentiated) of Brown and others (1980a), and Qal (recent alluvium and sedimentary deposits, undivided) of Brown (1982).

Qaf **fan deposits (Holocene and Upper Pleistocene[?])**—Unconsolidated, poorly sorted, poorly graded deposits of boulders, cobbles, pebbles, granules, sand, silt, clay, and woody debris preserved in fan-shaped accumulations at the transition between low-gradient valley floodplains and steeper upland drainages (Plates 1 and 2). Fan surfaces are characterized by anastomosing, intermittent fluvial channels formed where pools or obstructions such as log jams or debris flow levees create flow diversions. Sediment accumulates on the fan surface through normal fluvial deposition, avulsions, and lateral migration as streams emerge from upland settings and the gradient falls below the threshold for further sediment transport. Fans also accumulate during episodic high-discharge events as accumulations of soil, colluvium, large woody debris, or as landslide deposits are remobilized and transported down slope as fast-moving sediment gravity flows (hyperconcentrated floods and debris flows). The unit may locally include rapidly deposited talus from rockfall in steep drainages. Fans typically have a steep gradient at the apex, moderate gradient through the middle section, and low gradient near the toe. Individual fans mapped are as small as 0.005 hectares (0.01 acres) and as large as 57 hectares (143 acres). The local thickness of alluvial fan deposits is variable but is probably <15 m (<50 ft). Fan deposits are considered to be Holocene and Late Pleistocene in age on the basis of stratigraphic position and a lack of more precise age indicators. Partly equivalent to Qal (valley fill) of Piper and others (1939), Qf (alluvial-fan deposits), Qal (alluvium), and Qs (sedimentary deposits) of Greene (1972) and Greene and others (1972), Qf (alluvial-fan deposits) and Qs/Qal (alluvium and Holocene sedimentary

deposits, undifferentiated) of Brown and others (1980a), and units Qf (alluvial fan deposits) and Qal (recent alluvium and sedimentary deposits, undivided) of Brown (1982).

Figure 5-2. Map showing the distribution of alluvium (Qa) and fan delta deposits (Qfd) of the Silvies River. Base map is a 1-m lidar DEM with a stretched minimum-maximum multi-color ramp from 1,268 to 1,254 m (4,160 and 4,113 ft; upper elevation of the fan apex and low elevation in the study area). The DEM is overlain by a lidar-derived hillshade set at 60 percent transparency. White dashed lines are geologic contacts. The horizontal red line in the upper part of the figure is the boundary between the Poison Creek and Burns 7.5' quadrangles. Qma is marsh and alluvial deposits.

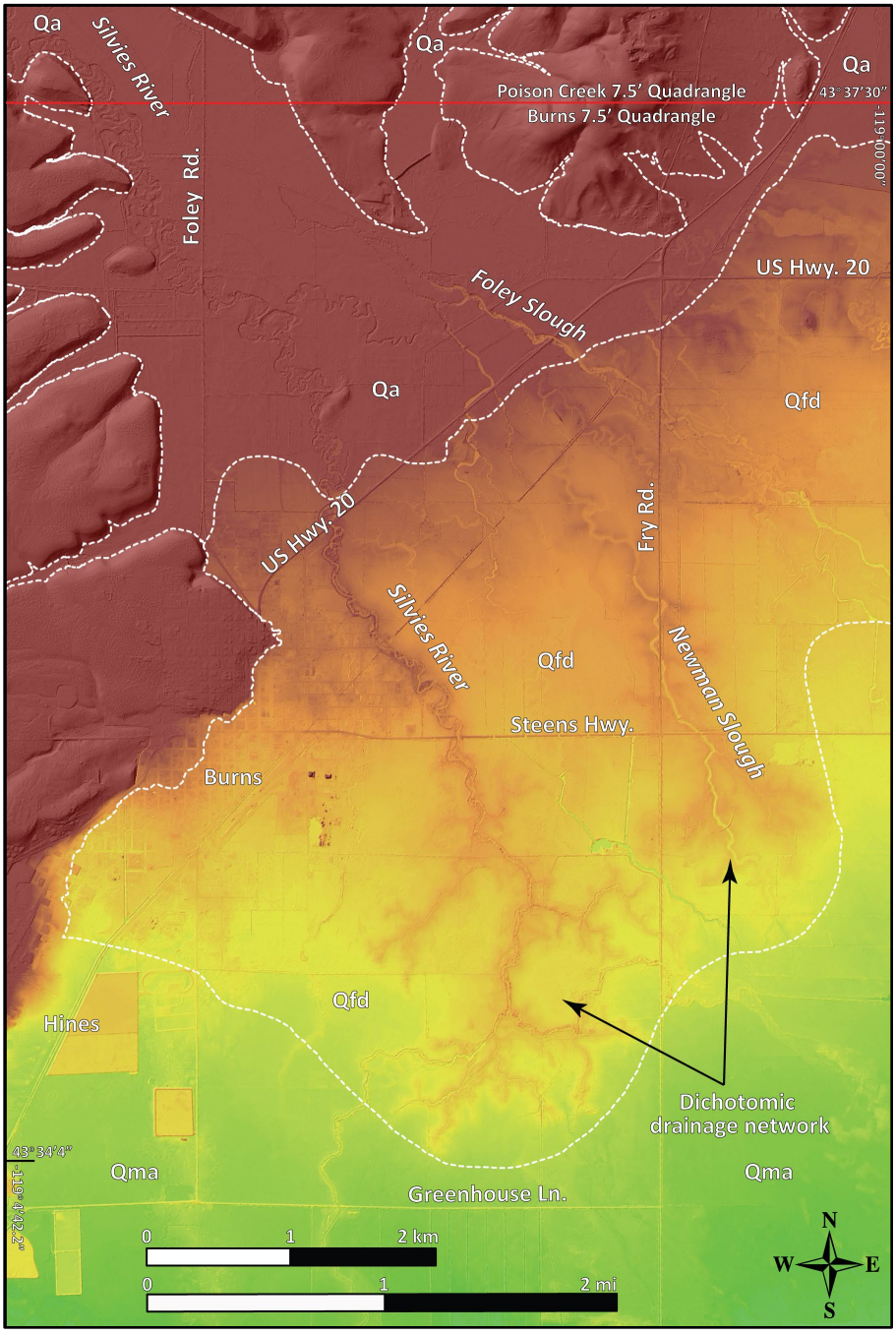

Qls **landslide deposits (Holocene and Upper Pleistocene[?])**—Unconsolidated, chaotically mixed masses of rock and soil deposited by landslides (e.g., slides, debris flows, rock avalanches; Plates 1 and 2). Deposits may consist of individual slide masses or may form large complexes resulting from reactivation of older landslide terrain. Landslide terrain is characterized by sloping hummocky surfaces, closed depressions, springs and wet seeps, and, locally, open ground fissures. Toes to more recent deposits retain convex-up, fan-shaped morphologies. Slides are often traceable uphill to head scarps or failure surfaces. In deeper landslides, these head scarps commonly expose bedrock. The unit locally includes rock fall, large talus piles, shallow-seated landslides of colluvium, rapidly emplaced debris flow deposits, and deeper bedrock slides. Individual slides mapped are as small as 0.007 hectares (0.01 acres) and as large as 19.5 hectares (48 acres). A majority of mapped landslide deposits are simple rotational or shallow-seated earthflow-type features that occur along major drainages, originating on sparsely vegetated, moderately to steep slopes underlain by weakly consolidated rocks (e.g., **Tmst**, **QTst**). Thickness of landslide deposits is highly varied but may be more than several tens of meters in larger deposits. Landslide deposits range in age from Late Pleistocene to those that have been recurrently active in relatively recent time. Large areas mapped as Quaternary landslide deposits typically include many discrete deposits of varying age that have not been differentiated here. Landslide deposits are typically referred to as clay, boulders, rock, or rock and clay in water well logs.

Qc **colluvium (Holocene and Upper Pleistocene[?])**—Unconsolidated and unsorted mixtures of locally derived volcanic and sedimentary rock and soil deposited in rockfall and talus cones beneath steep slopes (Plates 1 and 2). Shown as a separate unit on the map where the deposit completely obscures the underlying bedrock. Thickness of colluvial deposits is highly varied; maximum thickness is several meters. The unit is assigned a Holocene and Late Pleistocene age on the basis of stratigraphic position. Partly equivalent to Qc (colluvium and colluvium blanketed bedrock) of Brown (1982).

Qoaf **older fan deposits (Holocene and Upper Pleistocene[?])**—Unconsolidated to partly cemented, poorly sorted and poorly graded deposits of cobble- and boulder-dominated gravel, sand, and silt principally found in broad aprons fringing upland areas west and south of Burns (Plate 2). Deposits grade down slope from coarse, clay-rich boulder gravels to fine- to medium-grained gravel, sand, and silt. Partial cementing of deposits by caliche ($CaCO_3$) is common. Locally, older alluvial fan deposits are dissected by deeply incised ephemeral, alluvium-filled channels deposited during periods of high-water flow. Toward the hill-front on the west, older fans (**Qoaf**) are onlapped by younger fans (**Qaf**) emanating from modern drainages. On the east, older fans (**Qoaf**) terminate in abrupt step-like toes that are infilled by younger alluvial fan (**Qaf**) and marsh and alluvial deposits (**Qma**). Thickness of older alluvial fan deposits ranges between 18 and 30 m (60 to 100 ft). Older alluvial fans are likely largely Late Pleistocene age on the basis of deeply incised surface channels and stratigraphic position. However, some areas mapped as older alluvial fan deposits are likely to have been active into early Holocene time. Partly equivalent to Qf (alluvial fan deposits) of Brown and others (1980a) and Brown (1982).

Angular unconformity to disconformity

5.3 Upper Cenozoic volcanic and sedimentary rocks

5.3.1 Lower Pleistocene to Upper Miocene sedimentary rocks

QTst **sedimentary rocks (lower Pleistocene[?] to upper Miocene[?])**—Dissected and deeply eroded remnants of semi-consolidated sedimentary deposits exposed as rounded hills above the Rattlesnake Tuff (**Tmtr**) in the southeast corner of the Poison Creek 7.5′ quadrangle, across the northern part of the Burns 7.5′ quadrangle, and in the subsurface of the Harney Valley (**Figure 5-3**: Plates 1 and 2). Discontinuous exposures also lie across the tuff of Wheeler Springs (**Tmtwh**) and trachyandesite flow and vent deposits (**Tmat**, **Tmvt**) west and southwest of the city of Burns (Plate 2). In the Burns area, the unit is chiefly composed of 1) weakly stratified and poorly sorted boulder-cobble gravel containing rhyolite and pumice fragments locally derived from the rhyolite of Burns Butte (**Tmrb**) and the tuff of Wheeler Springs (**Tmtwh**) (see geochemical data in geodatabase and appendix) or 2) white (N9) to yellowish gray (5GY 8/1) and light gray (N7) massive to stratified deposits of pumiceous-tuffaceous claystone, siltstone, sandstone and interlayered air-fall tuff (**Figure 5-3b-c**). The unit as mapped in Burns 7.5′ quadrangle includes a prominent, northeast-trending ridge underlain by semi-consolidated tuffaceous rocks to the north of Burns (Plate 2; **Figure 5-3c**). Previous workers portray this ridge as rhyodacite (Greene, 1972; Greene and others, 1972), rhyolite of Burns Butte (**Tmrb**) (Brown and others, 1980a), or Rattlesnake Tuff (**Tmtr**) (Brown, 1982). In the southeast part of the Poison Creek 7.5′ quadrangle (Plate 1) and northeast part of the Burns 7.5′ quadrangle (Plate 2) **QTst** deposits consist largely of coarse-grained sand and well-sorted conglomerate containing subrounded to rounded welded tuff pebbles and small cobbles (**Figure 5-3d**). Thickness of unit **QTst** is variable in the Poison Creek and Burns 7.5′ quadrangles, ranging between 10 and 45 m (33 and 148 ft). Well log interpretations of the Weed and Poteet and HARN 52747 EOARC wells indicate the unit may be 81 to 104 m thick (265 to 340 ft) beneath the Harney Valley (**Table 2-1**, Plate 2, cross sections A-A′ and B-B′). The unit is used widely as a source of construction aggregate and crushed stone in the map area (Plates 1 and 2; Niewendorp and Geitgey, 2009).

Unit **QTst** is partly equivalent to the Harney Formation of Piper and others (1939), QTtg (terrace gravels) of Greene (1972) and Greene and others (1972), QTg (pediment gravel) and QTs (tuffaceous sedimentary rocks) of Walker (1977), QTsg (Pliocene to Pleistocene[?] tuffaceous sedimentary rocks) of Brown and others (1980a) and Brown (1982). According to Brown and others (1980), rocks equivalent to **QTst** are present in the type section of the Harney Formation at Wright Point (Walker, 1977, 1979; Niem, 1974) ~6.2 km (~3.8 mi) to the southeast of the Burns 7.5′ quadrangle. The unit is assigned a lower Pleistocene (?) to upper Miocene (?) age on the basis of stratigraphic position.

Figure 5-3. Examples of unit QTst sedimentary rocks in the Burns 7.5' quadrangle (Plate 2). (A) Quarry exposure off Switch Canyon Road of poorly sorted boulder-cobble gravel and weakly stratified tuffaceous sandstone. Deposits at this outcrop contain rhyolite and pumice fragments locally derived from the rhyolite of Burns Butte (Tmrb) and the tuff of Wheeler Springs (Tmtwh), respectively (43.56237, −119.10670 WGS84 geographic coordinates; 4837165mN, 338828mE WGS84 UTM Zone 11 coordinates). View is looking north. (B) Thinly bedded tuffaceous, pumice-bearing sandstone exposed along U.S. Highway 20 southwest of Hines (43.68316, −119.00457 WGS84 geographic coordinates; 4837165mN, 338828mE WGS84 UTM Zone 11 coordinates). View is looking east. (C) Well-stratified, pumice-bearing sandstone and siltstone exposed west of Burns (43.68316, −119.00457 WGS84 geographic coordinates; 4837165mN, 338828mE WGS84 UTM Zone 11 coordinates). View is looking north. (D) Weakly consolidated pebble-cobble conglomerate exposed north of Switchback Canyon Road (43.68316, −119.00457 WGS84 geographic coordinates; 4837165mN, 338828mE WGS84 UTM Zone 11 coordinates). Scale bars are 1 m (3.3 ft) and 0.5 m (1.6 ft) high. Photo credits: Carlie J.M. Duda, 2018 and 2019.

5.3.2 Upper Miocene volcanic and sedimentary rocks

Upper Miocene stratigraphy in the map area includes three prominent cliff- and bench-forming ash-flow tuffs (**Tmtd**, **Tmtp**, **Tmtr**), locally separated from one other by less well-exposed tuffaceous sedimentary rocks (**Tmst**) (**Figure 5-4**; Plates 1 and 2). West and northwest of the city of Burns, ash-flow tuffs (**Tmtr**, **Tmtp**) are associated with a bimodal suite of late Miocene (ca. 8.4 to 7.1 Ma) caldera-filling rhyolitic tuffs (**Tmtpi**, **Tmtw**, **Tmtwh**), exogenous rhyolite domes and flows (**Tmrg**, **Tmrb**), and basaltic trachyandesite and trachyandesite flows, dikes, and vent deposits (**Tmat**, **Tmvt**) (**Figure 5-5, Figure 5-6**; Plate 2). XRF geochemical analyses of whole-rock samples were obtained on 168 samples from the Poison Creek, Burns, Burns Butte (outside of present mapping area), and Poison Creek Slough 7.5′ (outside of present mapping area) quadrangles. Representative major- and trace-element data for upper Miocene units are shown in **Table 5-1**, **Figure 5-6**, and **Figure 5-7** (see geochemical data in geodatabase and appendix).

Figure 5-4. Stratigraphic section of tuffaceous sedimentary rocks (Tmst) and interbedded ash-flow tuffs in Devine Canyon in the Poison Creek 7.5' quadrangle (Plate 1). Tmtd is the 9.63/9.74 Ma Devine Canyon Ash-flow Tuff; Tmtp is the 8.41 Ma Prater Creek Ash-flow Tuff; Tmtr is the 7.093 Ma Rattlesnake Tuff. Tuffaceous sedimentary rocks form vegetated shallow slopes. Steeper cliffs are welded ash-flow tuff marker beds. (A) The stratigraphic section shown in A is the type section locality of the Devine Canyon Ash-flow Tuff (Tmtd) designated by Greene (1973) and Walker (1979) (43.70026, −119.01924 WGS84 geographic coordinates; 4840564mN, 337294mE WGS84 UTM Zone 11 coordinates). View is looking west. (B) The stratigraphic section shown in B is the type section locality of the Prater Creek Ash-flow Tuff (Tmtp) designated by Walker (1979) (43.68316, −119.00457 WGS84 geographic coordinates; 4837165mN, 338828mE WGS84 UTM Zone 11 coordinates). View is looking southeast. Photo credit: (A) Jason D. McClaughry, 2018; (B) Robert A. Houston, 2017.

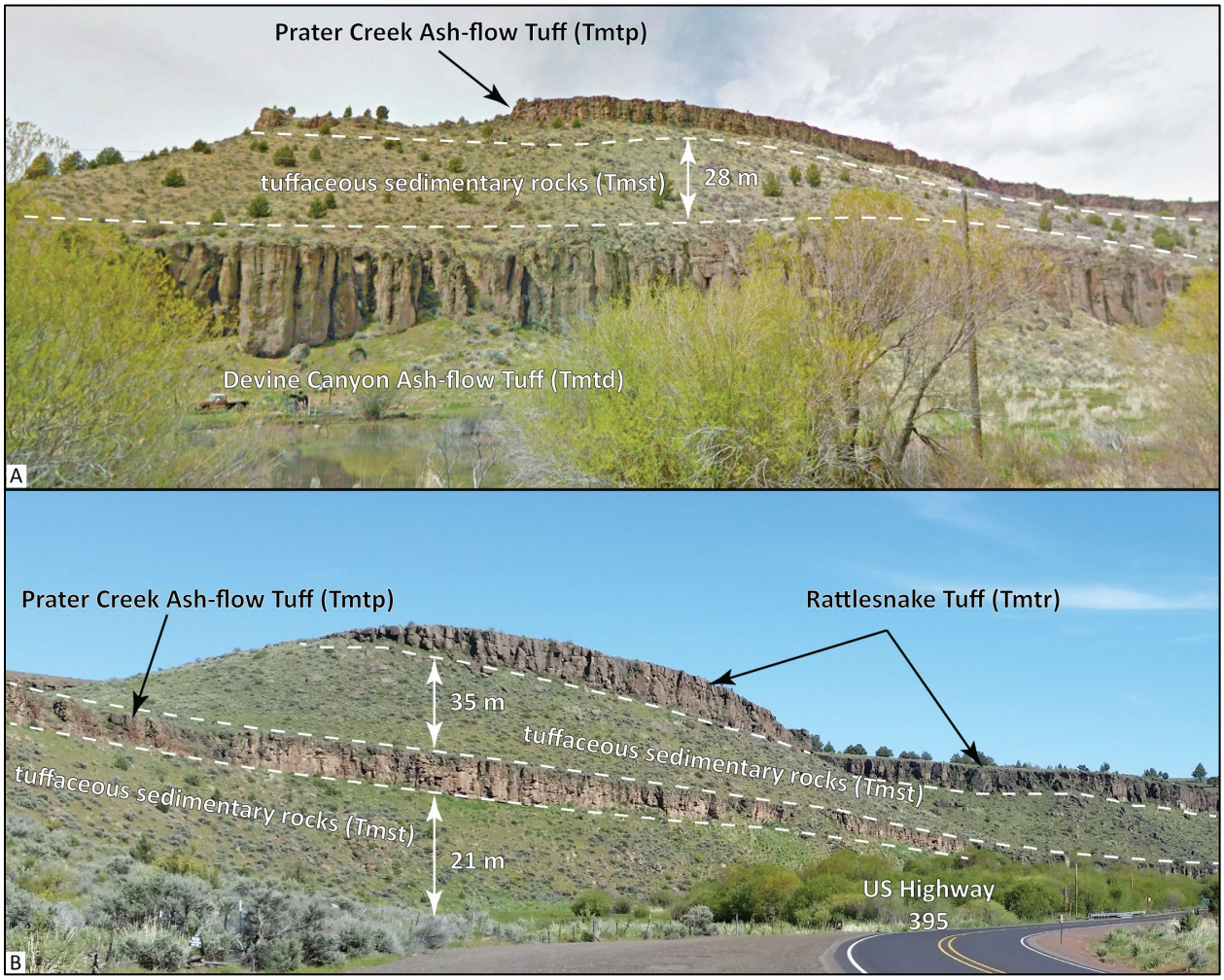

Figure 5-5. Basaltic trachyandesite (Tmat) exposed west of the Silvies River in the Poison Creek 7.5’ quadrangle (Plate 1) (43.66616, –119.11520 WGS84 geographic coordinates; 4836764mN, 329547mE WGS84 UTM Zone 11 coordinates). The section here is marked by a basal unit of Prater Creek Ash-flow Tuff (Tmtp) overlain by a younger basaltic trachyandesite flow (Tmat; middle outcrop) and the capping Rattlesnake Tuff (Tmtr). Sedimentary strata of unit Tmst are absent along the Prater Creek-Rattlesnake contact at this locality. Dashed white lines are geologic contacts. View is looking north. Photo credit: Jason D. McClaughry, 2018.

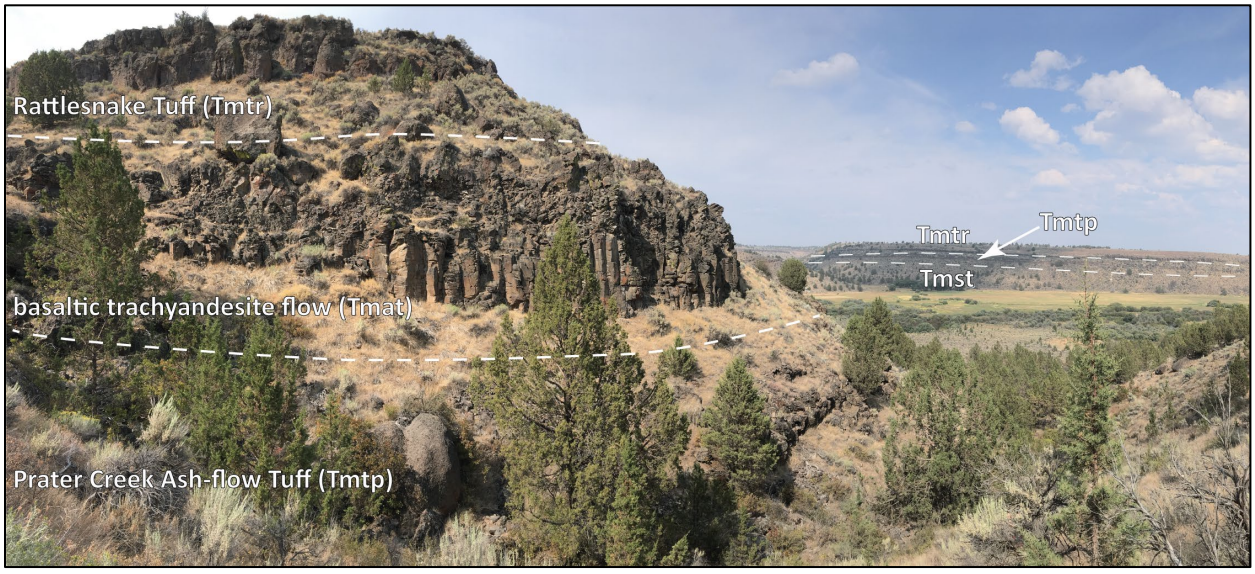

Figure 5-6. Total alkali ($Na_2O + K_2O$) vs. silica (SiO_2) (TAS) classification showing whole-rock XRF analyses on volcanic rocks in the Burns area (normalized to 100 percent anhydrous). Plot include 168 analyses obtained for this study and those compiled from previous studies (MacLean, 1994; Ford, 2012; M. Ferns, unpublished data, 2015; R. Houston, unpublished data, 2016; Houston and others, 2018; Niewendorp and others, 2018). TAS graph fields are from Le Bas and others (1986), Le Maitre and others (1989), and Le Maitre and others (2004). Red-dashed line is the dividing line between alkaline (above), subalkaline/tholeiitic (below) fields after Cox and others (1979).

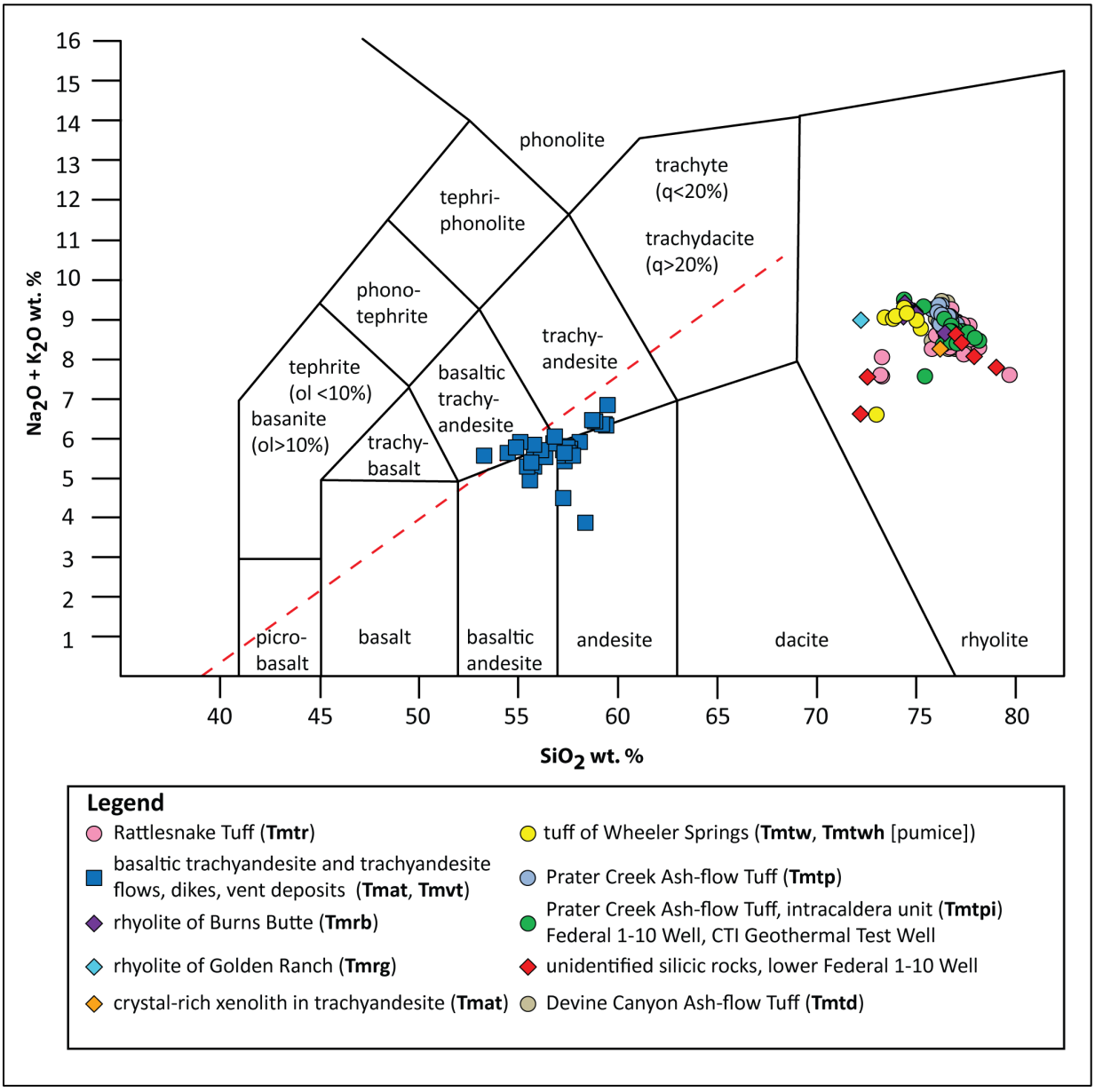

Table 5-1. Representative XRF analyses for late Miocene volcanic rocks sampled from the Poison Creek and Burns 7.5' quadrangles (2 tables).

Sample No.	61 PCBJ 18	HBB18-006	131 BRHC 19	75 BRHC 18	63 PCBJ 18	078 BRHC 18	094a BRHC 19	32 PCBJ 18	68 PCBJ 18	69 PCBJ 18	9 BRHC 18	147 BRHC 19
Geographic Area	Silvies River	Devine Canyon	Burns Butte	Burns Butte	Silvies River	US Hwy 20 at Hines	S. of US Hwy 20	Silvies River	Silvies River	Silvies River	Burns Butte	N. of US Hwy 20
Formation	Rattlesnake Tuff	Rattlesnake Tuff	na	na	na	na	na	na	na	na	na	na
Member	na	na	Silvies River caldera	Silvies River caldera	Silvies River caldera	Silvies River caldera	Silvies River caldera	Silvies River caldera	Silvies River caldera	Silvies River caldera	Silvies River caldera	Silvies River caldera
MAP_UNIT_N	Rattlesnake Tuff	Rattlesnake Tuff	basaltic trachyand. & trachyand. flows	basaltic trachyand. & trachyand. flows	basaltic trachyand. & trachyand. flows	basaltic trachyand. & trachyand. flows	basaltic trachyand. & trachyand. vent	basaltic trachyand. & trachyand. vent	basaltic trachyand. & trachyand. vent	xenolith in basaltic trachyand. vent	rhyolite of Burns Butte	rhyolite of Golden Ranch
MAP_UNIT_L	Tmtr	Tmtr	Tmat	Tmat	Tmat	Tmat	Tmvt	Tmat	Tmvt	Tmvt	Tmrb	Tmrg
UTM_N (NAD 83)	4837118	4843351	4825912	4824524	4836968	4822952	4820622	4834357	4835949	4835955	4827927	4820397
UTM_E (NAD 83)	329293	338203	328604	329260	329467	331750	329992	329693	329622	329591	329070	328273
Age (Ma)	7.093	7.093	nd	nd	nd	nd	nd	nd	nd	nd	7.68	8.03
Map No.	PG24	PG38	BG57	BG43	PG22	BG13	BG5	PG6	PG17	PG18	BG68	BG4
Oxides, weight percent												
SiO_2	76.48	76.77	55.87	56.12	55.46	56.31	55.94	57.51	57.34	76.28	74.93	72.30
Al_2O_3	12.60	12.09	17.25	17.32	17.43	17.35	17.68	16.50	16.48	11.56	13.51	14.44
TiO_2	0.18	0.19	1.07	1.08	1.14	1.08	1.10	1.25	1.25	0.26	0.21	0.37
FeO*	1.68	1.75	7.76	7.87	7.89	7.87	8.05	7.86	8.01	2.77	1.57	2.08
MnO	0.10	0.07	0.14	0.12	0.15	0.13	0.10	0.15	0.16	0.08	0.02	0.05
CaO	0.48	0.46	7.57	7.39	7.87	7.60	7.51	6.99	7.46	0.53	0.52	1.26
MgO	0.12	0.22	4.28	4.08	4.29	3.67	3.20	3.54	3.21	0.14	0.09	0.37
K_2O	4.93	4.33	1.94	1.85	1.80	1.84	1.99	2.07	1.89	4.98	5.06	4.76
Na_2O	3.39	4.08	3.61	3.67	3.45	3.66	3.91	3.62	3.72	3.25	4.08	4.27
P_2O_5	0.03	0.05	0.51	0.49	0.51	0.50	0.52	0.50	0.50	0.14	0.03	0.09
LOI	4.04	1.12	0.55	1.74	0.73	1.34	1.53	0.46	1.10	1.55	0.73	0.50
Total_I	95.37	98.09	98.77	97.87	98.64	98.04	97.91	99.03	98.48	97.80	98.70	98.92
Trace Elements, parts per million												
Ni	5	4	41	34	38	36	32	20	18	3	2	10
Cr	2	5	52	49	55	54	53	31	32	5	2	6
Sc	5	5	21	20	23	19	21	23	23	1	4	4
V	6	13	166	174	178	171	168	190	180	9	7	23
Ba	663	982	1,280	788	791	791	807	913	955	217	595	1,081
Rb	88	85	24	25	22	28	32	30	29	70	115	105
Sr	17	33	561	528	553	528	539	408	405	29	29	101
Zr	300	314	152	153	150	150	157	206	206	513	258	289
Y	93	89	23	23	23	21	23	30	29	72	49	31
Nb	30.0	28.5	8.9	10.0	9.7	8.9	9.3	13.5	13.5	41.3	28.4	16.3
Ga	18	20	18	18	18	18	19	18	18	24	18	16
Cu	4	15	67	80	83	42	72	56	60	9	9	10
Zn	105	102	81	81	84	81	81	86	92	120	33	35
Pb	19	17	8	8	7	6	8	8	7	14	15	12
La	39	44	25	24	26	22	27	26	32	104	43	28
Ce	88	80	50	46	53	48	50	53	58	193	70	47
Th	8	7	2	3	2	2	1	2	2	7	9	10
Nd	46	53	24	25	27	22	25	27	29	83	34	20
U	3	3	2	1	2	2	1	2	1	3	4	5

Major element determinations have been normalized to a 100-percent total on a volatile-free basis and recalculated with total iron expressed as FeO*; nd – no data for radiometric ages, na - not applicable or no information about formation. LOI, Loss on Ignition; Total_I, original analytical total.

Table 5-1, continued. Representative XRF analyses for late Miocene volcanic rocks sampled from the Poison Creek and Burns 7.5' quadrangles.

Sample No.	**45b BRHC 18**	**66 BRHC 18**	**69 BRHC 18**	**64 PCBJ 18**	**HBB18-005**	**HARN 50087 670-680**	**HARN 50087 720-810**	**HARN 50087 1200-1300**	**HARN 50087 1560-1600**	**HARN 50087 1900-1940**	**HBH008-17**	**125 PCBJ 18**	**131 PCBJ 18**
Geographic Area	W. of Hines	Burns Butte	Burns Butte	Silvies River	Devine Canyon	Hines	Hines	Hines	Hines	Hines	Devine Canyon	Devils Garden	Devils Garden
Formation	na	na	na	na	na	na	na	na	na	na	na	na	na
Member	Silvies River caldera	Silvies River caldera	Silvies River caldera	Silvies River caldera	Silvies River caldera	Silvies River caldera	Silvies River caldera	Silvies River caldera	Silvies River caldera	Silvies River caldera	Silvies River caldera	Silvies River caldera	Silvies River caldera
MAP_UNIT_N	tuff of Wheeler Springs (pumice)	tuff of Wheeler Springs	tuff of Wheeler Springs	Prater Creek Ash-flow Tuff	Prater Creek Ash-flow Tuff	Prater Creek Ash-flow Tuff, intracalder a unit	Prater Creek Ash-flow Tuff, intracalder a unit	Prater Creek Ash-flow Tuff, intracalder a unit	Prater Creek Ash-flow Tuff, intracalder a unit	Prater Creek Ash-flow Tuff, intracalder a unit	Devine Canyon Ash-flow Tuff	Devine Canyon Ash-flow Tuff	Devine Canyon Ash-flow Tuff
MAP_UNIT_L	Tmtwh	Tmtw	Tmtw	Tmtp	Tmtp	Tmtpi	Tmtpi	Tmtpi	Tmtpi	Tmtpi	Tmtd	Tmtd	Tmtd
UTM_N (NAD 83)	4825250	4824828	4824842	4836978	4843201	4824014	4824014	4824014	4824014	4824014	4843108	4845246	4846121
UTM_E (NAD 83)	330429	328547	328426	329500	338547	331853	331853	331853	331853	331853	338654	331068	328940
Age (Ma)	nd	nd	nd	8.41	8.41	nd	nd	nd	nd	nd	9.63/9.74	9.63/9.74	9.63/9.74
Map No.	BG52	BG46	BG47	PG23	PG36	BG26	BG27	BG33	BG38	BG41	PG35	PG40	PG45
Oxides, weight percent													
SiO_2	73.04	74.00	74.54	76.78	76.64	76.47	75.37	76.85	76.72	76.78	76.63	76.36	77.01
Al_2O_3	14.83	13.97	13.66	11.88	11.85	12.27	12.40	11.64	11.92	11.18	11.61	11.75	11.48
TiO_2	0.26	0.22	0.21	0.14	0.15	0.12	0.14	0.12	0.13	0.15	0.26	0.25	0.21
FeO*	1.95	1.81	1.61	1.91	2.21	1.77	2.05	2.19	2.11	3.12	2.65	2.80	2.73
MnO	0.05	0.06	0.05	0.03	0.02	0.03	0.05	0.11	0.05	0.08	0.09	0.07	0.10
CaO	1.24	0.68	0.62	0.14	0.11	0.25	0.42	0.28	0.37	0.20	0.35	0.16	0.14
MgO	2.03	0.16	0.14	0.02	0.15	0.10	0.14	0.07	0.04	0.09	0.16	0.05	0.06
K_2O	4.71	4.97	5.11	4.65	4.59	4.95	5.09	4.70	4.55	4.63	4.47	4.74	4.63
Na_2O	1.84	4.06	4.01	4.35	4.26	4.01	4.20	3.97	4.11	3.74	3.76	3.79	3.60
P_2O_5	0.05	0.07	0.04	0.09	0.02	0.02	0.15	0.05	0.01	0.02	0.03	0.03	0.04
LOI	9.19	0.68	0.69	0.00	0.94	1.22	1.34	0.93	3.42	1.43	1.41	0.59	1.10
Total_I	90.32	98.78	98.94	99.56	98.66	98.48	98.37	98.71	96.17	98.29	97.57	99.03	98.53
Trace Elements, parts per million													
Ni	7	8	5	3	4	4	5	10	4	5	7	2	3
Cr	4	4	2	3	5	3	5	19	5	14	7	3	3
Sc	5	5	4	1	2	0	0	2	1	0	2	2	1
V	14	10	6	3	9	8	10	4	1	8	9	10	10
Ba	510	641	618	60	62	228	212	177	194	64	210	139	208
Rb	90	114	115	105	101	109	121	109	112	104	74	84	100
Sr	76	35	31	13	10	46	17	16	12	19	27	15	26
Zr	261	284	281	505	514	501	530	442	497	576	604	699	880
Y	48	68	60	55	72	65	80	65	73	75	77	69	23
Nb	26.2	27.2	27.4	45.2	44.1	42.8	44.0	39.4	41.1	38.2	46.3	52.3	62.4
Ga	18	19	18	23	21	22	23	21	21	22	25	27	27
Cu	13	8	8	4	7	7	9	16	13	17	7	4	7
Zn	39	29	47	79	105	95	118	107	103	122	128	125	131
Pb	16	11	19	21	18	35	18	38	24	24	16	17	22
La	39	45	45	63	56	58	61	53	56	58	95	105	39
Ce	65	93	79	127	100	92	116	107	110	127	177	201	156
Th	9	10	11	9	8	9	9	8	9	8	8	7	10
Nd	29	41	38	41	52	37	54	49	52	53	85	89	31
U	3	2	4	4	3	4	3	2	3	1	3	3	2

Major element determinations have been normalized to a 100-percent total on a volatile-free basis and recalculated with total iron expressed as FeO*; nd – no data for radiometric ages, na - not applicable or no information about formation. LOI, Loss on Ignition; Total_I, original analytical total.

Figure 5-7. Chemical variation diagram (zirconium versus niobium) showing geochemical groupings for late Miocene volcanic rocks in the Burns area. Plot include 168 analyses obtained for this study and those compiled from previous studies (MacLean, 1994; Ford, 2012; M. Ferns, unpublished data, 2015; R. Houston, unpublished data, 2016; Houston and others, 2018; Niewendorp and others, 2018).

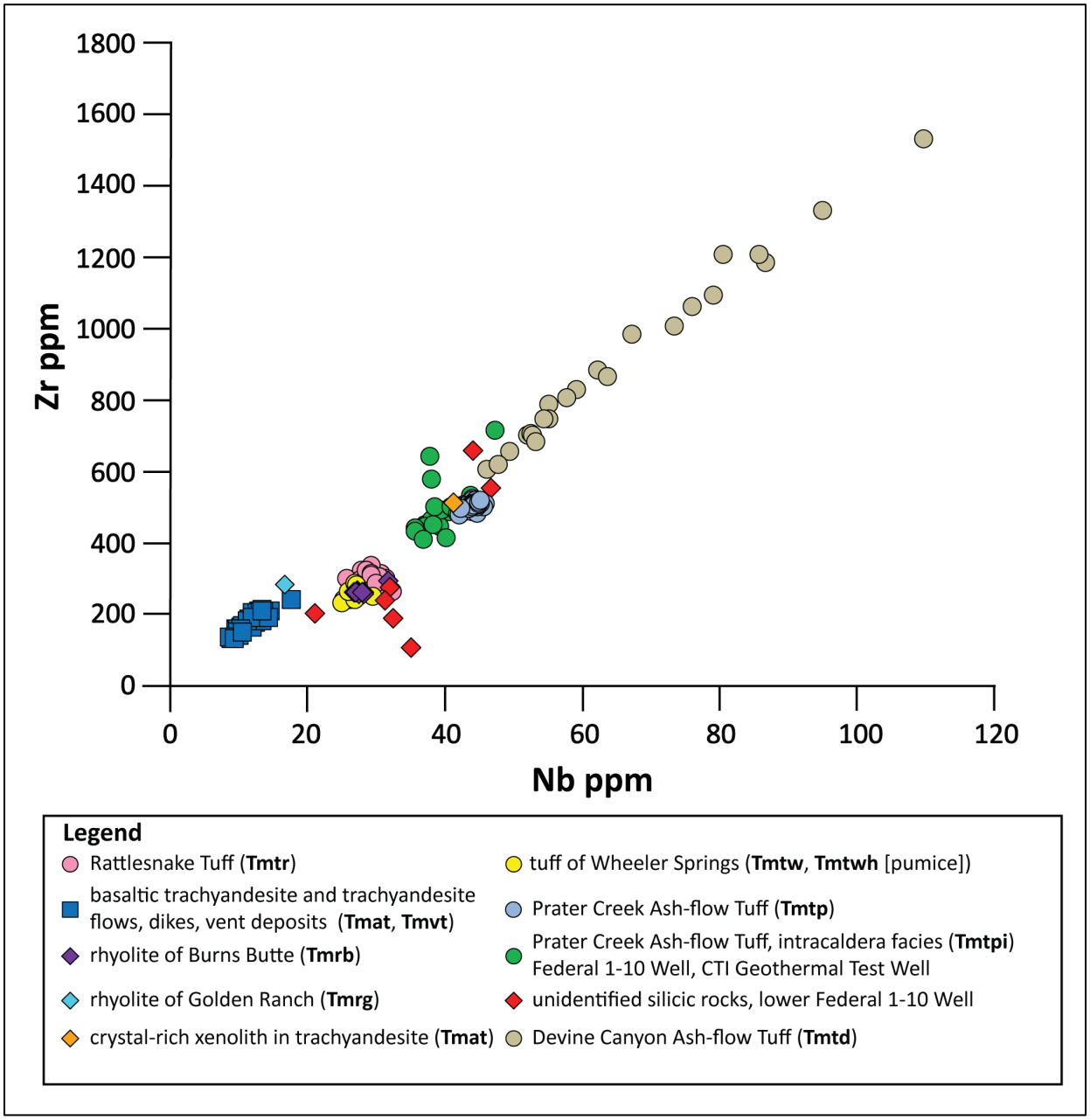

Tmtr **Rattlesnake Tuff (upper Miocene)**—Vitric, phenocryst-poor, pumice- and lithic-rich tuff capping a southern-dipping section of ash-flow tuff and interbedded tuffaceous sedimentary rocks (**Tmst**) between the northern boundary of the Poison Creek 7.5′ quadrangle (Plate 1) and the city of Burns (Plate 2). Over much of the map area, the unit forms distinctive outcrop cliffs and rimrock that can be easily traced in 1-m lidar DEMs and air photographs (**Figure 5-4**, **Figure 5-5**, **Figure 5-8**). The tuff extends into the subsurface below the Harney Valley in the eastern part of the Burns 7.5′ quadrangle (Plate 2); the tuff is interpreted to be present in the 131 to 152 m (430 to 500 ft) depth interval of the Weed and Poteet #1 well and is encountered in the 154 to 169 m (505 to 555 ft) depth interval of the HARN 52747 EOARC well (**Table 2-1**). Erosional remnants of the Rattlesnake Tuff (**Tmtr**) are also present in the southwest corner of the Burns 7.5′ quadrangle (Plate 2), overlying the older rhyolite of Golden Ranch (**Tmrg**) and tuff of Wheeler Springs (**Tmtwh**) (**Figure 5-1**). The type section of the Rattlesnake Tuff (**Tmtr**) is located along U.S. Highway 395 on the boundary of the Poison Creek and Devine Ridge South 7.5′ quadrangles (**Figure 5-9**; Plate 1; 43.659404, −118.998954 WGS84 geographic coordinates; Streck and Grunder, 1995).

Throughout much of the Poison Creek 7.5′ quadrangle the Rattlesnake Tuff (**Tmtr**) directly overlies the Prater Creek Ash-flow Tuff (**Tmtp**) (Plate 1; **Figure 5-4b, Figure 5-8**). South and west of the Silvies River in the Poison Creek 7.5′ quadrangle, the Rattlesnake Tuff (**Tmtr**) is separated from the Prater Creek Ash-flow Tuff (**Tmtp**) by a section of tuffaceous sedimentary rocks (**Tmst**) and basaltic trachyandesite to trachyandesite lavas (**Tmat**) and vent deposits (**Tmvt**) (**Figure 5-5**). East of the Silvies River and south of Fenwick Canyon and the intersection of Poison Creek and Devine Canyon, tuffaceous sedimentary rocks (**Tmst**) are present along the Rattlesnake-Prater contact; trachyandesite lavas are largely not present east and north of the Silvies River (Plate 1).

The Rattlesnake Tuff (**Tmtr**) in the map area occurs as a single cooling unit, displaying both vertical and lateral variations in welding and crystallization facies; not all facies are present at all localities. Welding facies of the Rattlesnake Tuff (**Tmtr**) in the map area are consistent with those defined by Streck (1994) and Streck and Grunder (1995) including 1) a 2 to 4 m thick (6.6 to 13 ft) basal strongly welded tuff (vitrophyre), 2) partially welded tuff with fiamme, and 3) partially welded tuff with pumice (**Figure 5-9**, **Figure 5-10, Figure 5-11a-c**). Partially welded tuff contains devitrified, moderately to completely flattened black, white, and banded fiamme up to 10 cm (3.9 in) in diameter (**Figure 5-11c**). Poly-compositional lithics consist of angular, moderate reddish brown (10R 4/6) fragments as much as 1 cm (0.5 in) in length that are supported in a devitrified glass shard and crystal groundmass.

The thickest sections of the Rattlesnake Tuff exposed in the central and southern parts of the Poison Creek 7.5′ quadrangle (Plate 1) and northern part of the Burns 7.5′ quadrangle (Plate 2) are associated with a thick basal zone of lithophysae, a crystallization facies overprinting pervasively devitrified, partially welded tuff (**Figure 5-8a**, **Figure 5-10b, Figure 5-11d**). Individual lithophysae are 1 to 3 cm (0.4 to 1.1 in) across, with the concentration of lithophysae increasing upsection. At the type section along U.S. Highway 395, a >19 m (>62 ft) thick zone of pervasively devitrified lithophysae lies near the base of the unit, directly overlying a <2 m (<6.5 ft) thick partially welded to strongly welded vitric tuff (vitrophyre) and associated non-welded, laminated basal surge deposits (**Figure 5-9**). The lithophysal zone grades upward to hackly jointed, massively bedded partially welded vitric tuff with a eutaxitic texture defined by aligned fiamme.

Zones defined by partially welded tuff with fiamme and partially welded tuff with pumice form rugged, prominent cliffs and ridge caps typically weathering to tightly packed boulder- to pebble-

sized, platy, angular fragments (**Figure 5-4**, **Figure 5-8**). Adjacent talus slopes are often mantled by toppled meter-scale boulders. Lithophysal horizons also form prominent bench and cliff features. However, unlike partially welded zones, these rocks weather to angular, cobble to sand-sized fragments with occasional meter-sized blocks spalled from more extensive outcrops (**Figure 5-10b**).

The Rattlesnake Tuff attains a maximum thickness of 40 m (130 ft) in the southern half of the Poison Creek 7.5′ quadrangle (Plate 1), thinning to the northwest, where the rock has largely been eroded away, exposing rock of underlying units (**Tmtp**, **Tmst**, **Tmtd**). Scattered remnants in the northwestern corner of the Poison Creek 7.5′ quadrangle have a maximum thickness of 14 m (46 ft). South into the Burns 7.5′ quadrangle (Plate 2), Rattlesnake Tuff (**Tmtr**) exposed at the surface and present in the subsurface ranges between 12 and 21 m thick (40 and 70 ft).

Typical hand samples of the Rattlesnake Tuff (**Tmtr**) are very pale orange (10YR 8/2), to very light gray (N7), to medium gray (N5), and light brownish gray (5YR 6/1), containing < 3 percent quartz, subhedral to euhedral, zoned anorthoclase and anhedral to euhedral clinopyroxene (ferrohedenbergite) microphenocrysts and phenocrysts < 2 mm (< 0.01 in) distributed within a vitric groundmass (**Figure 5-11a-d**). The tuff is petrographically characterized by ~2 percent quartz and feldspar phenocrysts, ~1 percent ferrohedenbergite phenocrysts, ~15 percent lithic fragments, ~15 percent pumice, and 55 percent devitrified glass-shard groundmass (**Figure 5-11e-f**). The original vitroclastic texture of the tuff is retained but is locally overprinted by very fine elongated crystals forming axiolitic structures. Samples obtained from this unit in the map area have a high-silica rhyolitic composition with 75.84 to 78.18 weight percent SiO_2, 11.77 to 12.73 weight percent Al_2O_3, 1.37 to 2.20 weight percent FeO* 2.99 to 4.08 weight percent Na_2O, and 4.33 to 5.38 weight percent K_2O. The tuff also contains 238 to 319 ppm Zr, 25.4 to 30.4 ppm Nb, 88 to 97 ppm Y, 75 to 90 ppm Ce, and 35 to 44 ppm La (**Figure 5-6**, **Figure 5-7**, **Table 5-1**).

The Rattlesnake Tuff has a reversed magnetic polarity (Parker, 1974; Thormahlen, 1984; Smith, 1986a,b; Streck, 1994) and is assigned a late Miocene age on the basis of stratigraphic position and an $^{40}Ar/^{39}Ar$ age of 7.093 ± 0.015 Ma (Streck and Grunder, 1995; Jordan and others, 2004). An older, less precise K/Ar age of 6.82 ± 0.33 Ma was reported for the Rattlesnake Tuff (**Tmtr**) by Greene (1973) in the southwest corner of the Poison Creek 7.5' quadrangle (Plate 1). The unit is equivalent to the Rattlesnake Ash-flow Tuff formally described by Walker (1979) and later renamed to Rattlesnake Tuff by Streck and Grunder (1995) (**Figure 5-6**). The Rattlesnake Tuff has an estimated eruptive volume of 280 km^3 (67 mi^3) occurring as a thick deposit that originally covered > 35,000 km^2 (> 13,500 mi^2) (Streck and Grunder, 1995). Although no caldera source related to the tuff is exposed, from pumice size and distance correlations, Streck (1994) proposed a vent located at Capehart Lake in the western part of the Harney Basin (**Figure 2-3**).

Figure 5-8. Stratigraphic section of Prater Creek Ash-flow Tuff (Tmtp) and Rattlesnake Tuff (Tmtr) exposed in Fenwick Canyon in the central part of the Poison Creek 7.5' quadrangle (Plate 1). (A) View looking northwest into the mouth of Fenwick Canyon (43.66718, −119.06048 WGS84 geographic coordinates; 4836972mN, 333877mE WGS84 UTM Zone 11 coordinates). (B) View looking west in the base of Fenwick Canyon (43.67394, −119.06794 WGS84 geographic coordinates; 4836764mN, 329547mE WGS84 UTM Zone 11 coordinates). Photo credit: (A-B) Jason D. McClaughry, 2018.

Figure 5-9. Type locality of the Rattlesnake Tuff (Tmtr) located ~16 km (~10 mi) north of Burns along the west side of U.S. Highway 395. An outcrop photograph and a line drawing of zonal variations in the exposure of Rattlesnake Tuff (Tmtr) are shown side by side (figure modified after Streck and others [1999], Streck and Ferns [2004], and Niewendorp and others [2018]). Scale bar in upper photograph is 1 m (3.3 ft) high; scale bar in lower photograph is 22 m (72.2 ft) high. Both photographs taken from U.S. Highway 395 looking west-southwest. (43.65940, −118.99895 WGS84 geographic coordinates; 4835986mN, 338820mE WGS84 UTM Zone 11 coordinates). Photo credit: Clark A. Niewendorp, 2017.

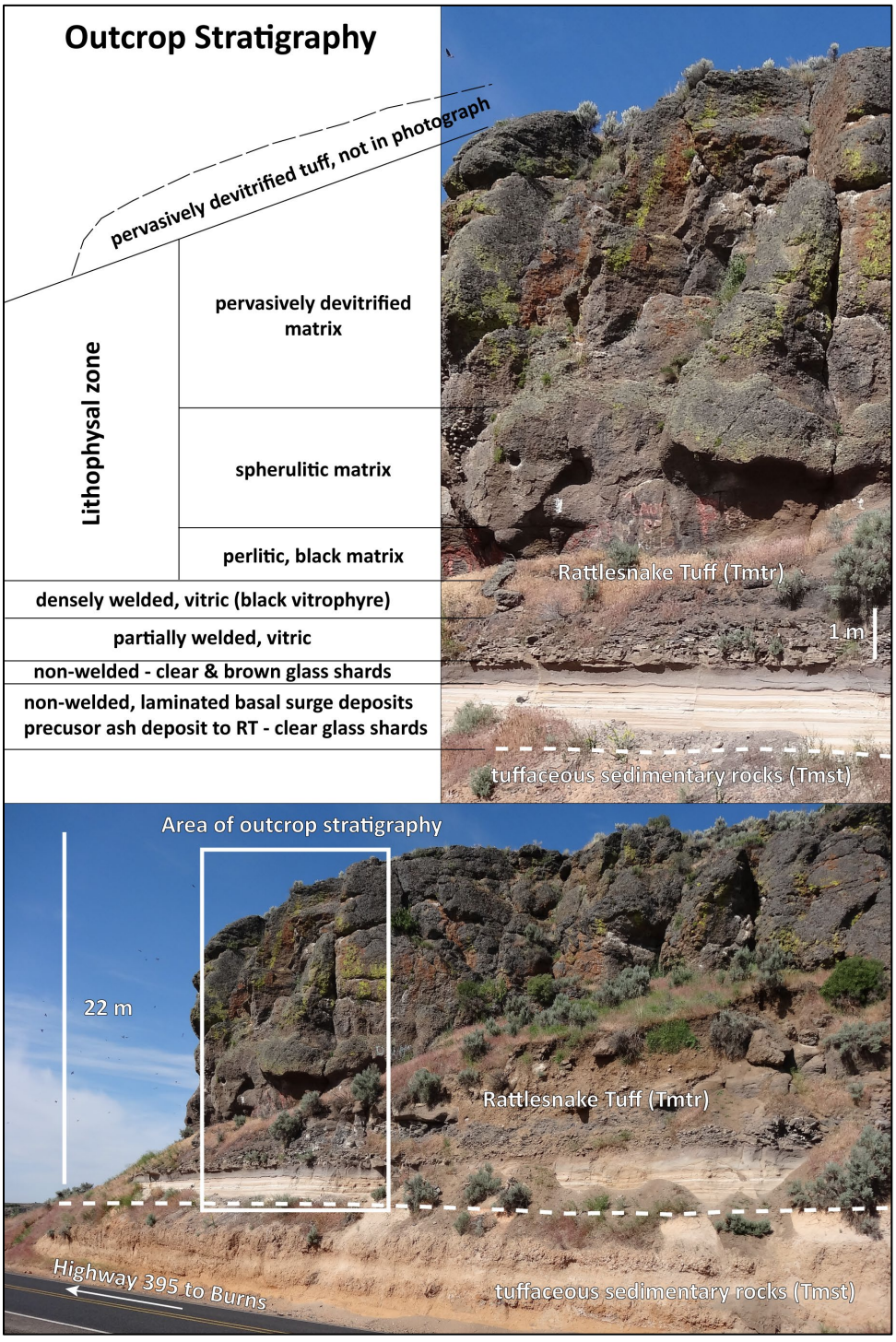

Figure 5-10. Examples of Rattlesnake Tuff (Tmtr) outcrops. (A) Platy, tabular jointed partially welded tuff (43.64325, −119.10931 WGS84 geographic coordinates; 4834413mN, 329875mE WGS84 UTM Zone 11 coordinates). View is looking north. (B) Massive, lithophysal tuff (43.66684, −119.11826 WGS84 geographic coordinates; 4837050mN, 329220mE WGS84 UTM Zone 11 coordinates). View is looking northeast. Person for scale in both photographs is 1.6 m tall (62 in); scale bar is 1 m (3.3 ft) high. Photo credit: (A-B) Jason D. McClaughry, 2018.

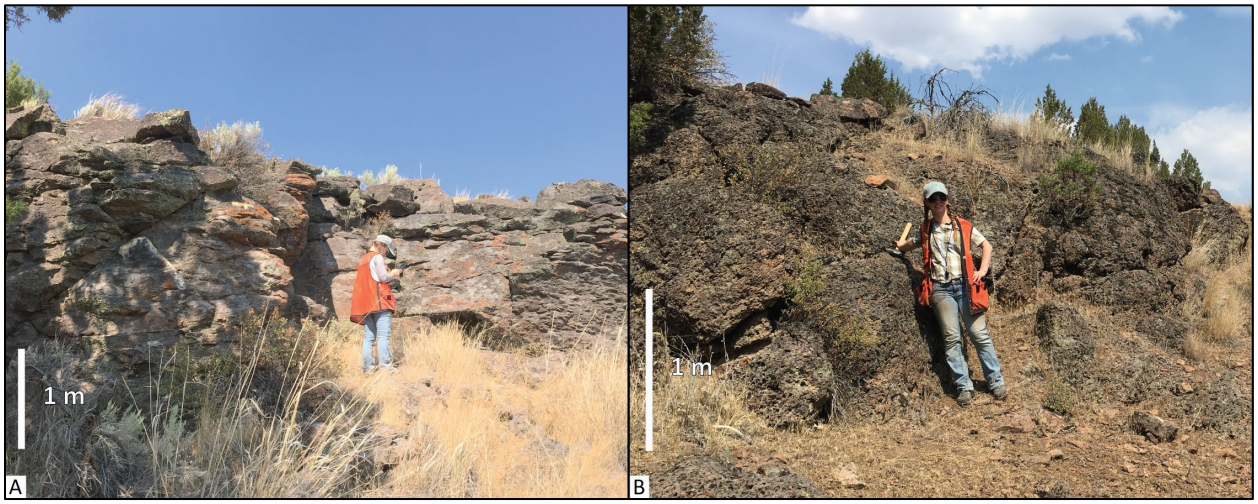

Figure 5-11. Hand sample and thin-section photographs showing textural variations in the Rattlesnake Tuff (Tmtr). (A) Partially welded tuff with pumice (sample 85 PCBJ 18). (B) Partially welded tuff with fiamme (sample 89 PCBJ 18). (C) Partially welded tuff with banded pumice and fiamme (sample 61 PCBJ 18). (D) Lithophysal tuff (sample 58 PCBJ 18). (E) Photomicrograph of a mafic lithic fragment surrounded by glass shards displaying compaction foliation under cross-polarized light. Scale bar is 1 mm (0.04 in) in length (sample HAH0170-16). (F) Same view as (E), under plane-polarized light. Abbreviations: af - alkali feldspar, qtz - quartz, Lithic Frag. - lithic fragment. Photo credit: (A-D) Jason D. McClaughry, 2018; (E-F) Robert A. Houston, 2017.

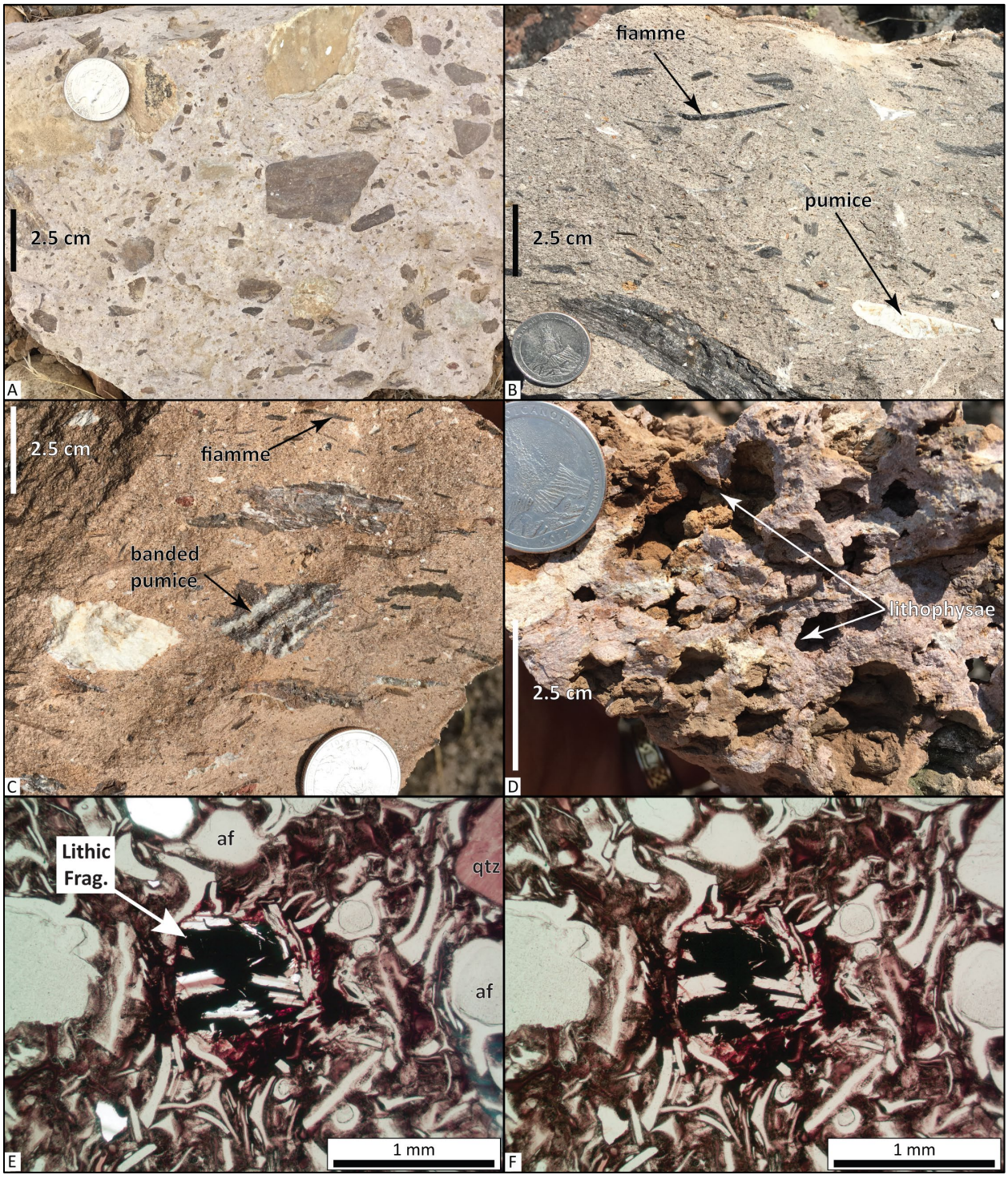

Tmat **basaltic trachyandesite and trachyandesite flows and dikes (upper Miocene)**—Dense non-vesicular to vesicular, aphyric basaltic trachyandesite and trachyandesite lava flows and dikes exposed in the southwest corner of the Poison Creek 7.5′ quadrangle (Plate 1) and the western edge of the Burns 7.5′ quadrangle (Plate 2). The unit consists of 1- to 10-m-thick (3.3 to 33 ft) grayish black (N2) dense and commonly distinctly flow-banded lava flows with rubbly, highly vesiculated flow tops and interbedded moderate red (5R 4/6) to black (N1) scoriaceous ʻAʻā flow-foot breccia (**Figure 5-12**). Dense, non-vesicular lavas form distinctive bench and cliff outcrops, typically characterized by blocky, platy, or hackly jointing (**Figure 5-5**, **Figure 5-13**). Well-defined columnar jointing is present at the base of at least one flow in the area west of the Silvies River in the Poison Creek 7.5′ quadrangle (**Figure 5-5**; Plate 1). Flows exposed in the Poison Creek 7.5′ quadrangle (Plate 1) contain sporadic small boulder-sized, subrounded xenoliths of white, coarse-grained, and crystal-rich rhyolite (**Figure 5-14**). The lavas commonly weather to platy slabs and irregular blocks, forming extensive talus slopes beneath cliff-forming outcrops. Composite thickness of flow units may locally be up to 70 m (230 ft). The unit is a source of construction aggregate in the map area, hosting several quarry sites (e.g., Fivemile Quarry, **Figure 5-13**; Plate 1; Niewendorp and Geitgey, 2009).

The unit includes several flow sequences erupted from different vent complexes, but they are not mapped separately here due to similar appearing lithology and narrow chemical ranges (**Figure 5-6**, **Figure 5-7**, **Table 5-1**). Typical basaltic trachyandesite or trachyandesite hand samples are commonly streaked or mottled, medium bluish gray (5B 5/1), light bluish gray (5B 7/1), dusky blue (5PB 3/2), or very light gray (N8) and aphyric to very sparsely microporphyritic with blocky plagioclase and pyroxene microphenocrysts <1 mm (< 0.04 in) across contained within a fine-grained crystalline groundmass of trachytic plagioclase microlites. Lithologic variations may be dense and non-vesicular to highly vesicular, commonly showing flow banding defined by elongation of groundmass plagioclase and microvesicles (**Figure 5-15a-b**). **Tmat** flows have a range of petrographic textures including 1) 63 PCBJ 18: fine-grained aphyric basaltic trachyandesite with < 1 percent euhedral to subhedral, blocky prismatic plagioclase microphenocrysts < 1 mm distributed within an equigranular holocrystalline groundmass of plagioclase, intergranular pyroxene, and < 1 percent (vol.) opaque oxides (**Figure 5-15c-d**), and 2) 32 PCBJ 18: very fine grained aphyric trachyandesite flows with abundant trachytic plagioclase contained within a hypocrystalline to hypohyaline groundmass. Blocky prismatic euhedral to anhedral plagioclase and clinopyroxene microphenocrysts larger than the groundmass, but <0.1 mm (0.004 in) are scattered through the rock (1 to 2 percent vol.) (**Figure 5-15e-f**). Samples obtained from the unit in the map area have a basaltic trachyandesite or trachyandesite chemical composition with 53.29 to 59.51 weight percent SiO_2, 16.32 to 18.73 weight percent Al_2O_3, 0.97 to 1.36 weight percent TiO_2, 6.66 to 8.83 weight percent FeO*, 2.41 to 4.25 weight percent Na_2O, 1.16 to 2.55 weight percent K_2O, 18 to 41 ppm Ni, 10 to 64 ppm Cr, 351 to 573 ppm Sr, 127 to 237 ppm Zr, and 9.1 to 17.8 ppm Nb (**Figure 5-6**, **Figure 5-7**, **Table 5-1**).

Tmat flows have reversed magnetic polarity and are assigned a late Miocene age on the basis of stratigraphic position above the 8.41 Ma Prater Creek Ash-flow Tuff (**Tmtp**) and below the 7.1 Ma Rattlesnake Tuff (**Tmtr**) (Plate 1). Brown (1982) reported a K/Ar age of 8.6 ± 0.3 Ma from this unit east of Burns Butte (Brown's Taw unit), but the reported age is considered too old on the basis of stratigraphic position and more precise ages obtained on adjacent units. **Tmat** flows dated by Brown (1982) lie stratigraphically above and infill erosional topography formed on the 7.68 Ma rhyolite of Burns Butte (**Tmrb**; $^{40}Ar/^{39}Ar$; Jordan and others, 2004), west of the city of Burns.

Along U.S. Highway 20, in the southwestern part of the Burns 7.5′ quadrangle flows (**Tmat**) and vent deposits (**Tmvt**) overlie the 8.03 Ma rhyolite of Golden Ranch (**Tmrg**; K/Ar; Fiebelkorn and others, 1982, 1983; Plate 2).

Basaltic trachyandesite or trachyandesite flows in the map area were erupted from still extant cinder- and dike-capped vents forming high ground between Mud Ridge (Burns Butte 7.5′ quadrangle) and the Silvies River (Poison Creek 7.5′ quadrangle, Plate 1) and a narrow belt of volcanoes forming high buttes between Burns Butte proper and U.S. Highway 20 in the southwest corner of the Burns 7.5′ quadrangle (Plate 2). Partly equivalent to Qbh (late basalt) and Th (Harney Formation) of Piper and others (1939), Ta (andesite) and QTmv (mafic vent complexes) of Greene (1972) and Greene and others (1972), Tob (olivine basalt) and Tmv (mafic vent rocks) of Walker (1977), Tma (andesites) and QTmv (Upper Pliocene mafic vent complexes) of Brown and others (1980a), and units Tmar (basaltic andesites of Rimrock Springs) and Taw (basaltic andesites of Willow Creek) of Brown (1982).

Figure 5-12. Basaltic trachyandesite flow (Tmat) exposed north of Switch Canyon Road in the Burns 7.5′ quadrangle (Plate 2). (A) The flow here consists of a grayish black (N2) dense lava flow core intercalated with moderate red (5R 4/6) to black (N1) scoriaceous ‘A‘ā flow-foot breccia (43.56671, −119.11857 WGS84 geographic coordinates; 4825930mN, 328912mE, WGS84 UTM Zone 11 coordinates). The letter B marks the location of photograph B. Arrow points to person in orange vest for scale. View is looking north. (B) Close-up photograph of outcrop of dense lava in shown in A (43.56708, −119.11822 WGS84 geographic coordinates; 4825971mN, 328941mE, WGS84 UTM Zone 11 coordinates). View is looking northeast. Scale bar is 1 m (3.3 ft) high. Photo credit: (A-B) Carlie J.M. Duda, 2018.

Figure 5-13. Trachyandesite flows (Tmat) exposed west of the Five Mile Quarry along the Silvies River in the Poison Creek 7.5' quadrangle (Plate 1) (43.65543, −119.09981 WGS84 geographic coordinates; 4835746mN, 330676mE WGS84 UTM Zone 11 coordinates). Tmst is tuffaceous sedimentary rocks. View is looking east. Photo credit: Jason D. McClaughry, 2018.

Figure 5-14. Rhyolite xenolith contained within a trachyandesite lava flow (Tmat) in the southwest part of the Poison Creek 7.5’ quadrangle (Plate 1) (43.65058, −119.12474 WGS84 geographic coordinates; 4835259mN, 328648mE WGS84 UTM Zone 11 coordinates). View is looking northeast. Scale bar is 0.5 m (1.6 ft) high. Photo credit: Jason D. McClaughry, 2018.

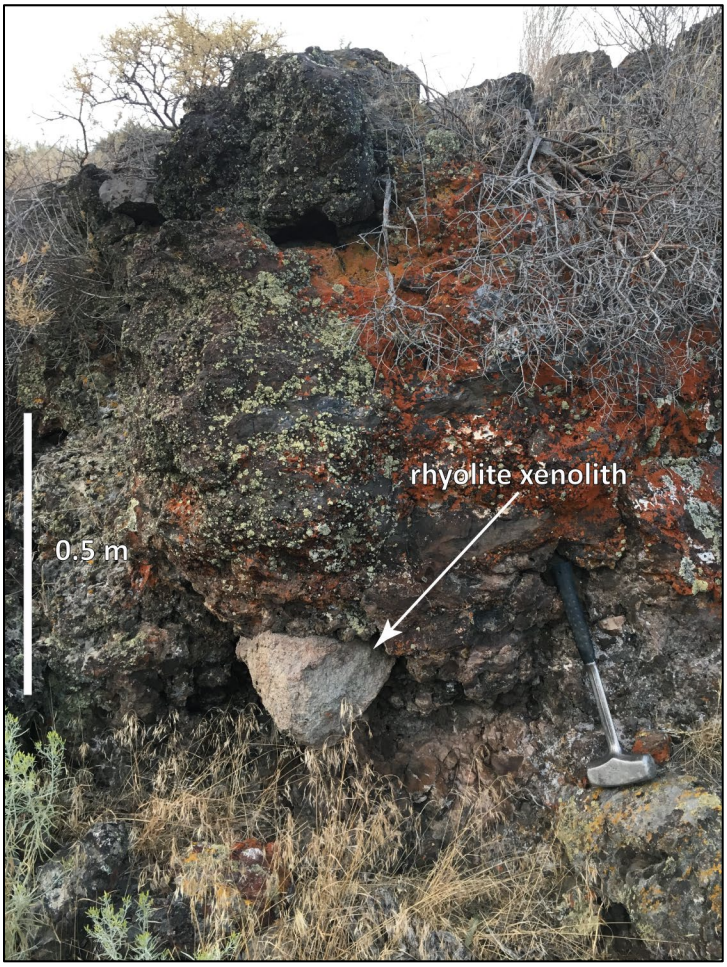

Figure 5-15. Hand sample and thin-section photographs showing textural variations in basaltic trachyandesite and trachyandesite lava flows (Tmat). (A) Hand sample of basaltic trachyandesite (Tmat) from the outcrop shown in Figure 5-5 (sample 63 PCBJ 18). (B) Hand sample of trachyandesite (Tmat) exposed beneath the Rattlesnake Tuff (Tmtr) northwest of Arntz Reservoir in the southwest part of the Poison Creek 7.5’ quadrangle (Plate 1) (sample 32 PCBJ 18). (C) Photomicrograph of sample 63 PCBJ 18 under cross-polarized light. Scale bar is 1 mm (0.04 in) in length. (D) Same view as (C), under plane-polarized light. (E) Photomicrograph of sample 32 PCBJ 18 under cross-polarized light. Scale bar is 1 mm (0.04 in) in length. (F) Same view as (E), under plane-polarized light. Abbreviations: p- plagioclase feldspar, px – pyroxene. Photo credit: (A-F) Jason D. McClaughry, 2018.

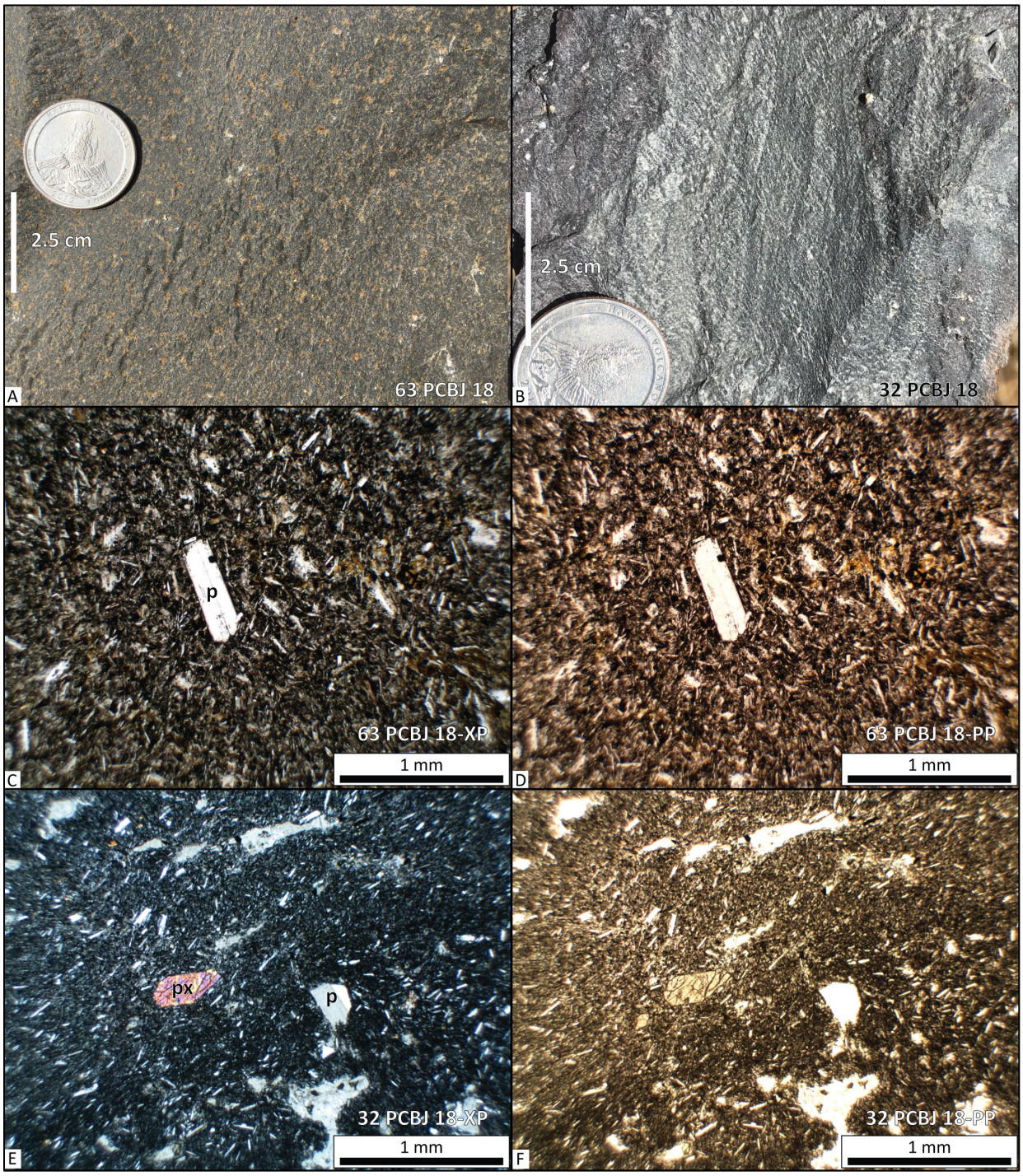

Tmvt **basaltic trachyandesite and trachyandesite vent deposits (upper Miocene)**—Weakly consolidated scoria, cinders, and palagonitic tuffs forming small shield volcanoes west of the Silvies River in the Poison Creek 7.5′ quadrangle and immediately west and southwest of Burns in the Burns 7.5′ quadrangle (**Figure 5-16**; Plates 1 and 2). Cinder deposits are moderate reddish brown (10R 4/6) to grayish black (N2) and typically massive to moderately bedded, containing numerous fluidal volcanic bombs (**Figure 5-17a-d**). Small low-lying mound-forming vents south of U.S. Highway 20 in the Burns 7.5′ quadrangle incorporate numerous thin flows and discontinuous ribbons of lava < 1 m (< 3.3 ft) thick. In the southwest part of the Poison Creek 7.5′ quadrangle, grayish red (10R 4/2) cinders forming a **Tmvt** vent contain 5 to 10 percent conspicuous xenoliths and feathered bands of grayish black (N2), rhyolitic crystal-rich rheomorphic tuff (**Figure 5-18a-d**). These xenoliths range in size from 2 mm (0.08 in) up to several meters across (**Figure 5-18b-c**). Typical xenolith hand samples contain 35 to 50 percent clear, euhedral to anhedral, prismatic sanidine crystals up to 8 mm (0.3 in) contained within a fresh grayish black (N2) glassy groundmass (**Figure 5-18d**). Petrographically, xenoliths contain 35 to 50 percent broken clear, euhedral to anhedral, prismatic sanidine up to 8 mm (0.3 in), < 2 percent subhedral clinopyroxene up to 0.5 mm (0.02 in), <1 percent anhedral resorbed quartz < 0.5 mm (0.02), 2 percent deformed pumice fiamme, and 1 to 2 percent andesite lithic fragments up to 0.5 mm (0.02 in) contained within a groundmass of contorted and folded cuspate glass shards. Perthitic textures are common in alkali feldspars (**Figure 5-19**). A xenolith sample obtained from the vent in the Poison Creek 7.5′ quadrangle (Plate 1) has a rhyolitic chemical composition with 76.28 weight percent SiO_2, 11.56 weight percent Al_2O_3, 2.76 weight percent FeO*, 3.25 weight percent Na_2O, and 4.98 weight percent K_2O. The rhyolite also contains 512 ppm Zr, 41.3 ppm Nb, 71 ppm Y, 103 ppm La, and 193 ppm Ce (**Figure 5-6**, **Figure 5-7**, **Table 5-1**). Chemical composition of the xenolith is similar to chemical analyses obtained from the underlying Prater Creek Ash-flow Tuff (**Tmtp**) (**Figure 5-6**, **Figure 5-7**, **Table 5-1**).

Cinder and scoria samples obtained from the **Tmvt** outcrops in the Poison Creek and Burns 7.5′ quadrangles (Plates 1 and 2) have a basaltic trachyandesite or trachyandesite chemical composition similar to flows of unit **Tmat** with 55.62 to 57.33 weight percent SiO_2, 16.47 to 18.12 weight percent Al_2O_3, 1.11 to 1.25 weight percent TiO_2, 7.93 to 8.37 weight percent FeO*, 2.84 to 3.72 weight percent Na_2O, 1.40 to 1.88 weight percent K_2O, 17 to 34 ppm Ni, 32 to 50 ppm Cr, 405 to 600 ppm Sr, 152 to 206 ppm Zr, and 9.7 to 13.5 ppm Nb (**Figure 5-6**, **Figure 5-7**, **Table 5-1**).

Tmvt vent deposits are assigned a late Miocene age on the basis of stratigraphic association with unit **Tmat**. A significant component of unconsolidated cinders has been eroded and reworked as an important clast component in younger sedimentary rocks of unit **QTst.** Extensively mined as an aggregate resource in the Burns 7.5′ quadrangle (**Figure 5-17a-c**; Plate 2). Partly equivalent to Qbh (late basalt) and Th (Harney Formation) of Piper and others (1939), QTmv (mafic vent complexes) of Greene (1972) and Greene and others (1972), Tob (olivine basalt) and Tmv (mafic vent rocks) of Walker (1977), QTmv (Upper Pliocene Mafic vent complexes) of Brown and others (1980a), and Tav (basaltic andesite vent complexes) of Brown (1982).

Figure 5-16. View looking south across Switch Canyon Road toward shield-forming basaltic trachyandesite flows, dikes, and vent deposits (Tmat, Tmvt). Sedimentary rocks of unit QTst underlie the area in the middle ground. (43.57029, −119.11814 WGS84 geographic coordinates; 4826325mN, 328956mE WGS84 UTM Zone 11 coordinates). Car for scale in the left-center part of the photograph. Photo credit: Carlie J.M. Duda, 2018.

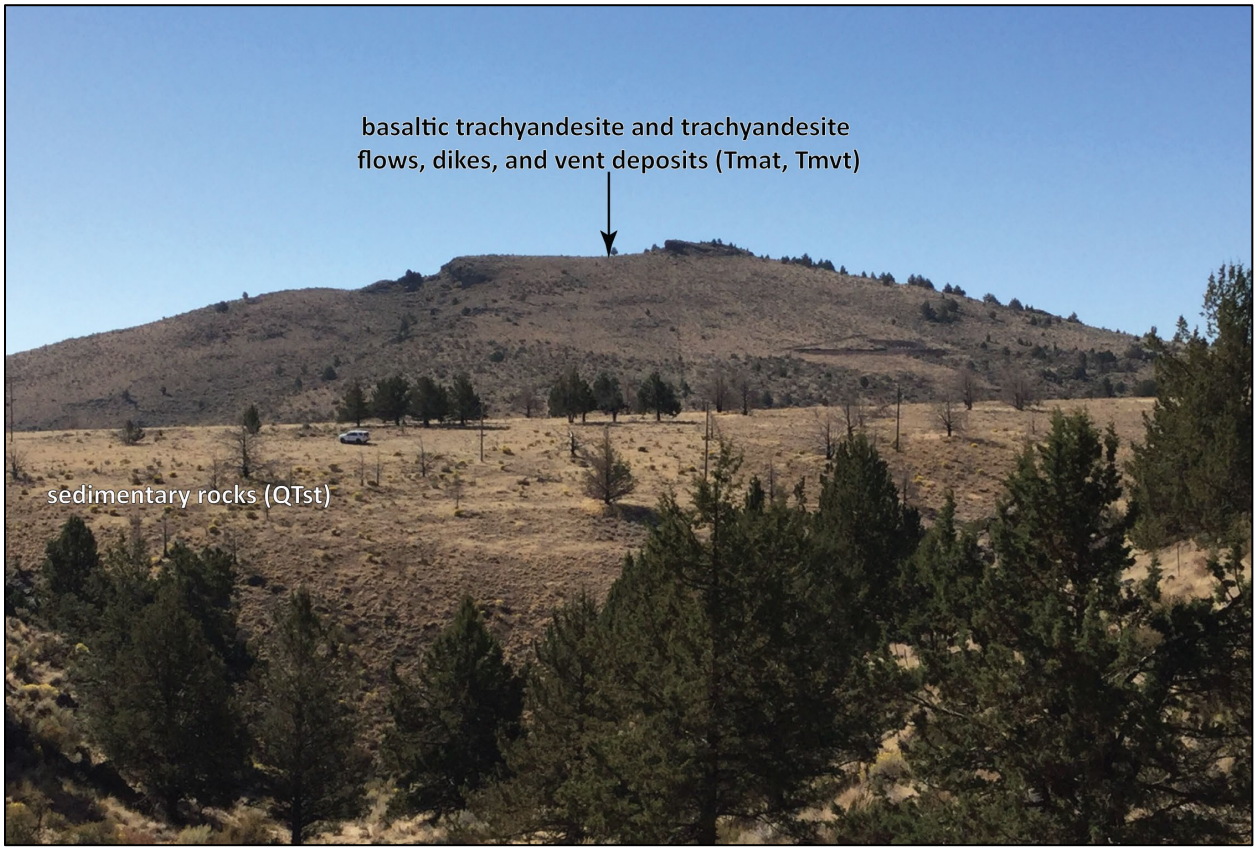

Figure 5-17. Basaltic trachyandesite and trachyandesite vent deposits (Tmvt). (A) Moderate reddish brown (10R 4/6) cinder deposits exposed in a quarry west of Hines in the Burns 7.5' quadrangle (Plate 2) (43.56032, −119.11007 WGS84 geographic coordinates; 4825204mN, 329581mE WGS84 UTM Zone 11 coordinates). View is looking east. (B) Meter-scale lava bomb exposed on the slopes above the outcrop in A (43.56063, −119.11082 WGS84 geographic coordinates; 329520mE, 4825238mN WGS84 UTM Zone 11 coordinates). (C) Grayish black (N2), moderately bedded cinders exposed in a quarry west of Hines in the Burns 7.5' quadrangle (Plate 2) (43.55980, −119.10578 WGS84 geographic coordinates; 329924mE, 4825135mN WGS84 UTM Zone 11 coordinates). View is looking east. (D) Quarry face in C contains numerous fluidal ribbon bombs. Photo credit: (A-D) Carlie J.M. Duda, 2018.

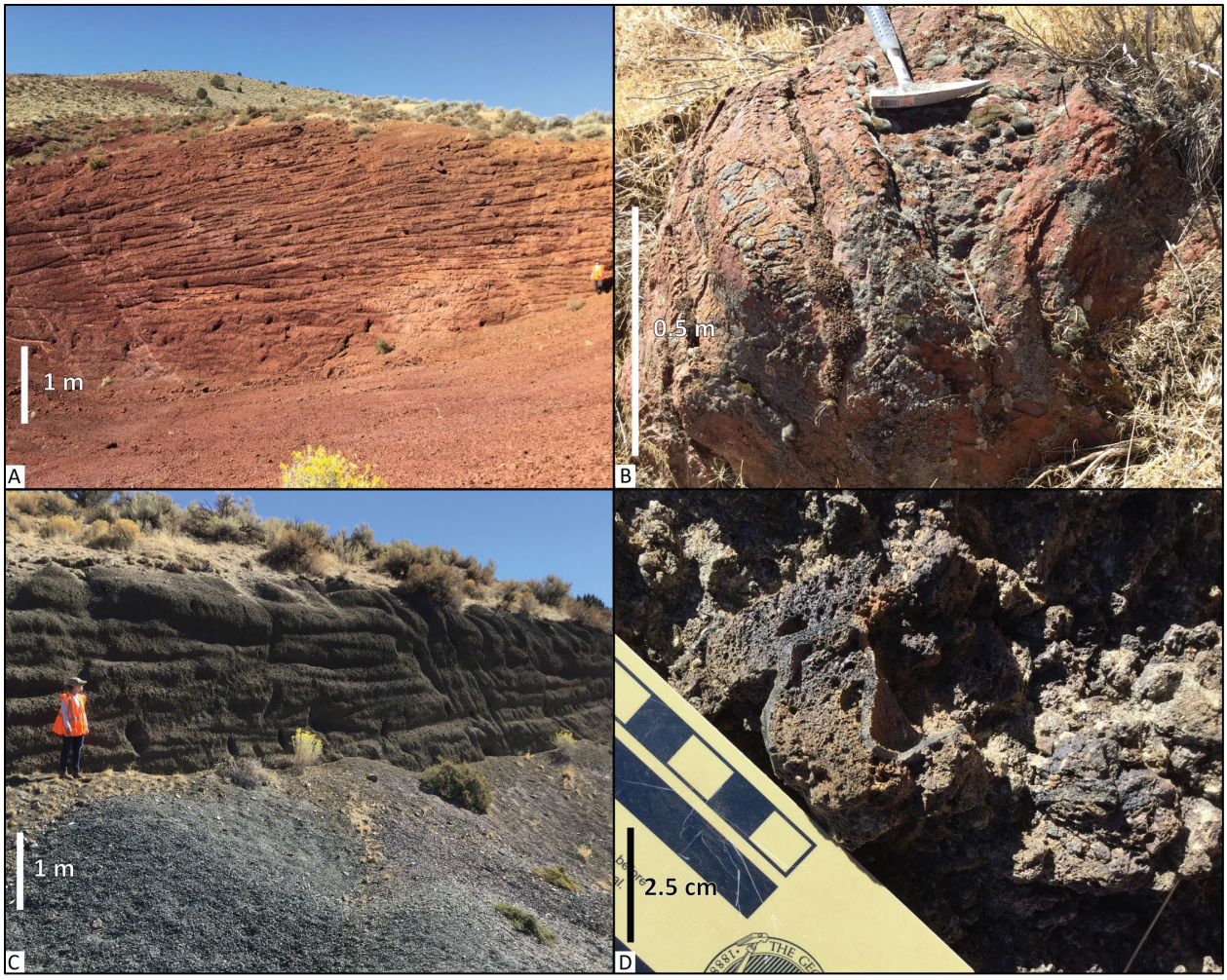

Figure 5-18. Basaltic trachyandesite vent (Tmvt).(A) Grayish red (10R 4/2) cinders forming a vent complex (Tmvt) in the southwestern part of the Poison Creek 7.5' quadrangle (Plate 1) (43.65698, −119.11332 WGS84 geographic coordinates; 329589mE, 4835955mN WGS84 UTM Zone 11 coordinates). View is looking east. (B, C) Cinders here contain 5 to 10 percent xenoliths up to 1 m (3.3 ft) across and feathered, cm-scale bands of grayish black (N2), rhyolitic crystal-rich rheomorphic tuff. (D) Xenoliths contain 35 to 50 percent clear, euhedral to anhedral, prismatic sanidine crystals up to 8 mm (0.3 in) contained within a fresh grayish black (N2) glassy groundmass. Photo credit: Jason D. McClaughry, 2018.

Figure 5-19. Thin section photographs of the crystal-rich mega xenolith shown in Figure 5-18b-d. (A) Photomicrograph of sample 69 PCBJ 18 under cross-polarized light. (B) Same view as (A), under plane-polarized light. Scale bar is 1 mm (0.04 in) in length. Abbreviations: af – alkali feldspar, qtz – quartz, px – pyroxene. Photo credit: (A-B) Jason D. McClaughry, 2019.

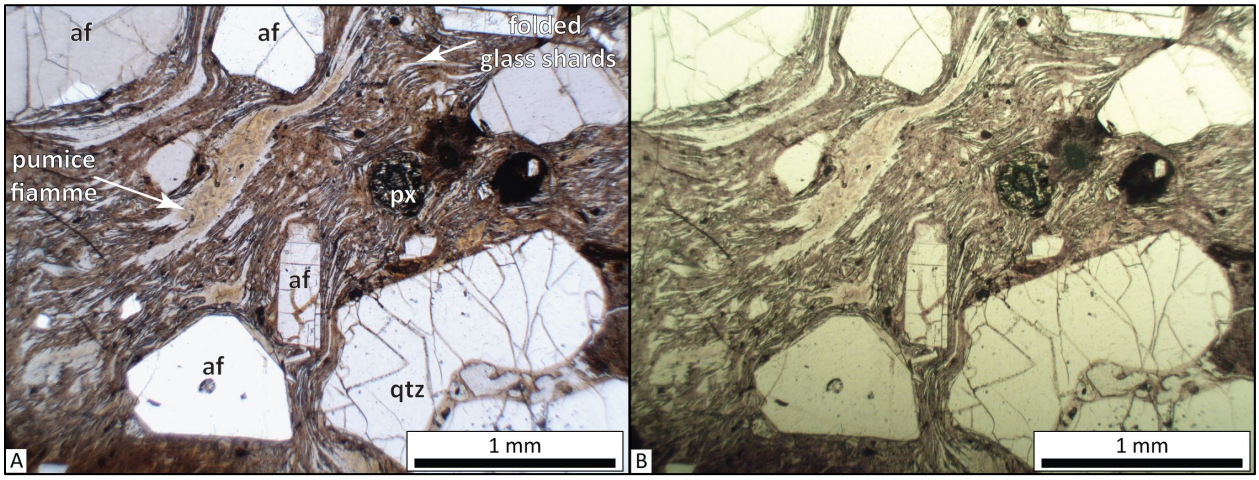

Tmrb **rhyolite of Burns Butte (upper Miocene)** — Flow banded, strongly flow-foliated aphyric rhyolite exposed in high hills due west of the city of Burns in the Burns 7.5′ quadrangle (Plate 2). The unit extends west into the Burns Butte 7.5′ quadrangle, where these rocks form Burns Butte. Rhyolite occurs in prominent outcrops up to 100 m (328 ft) high where incised by deep canyons (**Figure 5-20a**). Outcrops typically are characterized by distinct flow banding and horizontal to subvertical and vertical flow foliation with complex recumbent flow folds up to 20 m (66 ft) high (**Figure 5-20b**). The upper parts of flows are marked by faintly banded black (N9) to greenish black (5G 2/1) obsidian flow tops (Brown, 1982). Flow breccia, containing poorly sorted, faintly banded black (N9) to greenish black (5G 2/1) obsidian fragments, is present in a number of outcrops and may be related to carapace, basal, marginal, and internal autobrecciation (**Figure 5-20c**).

Typical hand samples of the rhyolite are medium light gray (N6) to light brownish gray (5YR 6/1) and medium bluish gray and aphyric with a very fine-grained cryptocrystalline groundmass. Hand sample textures range from strongly planar to contorted flow banded, sugary-textured rhyolite, to devitrified obsidian, or brecciated rhyolite (**Figure 5-21a-d**). The rhyolite is petrographically aphyric to very sparsely microporphyritic with < 1 percent subhedral, blocky to prismatic alkali feldspar, clinopyroxene/orthopyroxene, and quartz microphenocrysts up to 0.5 mm (0.02 in) contained within a cryptocrystalline, felty, and mottled groundmass of feldspar, pyroxene, and magnetite (**Figure 5-21e-f**). Plagioclase and pyroxene microphenocrysts occur as single crystals or in small clusters. Resorbed quartz grains up to 4.5 mm (0.2 in) are also present. Flow banding is apparent in thin section, defined by the trachytic alignment of plagioclase microlites alternating with bands of cryptocrystalline quartz. Samples obtained from this unit in the map area have a high-silica rhyolitic composition with 74.34 to 74.98 weight percent SiO_2, 13.39 to 13.61 weight percent Al_2O_3, 1.51 to 1.85 weight percent FeO*, 4.06 to 4.34 weight percent Na_2O, and 4.97 to 5.09 weight percent K_2O. The rhyolite also contains 255 to 293 ppm Zr, 26.8 to 31.8 ppm Nb, 31 to 54 ppm Y, 54 to 81 ppm Ce, and 32 to 54 ppm La (**Figure 5-6**, **Figure 5-7**, **Table 5-1**). Chemical composition of the rhyolite of Burns Butte (**Tmrb**) is indistinguishable from

analyses obtained from the underlying tuff of Wheeler Springs (**Tmtw**, **Tmtwh**) (**Figure 5-6**, **Figure 5-7**, **Table 5-1**).

The rhyolite of Burns Butte (**Tmrb**) has normal magnetic polarity and is assigned a late Miocene age on the basis of stratigraphic position above the 8.41 Ma Prater Creek Ash-flow Tuff (**Tmtp**) and below the 7.093 Ma Rattlesnake Tuff (**Tmtr**) (Plate 2). The unit intrudes and directly overlies the tuff of Wheeler Springs (**Tmtw**, **Tmtwh**). Jordan and others (2004) reported an $^{40}Ar/^{39}Ar$ age of 7.68 ± 0.04 Ma for a sample of the rhyolite (**Tmrb**) obtained on Burns Butte. Brown (1982) interpreted the rhyolite of Burns Butte to be older than the rhyolite of Golden Ranch (**Tmrg**) on the basis of outcrop relationships in the Burns Butte 7.5′ quadrangle. Green and others (1972) reported a K/Ar age of 7.82 ± 0.26 Ma for the rhyolite of Golden Ranch (**Tmrg**) (recalculated to 8.03 ± 0.26 Ma by Fiebelkorn and others, 1982, 1983). No outcrops exposing the relationship between the two units are known in the present map area.

The rhyolite of Burns Butte occurs as exogenous domes and flows erupted from vents forming high ground at Burns Butte (Burns Butte 7.5′ quadrangle). The unit is interpreted as a rhyolite dome complex situated along the eastern margin of the Silvies River caldera (Plate 2; **Figure 2-3**). Partly equivalent to Td (Danforth Formation) of Piper and others (1939), Tr (rhyodacite) of Greene (1972) and Greene and others (1972), Tvs (silicic vent rocks) of Walker (1977), Tmrb (rhyodacite of Burns Butte) of Brown and others (1980a), and Tmrb (rhyolite of Burns Butte) of Brown (1982).

Figure 5-20. Rhyolite of Burns Butte (Tmrb) exposed west of the city of Burns in the Burns 7.5' quadrangle (Plate 2). (A) Prominent outcrops, typically up to tens of meters high, are characterized by horizontal to subvertical and vertical flow foliation (43.57142, −119.11905 WGS84 geographic coordinates; 4826455mN, 328886mE WGS84 UTM Zone 11 coordinates). White arrow points to person for scale. View is looking northeast. (B) Complex isoclinal recumbent flow folds in rhyolite (43.57019, −119.11584 WGS84 geographic coordinates; 4826311mN, 329145mE WGS84 UTM Zone 11 coordinates). View is looking north. (C) Autobreccia with banded obsidian clasts (43.58299, −119.11784 WGS84 geographic coordinates; 4827734mN, 329015mE WGS84 UTM Zone 11 coordinates). Scale bars in B and C are 1 m (3.3 ft) tall. Photo credit: (A-C) Carlie J.M. Duda, 2018.

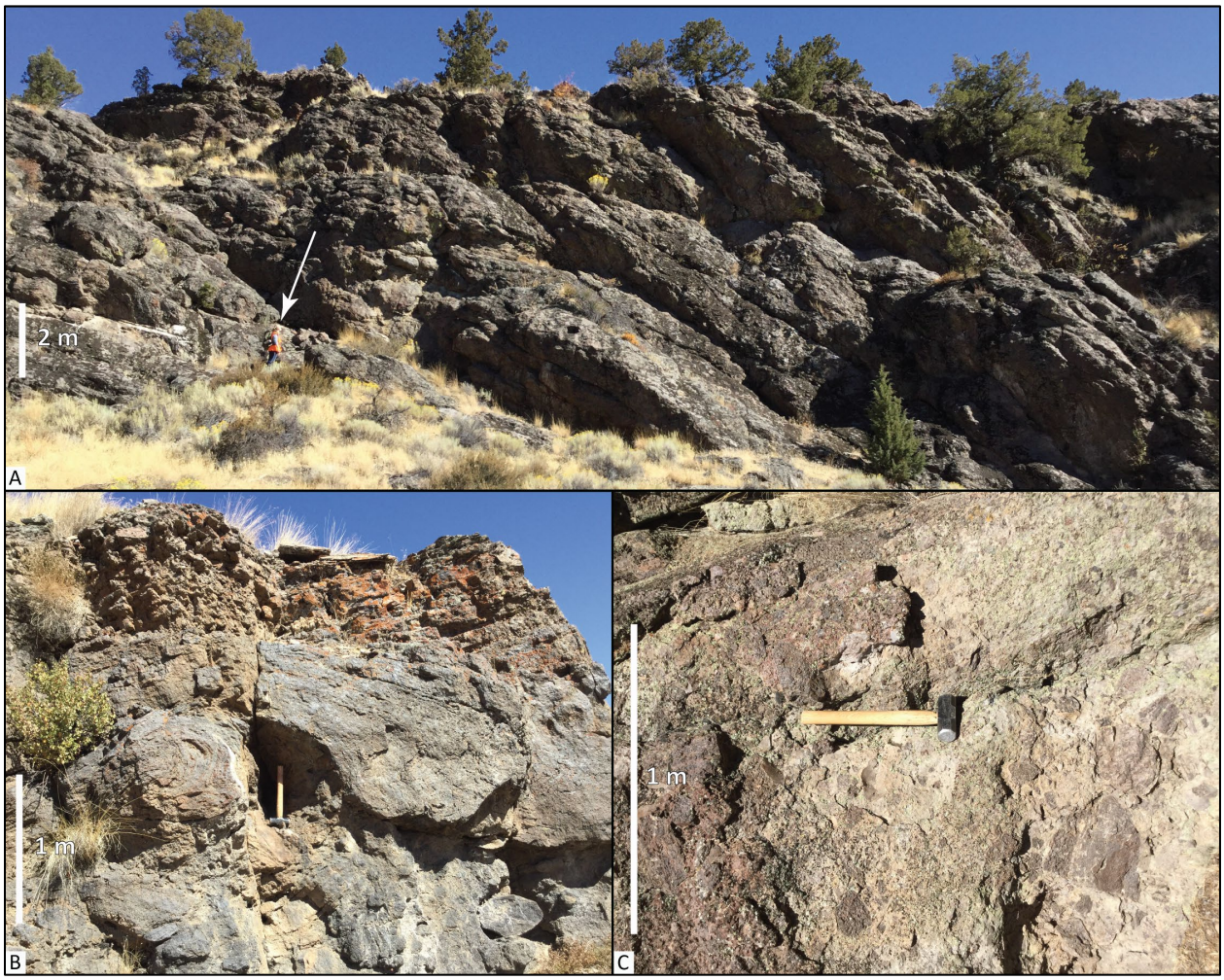

Figure 5-21. Hand sample and thin section photographs showing variations in the rhyolite of Burns Butte (Tmrb). (A) Planar flow banded. (B) Devitrified obsidian. (C) Contorted flow banded. (D) Breccia. Photomicrograph of sample 29 BRHC 18 under cross-polarized light. Scale bar is 1 mm (0.04 in) in length. (F) Same view as (E), under plane-polarized light. Abbreviations: qtz – quartz, px – pyroxene. Photo credit: (A-F) Carlie J.M. Duda, 2018.

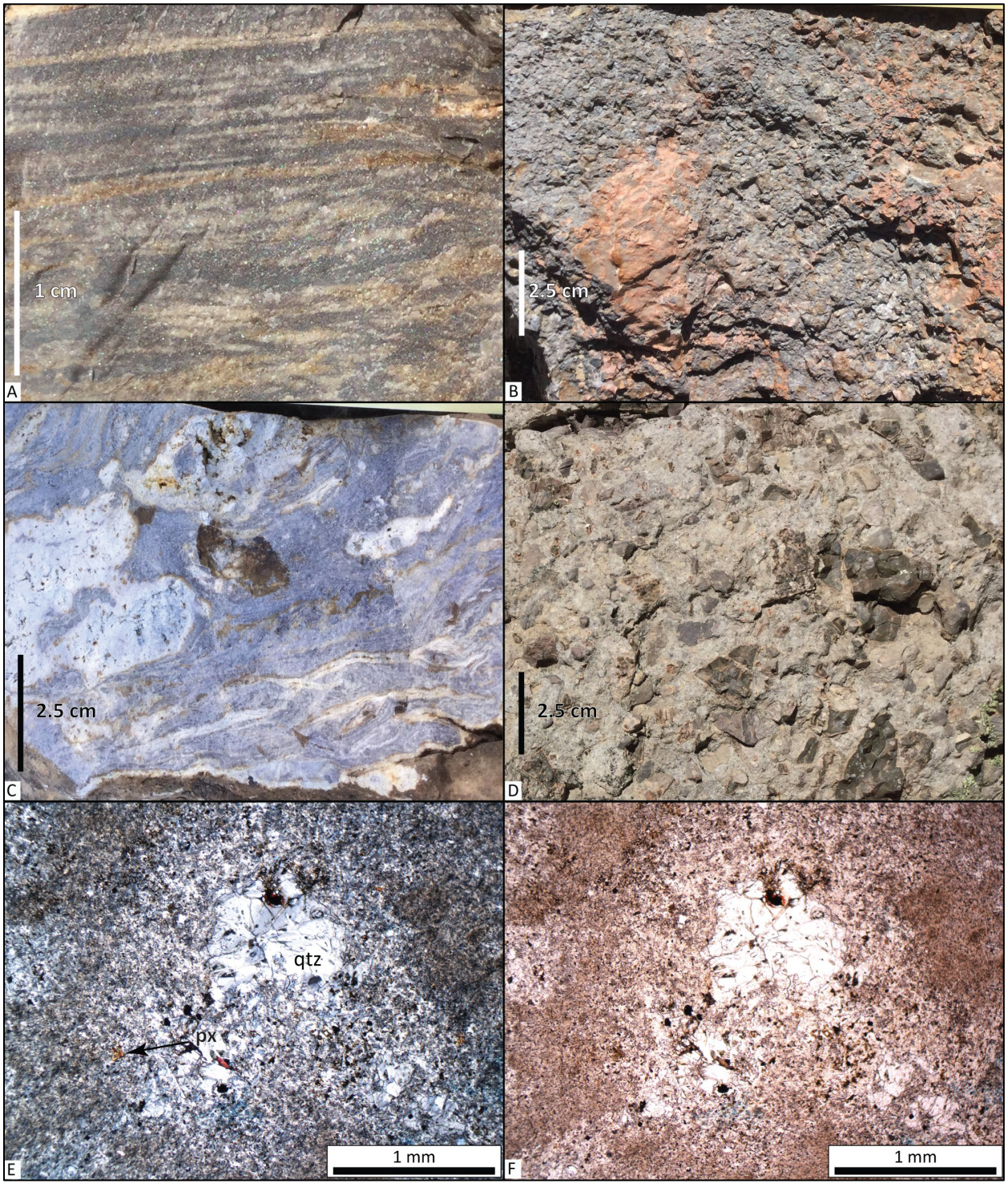

Tmrg **rhyolite of Golden Ranch (upper Miocene)**—Massive to crudely flow-foliated rhyolite exposed in low hills between Burns Butte, U.S. Highway 20, and the southern boundary of the Burns 7.5′ quadrangle (Plate 2). The unit extends west into the Burns Butte 7.5′ quadrangle. The rhyolite occurs in prominent outcrops up to 30 m (100 ft) high, characterized by blocky to subvertical to vertical tabular jointing (**Figure 5-22**). Outcrop surfaces observed in 1-m lidar DEMs south of U.S. Highway 20 retain complex compression ridges formed during lava flow emplacement (Plate 2).

Typical hand samples of the rhyolite are medium light gray (N6) and porphyritic to microporphyritic with phenocrysts and microphenocrysts of alkali feldspar up to 5 mm (0.2 in) and microphenocrysts of biotite, and sparse quartz contained within a devitrified, spherulitic groundmass (**Figure 5-23a**). The rhyolite is petrographically abundantly porphyritic to microporphyritic with 3 to 5 percent subhedral to anhedral, blocky to prismatic alkali feldspar phenocrysts and microphenocrysts <5 mm (0.2 in), 1 to 2 percent subhedral biotite microphenocrysts <1 mm (0.04 in), and 1 percent alkali feldspar-biotite glomerocrysts up to 5 mm (0.2 in) contained within a cryptocrystalline, felty, and mottled groundmass of feldspar, quartz, and magnetite (**Figure 5-23b-c**). Spherulitic overgrowths are common. Flow banding is apparent in thin section, defined by the trachytic alignment of alkali-feldspar and biotite, alternating with bands of cryptocrystalline quartz. Alkali feldspar are typically prismatic to blocky and twinned; dissolution of feldspar cores is common (**Figure 5-23b-c**). Samples obtained from this unit have a broad rhyolitic composition with 72.30 to 76.21 weight percent SiO_2, 12.71 to 14.44 weight percent Al_2O_3, 1.21 to 2.08 weight percent FeO*, 3.71 to 4.27 weight percent Na_2O, and 4.76 to 5.25 weight percent K_2O. The rhyolite also contains 195 to 289 ppm Zr, 16.3 to 26.1 ppm Nb, 31 to 36 ppm Y, 28 to 41 ppm La, and 47 to 76 ppm Ce (**Figure 5-6**, **Figure 5-7**, **Table 5-1**). Additional work on the rhyolite of Golden Ranch (**Tmrg**) in the Burns Butte 7.5′ quadrangle will better quantify the chemical makeup of this unit and its possible variations.

The rhyolite of Golden Ranch (**Tmrg**) is assigned a late Miocene age on the basis of stratigraphic position above the 8.41 Ma Prater Creek Ash-flow Tuff (**Tmtp**) and below the 7.093 Ma Rattlesnake Tuff (**Tmtr**) (Plate 2). The unit intrudes and directly overlies the tuff of Wheeler Springs (**Tmtw**, **Tmtwh**). Green and others (1972) reported a K/Ar age of 7.82 ± 0.26 Ma for the rhyolite of Golden Ranch (**Tmrg**) (recalculated to 8.03 ± 0.26 Ma by Fiebelkorn and others, 1982, 1983).

The rhyolite of Golden Ranch occurs as exogenous domes and flows erupted from vents forming high ground southeast of Burns Butte. The unit is interpreted as a rhyolite dome complex situated along the eastern margin of the Silvies River caldera (**Figure 2-3**; Plate 2). Partly equivalent to Td (Danforth Formation) of Piper and others (1939), Tr (rhyodacite) of Greene (1972) and Greene and others (1972), Tvs (silicic vent rocks) of Walker (1977), Tmrb (rhyodacite of Burns Butte) of Brown and others (1980a), and Tmrg (rhyolite of Golden Ranch) of Brown (1982).

Figure 5-22. The rhyolite of Golden Ranch (Tmrg), exposed in the southwestern part of the Burns 7.5’ quadrangle (Plate 2). (A) Massive to blocky- and platy-jointed rhyolite exposed north of U.S. Highway 20 (43.58299, −119.11784 WGS84 geographic coordinates; 4827734mN, 329015mE WGS84 UTM Zone 11 coordinates). View is looking east. (B) Tabular-jointed rhyolite exposed along U.S. Highway 20 southwest of Hines (43.58299, −119.11784 WGS84 geographic coordinates; 4827734mN, 329015mE WGS84 UTM Zone 11 coordinates). View is looking east. Photo credit: (A-B) Carlie J.M. Duda, 2019.

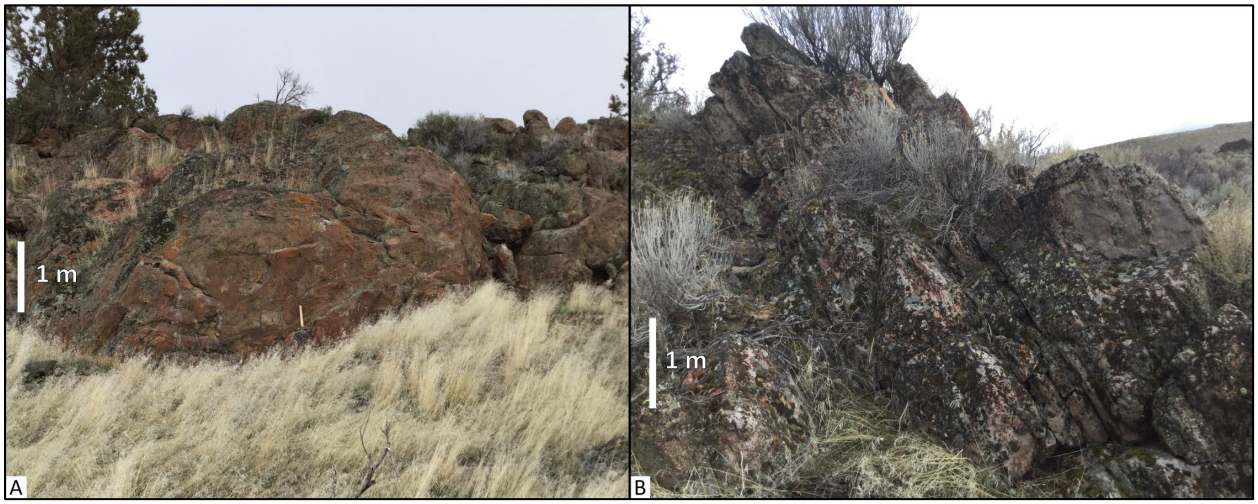

Figure 5-23. Hand sample and thin section photographs showing the rhyolite of Golden Ranch (Tmrg). (A) Alkali feldspar-biotite microporphyritic rhyolite with a devitrified, spherulitic groundmass. Photomicrograph of sample 147 BRHC 19 under cross-polarized light. (C) Same view as (B), under plane-polarized light. Scale bar is 1 mm (0.04 in) in length. Abbreviations: af – alkali feldspar; bt- biotite; qtz – quartz. Photo credit: (A-C) Carlie J.M. Duda, 2019.

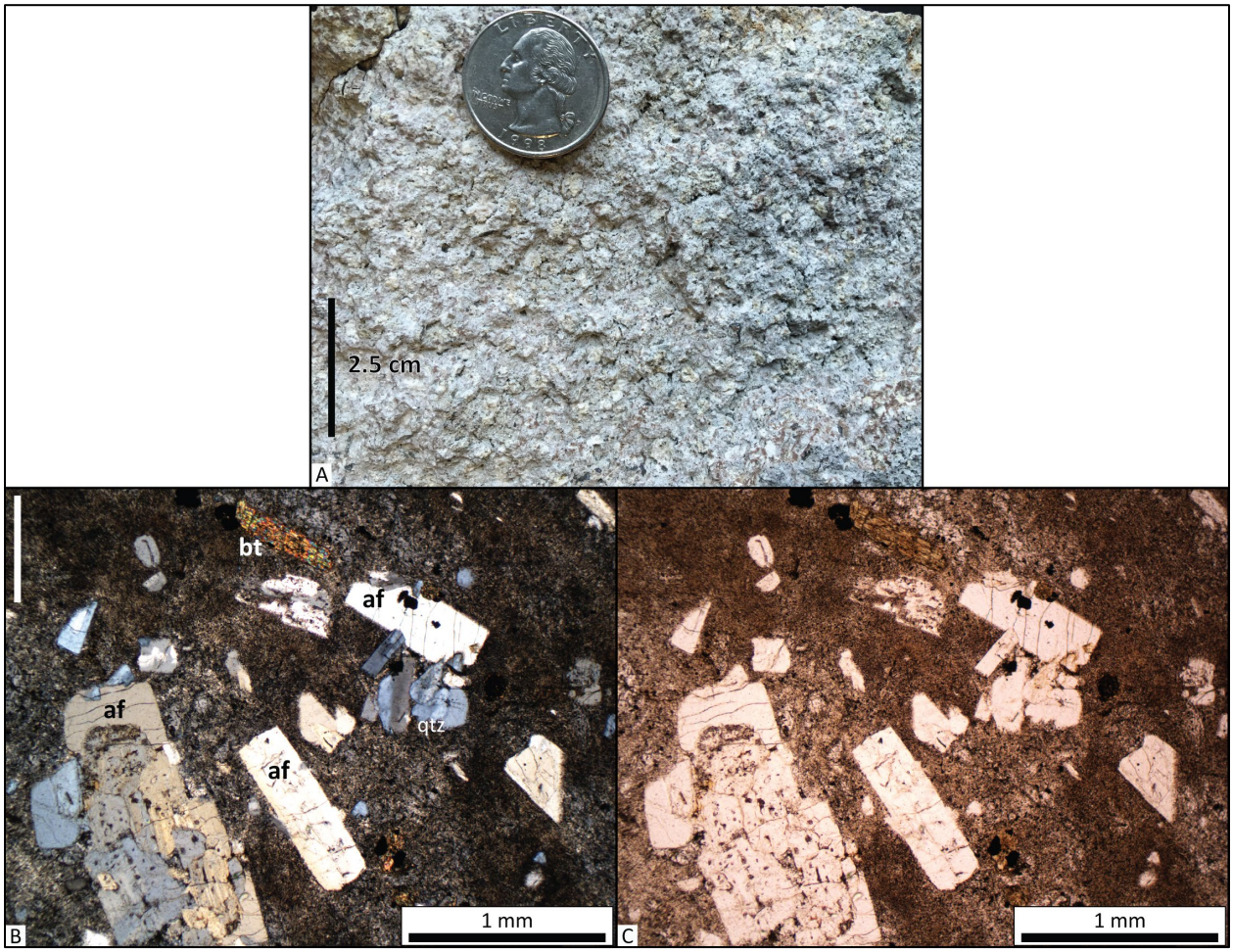

Tmri **rhyolite intrusive (upper Miocene)**—Light gray (N7) rhyolite occurring in rubbly exposures intruding the tuff of Wheeler Springs (**Tmtw**) along the southwest-central edge of Burns 7.5′ quadrangle (Plate 2). The unit description and mapped distribution of **Tmri** shown here is based solely on the work of Brown (1982); access to the privately held outcrop area was not available during the course of this study. Brown (1982) considered unit **Tmri** to represent a hypabyssal intrusive equivalent to the rhyolite of Golden Ranch (**Tmrg**).

Tmtwh **tuff of Wheeler Springs, non-welded lapilli tuff (upper Miocene)**—Semi-consolidated to consolidated, unwelded lithic-rich to lithic-poor rhyolitic lapilli-fall and lapilli-flow with minor intercalated ash-fall and ash-flow tuff and epiclastic rocks exposed between Burns Butte (Burns Butte 7.5′ quadrangle) and U.S. Highway 20 in the southwest part of the Burns 7.5′ quadrangle (**Figure 5-24**; Plate 2). The unit directly underlies the rhyolite of Burns Butte (**Tmrb**), rhyolite of Golden Ranch (**Tmrg**), and basaltic trachyandesite and trachyandesite flow (**Tmat**) and vent deposits (**Tmvt**). **Tmtwh** overlies the intracaldera unit of the Prater Creek Ash-flow Tuff (**Tmtpi**) in

the Federal 1-10 well. The non-welded tuff of Wheeler Springs (**Tmtwh**) is associated with a series of underlying welded tuffs exposed in the Burns 7.5′ quadrangle (Plate 2) and the Burns Butte 7.5′ quadrangle on the west (Brown, 1982). The unit is well exposed in 10- to 50-m-high (33 to 164 ft) outcrops in borrow pits, where it is characterized by massive to well-bedded meter-scale subunits (**Figure 5-24a-b**). **Tmtwh** is identified by an abundance of white (N9) inflated pumices up to 10 cm (4.2 in) across, fresh, black (N1) obsidian nodules up to 5 cm (2.1 in) across, and pebble- to boulder-sized, angular basaltic andesite to rhyolitic lithic fragments (**Figure 5-24c-d**). Brown (1982) interpreted the unit to represent at least 20 discrete eruptive events. Both the non-welded and welded phases of the tuff of Wheeler Springs (**Tmtw**, **Tmtwh**) are restricted in distribution, along the eastern margin of the Silvies River caldera (Plate 2, cross section B-B′).

Pumices sampled from this unit in the map area have rhyolitic compositions with 73.04 to 74.25 weight percent SiO_2, 13.76 to 14.83 weight percent Al_2O_3, 1.53 to 1.94 weight percent FeO*, 1.84 to 3.31 weight percent Na_2O, and 4.71 to 5.75 weight percent K_2O (**Table 5-1**). The rhyolite pumices also contain 252 to 261 ppm Zr, 24.2 to 28.4 Nb, 37 to 48 ppm Y, 34 to 40 ppm La, and 65 to 75 ppm Ce (**Figure 5-6**, **Figure 5-7**, **Table 5-1**). The unit is chemically indistinguishable from the underlying welded phases of the tuff of Wheeler Springs (**Tmtw**). Chemical composition of pumices in the non-welded part of the tuff of Wheeler Springs (**Tmtwh**) and welded tuff (**Tmtw**) are also indistinguishable from those obtained from the overlying rhyolite of Burns Butte (**Tmrb**). Spatial and geochemical association of the silicic units indicates the tuff of Wheeler Springs represents pyroclastic eruptions directly preceding and genetically related to later effusive exogenous dome growth and flows forming the rhyolite of Burns Butte (**Tmrb**). Brown (1982) indicated the unit apparently erupted from a vent either underlying or west of Burns Butte. Together, both non-welded and welded phases of the tuff of Wheeler Springs (**Tmtw**, **Tmtwh**) are chemically similar to the younger Rattlesnake Tuff (**Tmtr**) but are differentiated from the Rattlesnake Tuff (**Tmtr**) on the basis of their lower SiO_2, higher Al_2O_3, higher Sr, lower Y, and higher Rb (**Figure 5-7**, **Table 5-1**).

The tuff of Wheeler Springs, non-welded lapilli tuff (**Tmtwh**) is assigned a late Miocene age on the basis of stratigraphic position above the 8.41 Ma Prater Creek Ash-flow Tuff (**Tmtp**) and below the 7.68 Ma rhyolite of Burns Butte (**Tmrb**). The unit is used widely as a source of construction aggregate and crushed stone in the map area and can be mapped partially on the basis of prospect pits and mine excavations (Plate 2; Niewendorp and Geitgey, 2009). Equivalent to Tmlh (Hotchkiss lapilli member of the tuff of Wheeler Springs) of Brown (1982).

Figure 5-24. The tuff of Wheeler Springs, non-welded lapilli tuff (Tmtwh) exposed south of Switch Canyon Road in the Burns 7.5′ quadrangle (Plate 2) (43.56094, −119.09961 WGS84 geographic coordinates; 4825250mN, 330428mE WGS84 UTM Zone 11 coordinates). (A) Stratified pumice lapilli tuff. View is looking northwest. (B) Massive pumice-lapilli tuff. View is looking north. (C) White (N9) inflated pumice. (D) Fresh, black (N9) obsidian nodules. View in A and B is looking north. Photo credit: (A-D) Carlie J.M. Duda, 2018.

Tmtw **tuff of Wheeler Springs, welded tuff (upper Miocene)**—Sequence of devitrified, aphyric, crystal-vitric welded ash-flow tuffs exposed between Burns Butte (Burns Butte 7.5′ quadrangle) and U.S. Highway 20 in the southwest part of the Burns 7.5′ quadrangle (Plate 2). Brown (1982) subdivided the welded part of the tuff of Wheeler Springs (**Tmtw**) into five mappable units on the basis of lithologic criteria. Two of those members, the McGee and Sage Hen members, were mapped in the Burns 7.5′ quadrangle by Brown (1982). We do not distinguish the units of Brown (1982) here as 1) key outcrops likely observed by Brown (1982) are on private ground closed to entry and 2) several geochemical analyses obtained from accessible outcrops of subdivided members are indistinguishable.

The unit is typically preserved in bench-forming outcrops ranging from 5 to 30 m (16.4 to 98.4 ft) high in the Burns Butte and Burns 7.5′ quadrangles (**Figure 5-25a**; Plate 2). Outcrops show a range of welding facies from strongly welded devitrified tuff to highly expanded vitric tuff. Black

hydrated obsidian in the groundmass is common in vitric zones. Locally highly expanded areas show significant vapor-phase alteration of groundmass and pumice. In some cases, pumice has been completely altered to masses of crystobalite.

Typical hand samples of the tuff are moderate orange pink (10R 7/4), aphyric, and strongly welded, with pumice fiamme up to several centimeters (**Figure 5-25b**). Petrographically, the welded tuff of Wheeler Springs (**Tmtw**) is devitrified, characterized by well-developed vitroclastic texture with moderately preserved, cuspate glass shards to variably altered glass shards and pumice fiamme overgrown and replaced by fibrous cryptocrystalline quartz and radiating growths of quartz and feldspar (axiolites) (**Figure 5-25c-d**). Thin sections typically contain scattered prismatic alkali feldspar crystals < 1 mm (0.02 in) long and flow banded black-brown obsidian lithics. Samples obtained from this unit in the map area have a rhyolitic composition with 74.00 to 75.02 weight percent SiO_2, 13.42 to 13.97 weight percent Al_2O_3, 1.57 to 1.81 weight percent FeO*, 3.42 to 4.32 weight percent Na_2O, and 4.97 to 5.53 weight percent K_2O. The rhyolite also contains 240 to 284 ppm Zr, 26.6 to 27.5 ppm Nb, 42 to 68 ppm Y, 41 to 45 ppm La, and 72 to 93 ppm Ce (**Figure 5-6**, **Figure 5-7**, **Table 5-1**).

The tuff of Wheeler Springs, welded tuff (**Tmtw**) is assigned a late Miocene age on the basis of stratigraphic position above the 8.41 Ma Prater Creek Ash-flow Tuff (**Tmtp**) and below the 7.68 Ma rhyolite of Burns Butte (**Tmrb**). Partly equivalent to Tmtm/Tmts (McGee and Sage Hen Ash-flow tuff members of the tuff of Wheeler Springs) of Brown (1982).

Figure 5-25. Welded tuff of Wheeler Springs (Tmtw) exposed east of Burns Butte in the Burns 7.5′ quadrangle (Plate 2). (A) Massive- to blocky-jointed outcrop of strongly welded, devitrified tuff (43.55670, –119.12275 WGS84 geographic coordinates; 328546mE, 4824827mN WGS84 UTM Zone 11 coordinates). View is looking west. (B) Strongly welded tuff, containing pumice fiamme. (C,D) Thin section photomicrographs of hand sample 66 BRHC 18 shown in B. (C) Thin section under cross-polarized light showing a mixture of microphenocrysts of alkali feldspar and an obsidian lithic in a groundmass of relict cuspate glass shards. (D) Same view as (C), under plane-polarized light. Scale bar is 1 mm (0.04 in) in length. Abbreviation: af – alkali feldspar. Photo credit: (A-D) Carlie J.M. Duda, 2018 and 2019.

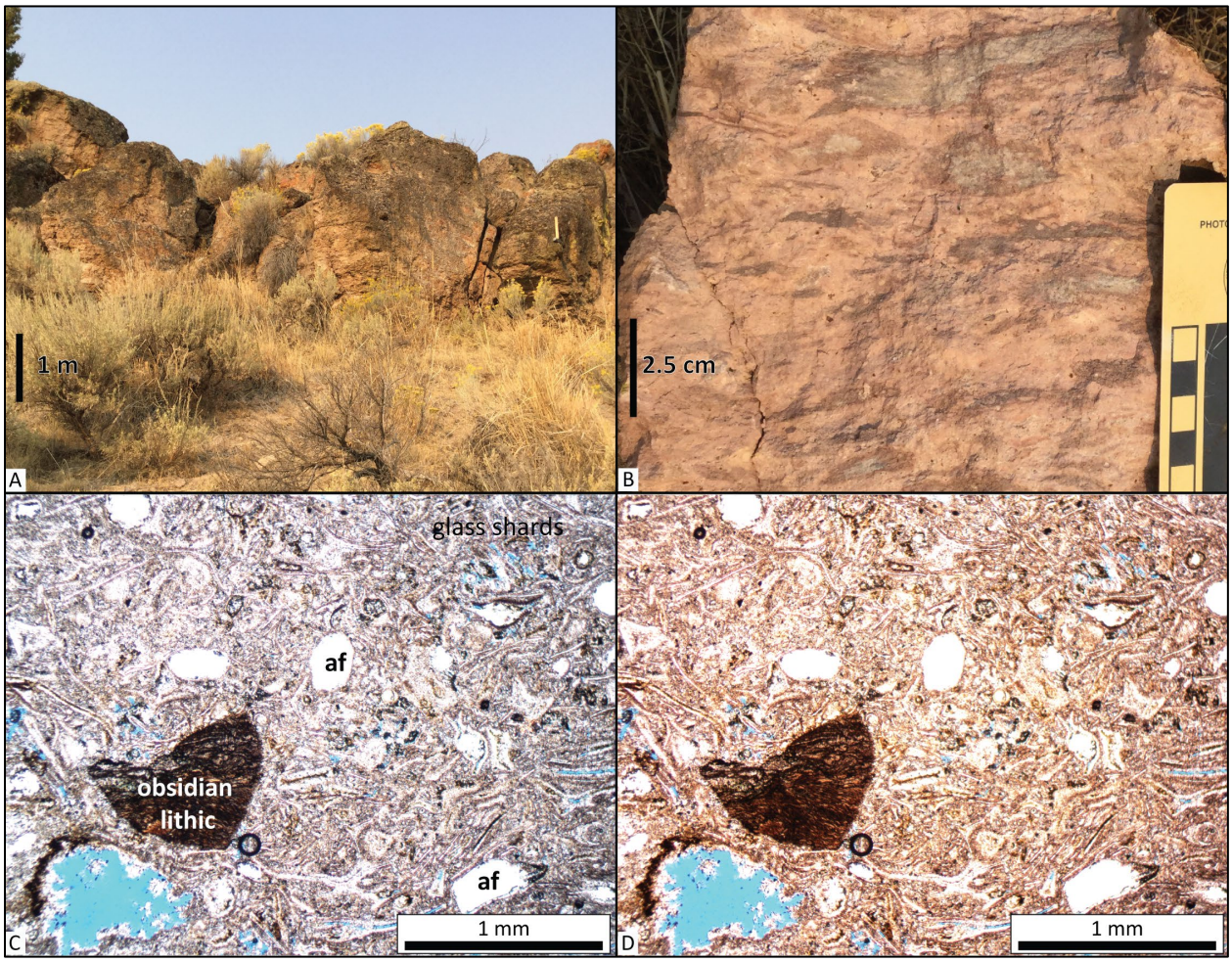

Tmtp **Prater Creek Ash-flow Tuff (upper Miocene)**—Devitrified, welded, crystal-poor ash-flow tuff exposed in a south-dipping section beneath the Rattlesnake Tuff (**Tmtr**) and above the Devine Canyon Ash-flow Tuff (**Tmtd**) in the Poison Creek 7.5′ quadrangle (**Figure 5-4**, **Figure 5-8**; Plate 1). In the southwest part of the Poison Creek 7.5′ quadrangle (Plate 1), west of the Silvies River a thick section of basaltic trachyandesite and trachyandesite (**Tmat**) lies between the older Prater Creek Ash-flow Tuff (**Tmtp**) and younger Rattlesnake Tuff (**Tmtr**) (**Figure 5-5**). The Prater Creek Ash-flow Tuff (**Tmtp**) projects into the subsurface below the Harney Valley as it enters the northern part of the Burns 7.5′ quadrangle (Plate 2). We interpret the unit to be present at the 231 to 243 m (760 to 800 ft) depth interval of the Weed and Poteet #1 well (Plate 2, cross sections A and B; **Table 2-1**). The type section of the Prater Creek Ash-flow Tuff (**Tmtp**) is defined by

Walker (1979) along Poison Creek and U.S. Highway 395 in the eastern part of the Poison Creek 7.5' quadrangle (Plate 1; 43.683167, −119.004576304 WGS84 geographic coordinates) (**Figure 5-4b**).

The Prater Creek Ash-flow Tuff (**Tmtp**) forms distinctive outcrop cliffs and rimrock that can be easily traced in 1-m lidar DEMs and air photographs throughout the Poison Creek area (**Figure 5-4**, **Figure 5-8**). Where exposed in the map area, the ash-flow tuff is 10 to 30 m (32 to 98 ft) thick occurring as a single cooling unit. The tuff is typically massive and strongly welded, exhibiting a eutaxitic texture and a distinctive platy jointing. There is also a lithophysal section, recognizable in many outcrops of **Tmtp**, exhibiting lenticular or crescent-shaped voids in the plane of compaction foliation (**Figure 5-26**). Flattened and devitrified pumice (fiamme) up to 5 cm (2 in) long (compaction ratio of 10:1) are present but not abundant. Lithics are a minor component (<3 percent vol.) and consist of angular poly-compositional lithic fragments as much as 2 cm (0.8 in) in length.

Typical fresh hand samples are pale blue (5PB 7/2), pinkish gray (5YR 8/1), light brown (5YR 5/2), to moderate reddish brown (10R 4/6) when weathered (**Figure 5-27a-b**). The tuff contains < 1 percent (vol.) crystal fragments of sanidine and quartz <0.5 mm (<0.01 in). The strongly welded, devitrified tuff commonly exhibits a distinctive spotted appearance. In thin section, the tuff is characterized by less than 1 percent sanidine and quartz crystal fragments in a devitrified glass-shard groundmass (**Figure 5-27c-f**). Locally, the tuff is zeolitized. Samples obtained from this unit in the map area have a high-silica peraluminous rhyolitic composition with 76.55 to 77.10 weight percent SiO_2, 11.59 to 11.98 weight percent Al_2O_3, 1.79 to 2.33 weight percent FeO*, 4.13 to 4.35 weight percent Na_2O, and 4.51 to 4.69 weight percent K_2O. The rhyolite tuff also contains 492 to 519 ppm Zr, 42.2 to 45.3 ppm Nb, 45 to 85 ppm Y, 86 to 127 ppm Ce, and 44 to 70 ppm La (**Figure 5-6**, **Figure 5-7**, **Table 5-1**). Chemical composition of the Prater Creek Ash-flow Tuff (**Tmtp**) is remarkably similar to and largely indistinguishable from geochemical analyses obtained over a 457 m (1,500 ft) interval of lithologically monotonous tuff (**Tmtpi)** in the lower part of the CTI well (n = 16 samples) and a >427 m (>1,400 ft) thick lithologically monotonous tuff interval in the Federal 1-10 well (n = 10 samples) (**Figure 5-7**, **Table 2-1, Table 5-1**).

The Prater Creek Ash-flow Tuff (**Tmtp**) is assigned a late Miocene age on the basis of stratigraphic position and an $^{40}Ar/^{39}Ar$ age of 8.41 ± 0.16 Ma (Jordan and others, 2004). The tuff has an estimated eruptive volume of ~200 km^3 (~48 mi^3), covering an outcrop area of ~9,615 km^2 (~3,713 mi^2) (Greene, 1973; Parker, 1974; Streck and Ferns, 2004). A possible caldera or vent source for the tuff was suggested at Double O Ranch (~25 km [15.6 mi] south of the map area) by Parker (1974), who argued on the basis of mineralogical and chemical similarities that the 8.28 ± 0.05 Ma rhyolite of Double O Ranch was a dome-flow complex associated with the Prater Creek eruptive center (unit Trr of Greene and others, 1972; date from Jordan and others, 2004; **Figure 2-3**). Meigs and others (2009) and Ford (2013) suggested a Prater Creek Ash-flow Tuff (**Tmtp**) eruptive center lying along the northern edge of Wright Point. Khatiwada and Keller (2015), on the basis of geophysical imaging, inferred a possible eruptive source area for the Prater Creek Ash-flow Tuff (**Tmtp**) in a similar location centered on Malheur Lake and Wright Point (northern caldera). Lithologic and geochemical data obtained during this study from a number of deep drill holes in this part of the Harney Basin, including the Federal 1-10, CTI well, Weed and Poteet #1, and #1 Fay (**Table 2-1**), now constrain the source of the Prater Creek Ash-flow Tuff (**Tmtp**) to the Silvies River caldera, lying beneath and west of the city of Burns (Plates 1 and 2; **Figure 2-3**).

The tuff was informally named the welded tuff of Prater Creek by Greene (1972) and Greene and others (1972); formally recognized as the Prater Creek Ash-flow Tuff by Walker (1979). Partly equivalent to Td (Danforth Formation) of Piper and others (1939) and Tat (silicic ash-flow tuff) of Walker (1977). Equivalent to Tmtp (Prater Creek Ash-flow Tuff) of Brown and others (1980a) and Brown (1982).

Figure 5-26. Lithophysal Prater Creek Ash-flow Tuff (Tmtp) exposed in Fenwick Canyon in the Poison Creek 7.5' quadrangle (Plate 1) (43.66683, –119.06470 WGS84 geographic coordinates; 333539mE, 4836939mN WGS84 UTM Zone 11 coordinates). View is looking north. Person for scale is 1.6 m (62 in) tall. Photo credit: Jason D. McClaughry, 2018.

Figure 5-27. Hand sample and thin section photographs showing the Prater Creek Ash-flow Tuff (Tmtp). (A) Hand sample of strongly welded, devitrified tuff. (B) Hand sample of lithophysal tuff. (C) Thin section under cross-polarized light. Sample number HAH064-16. Two fiamme displaying eutaxitic texture surrounded by a groundmass of vitric ash and glass shards. Scale bar is 1 mm (0.04 in) in length. (D) Same view as (C), under plane-polarized light. (E) Thin section under cross-polarized light. Sample number, HAH023-16. Broken alkali feldspar crystal fragment (labeled af) surrounded by a devitrified groundmass of vitric ash and glass shards. Eutaxitic texture is evident in plane-polarized light. Scale bar is 1 mm (0.04 in) in length. (F) Same view as (E), under plane-polarized light. Photo credits: (A-B) Jason D. McClaughry, 2018; (C-F) Robert A. Houston, 2017.

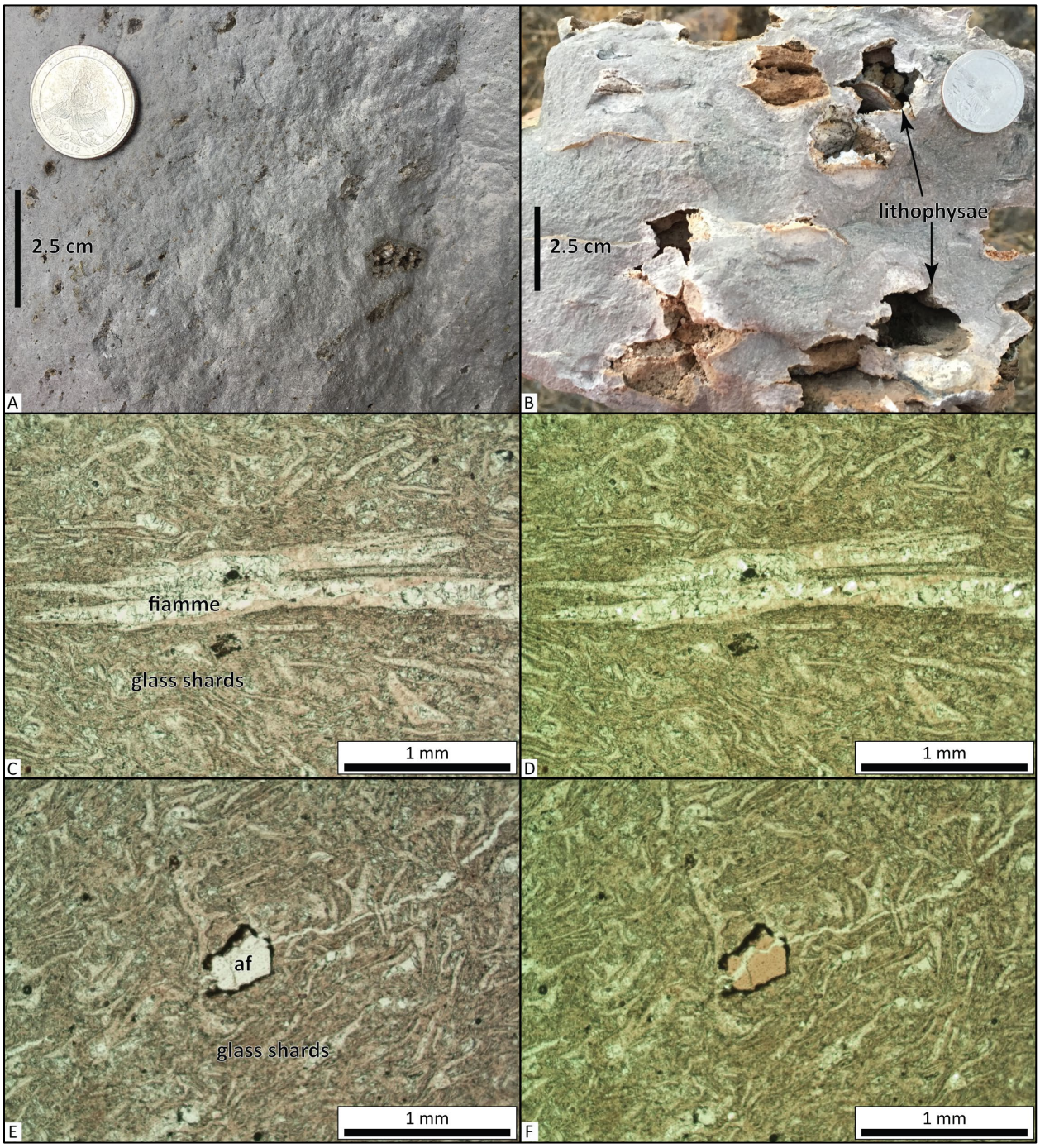

Tmtpi **Prater Creek Ash-flow Tuff, intracaldera unit (upper Miocene) (cross section only)**—Dusky yellow green (5GY 5/2) to light olive gray (5Y 5/2), fine-grained silicic tuff recovered from the CTI well located in Hines in the Burns 7.5′ quadrangle (Plate 1, cross sections) and the Federal 1-10 well in the Burns Butte 7.5′ quadrangle (**Figure 5-28a-b**, **Table 2-1**). The tuff is known only from drill cuttings and is not exposed at the surface. The unit, as defined here, forms a lithologically and geochemically monotonous thick interval exceeding 427 m (1,400 ft) in the Federal 1-10 well and >429 m (>1,406 ft) in the CTI well. The unit forms the bottom of the CTI well and may be of considerably greater thickness in that area.

The top of **Tmtpi** lies at an elevation of ~ 561 m (1,840 ft) above sea level (asl) in the Federal 1-10 well and at ~ 1,097 m (3,598 ft) asl in the CTI well. The **Tmtpi** sequence in the Federal 1-10 well is overlain by a >762 m (>2,950 ft) sequence of basaltic trachyandesite, trachyandesite, and minor dacite **(Tmat)**. Near the top of the mafic sequence, flows are interbedded with an ~37 m (~120 ft) thick non-welded ash-flow tuff unit, correlative to the tuff of Wheeler Springs, non-welded lapilli tuff (**Tmtwh**). The upper part of the mafic sequence above the Wheeler Springs Tuff is correlative with basaltic trachyandesite and trachyandesite flows exposed in the southwest part of the Poison Creek 7.5′ quadrangle. The uppermost part of the Federal 1-10 well was spudded into Rattlesnake Tuff (**Tmtr**). In the CTI well the **Tmtpi** sequence is directly overlain by ~61 m (200 ft) of silicic tuff correlated with the tuff of Wheeler Springs (**Tmtw**, **Tmtwh**) and above the tuff of Wheeler Springs interval by ~43 m (140 ft) of basaltic trachyandesite **(Tmat)**, and Rattlesnake Tuff (**Tmtr**).

Grain mount thin sections of cuttings from the monotonous tuff intervals in both the Federal 1-10 and CTI wells are dominated by fragments of silicic tuff where former glass shards and pumice have been recrystallized to radiating intergrowths of quartz and alkali feldspar forming a pervasive granophyric texture (**Figure 5-28c-f**). Granophyric overgrowths are arranged about sparse remnant euhedral to subhedral alkali feldspar crystals. Sparse lithics of plagioclase-pyroxene andesite are scattered through the thin sections. Magnetic grain separation indicates that the intervals studied are ~95 percent (vol.) granophyric silicic tuff and ~5 percent (vol.) mafic lithics. Samples (n =5) obtained from **Tmtpi** in the Federal 1-10 well, interval 899 m (2,950 ft) to 1,326 m (4,350 ft), have a high-silica peraluminous rhyolitic composition with 75.44 to 78.15 weight percent SiO_2, 10.36 to 11.37 weight percent Al_2O_3, 1.55 to 2.18 weight percent FeO*, 3.23 to 3.69 weight percent Na_2O, and 4.17 to 5.14 weight percent K_2O. The rhyolite also contains 408 to 479 ppm Zr, 36.0 to 42.0 ppm Nb, 59 to 73 ppm Y, 46 to 58 ppm La, and 88 to 106 ppm Ce. Samples (n= 16) obtained from this unit in the CTI well, interval 152 m (500 ft) to 596 m (1956) have a high-silica peraluminous rhyolitic composition identical to the Federal Well with 75.37 to 77.40 weight percent SiO_2, 11.18 to 12.40 weight percent Al_2O_3, 1.74 to 3.14 weight percent FeO*, 3.61 to 4.20 weight percent Na_2O, and 4.55 to 5.86 weight percent K_2O. The rhyolite also contains 439 to 712 ppm Zr, 35.8 to 47.5 ppm Nb, 59 to 81 ppm Y, 50 to 66 ppm La, and 92 to 131 ppm Ce (**Figure 5-6**, **Figure 5-7**, **Table 5-1**). Geochemical analyses from these monotonous tuff intervals in the lower parts of the CTI and Federal 1-10 wells are indistinguishable from analyses obtained from surface outcrops of the wide-ranging Prater Creek Ash-flow Tuff (**Tmtp**) (**Figure 5-7**, **Table 2-1, Table 5-1**).

The Prater Creek Ash-flow Tuff, intracaldera unit (**Tmtpi**) is assigned a late Miocene age on the basis of stratigraphic position. **Tmtpi** is considered the intracaldera tuff equivalent to the outflow unit forming the Prater Creek Ash-flow Tuff (**Tmtp**) on the basis of 1) monotonously identical lithology and geochemistry of cuttings over stratigraphic intervals exceeding 427 m (1,400 ft) in

vertical thickness, and 2) pervasive granophyric textures in silicic grains, which are related to slow cooling and crystallization of formerly glassy components (glass shards and pumice) in the central parts of very thick (several tens to hundreds of meters), densely welded ignimbrites (McPhie and others, 1993).

Figure 5-28. Representative cuttings and grain-mount thin sections from the Federal 1-10 and CTI wells. (A) Cuttings sample of silicic tuff from the 926 m (3,040 ft) depth interval of the Federal 1-10 well. (B) Cuttings sample of silicic tuff from the 308 to 311 m (1,010 to 1,020 ft) depth interval of the CTI well. (C) Federal 1-10 grain mount thin section under cross-polarized light. Sample number F-1-10-3040. (D) Same view as (C), under plane-polarized light. (E) CTI well grain mount thin section under cross-polarized light. Sample number HARN 50087-1010-1020. (F) Same view as (E), under plane-polarized light. Scale bar is 1 mm (0.04 in) in length in photos C to F. Thin sections show grains of fine-grained tuff with granophyric textures and sparse lithics of andesite. Granophyric textures are related to slow cooling and crystallization of formerly glassy components (glass shards and pumice) in the central parts of very thick, densely welded ignimbrites (McPhie and others, 1993). Photo credit: (A-F) Jason D. McClaughry, 2019.

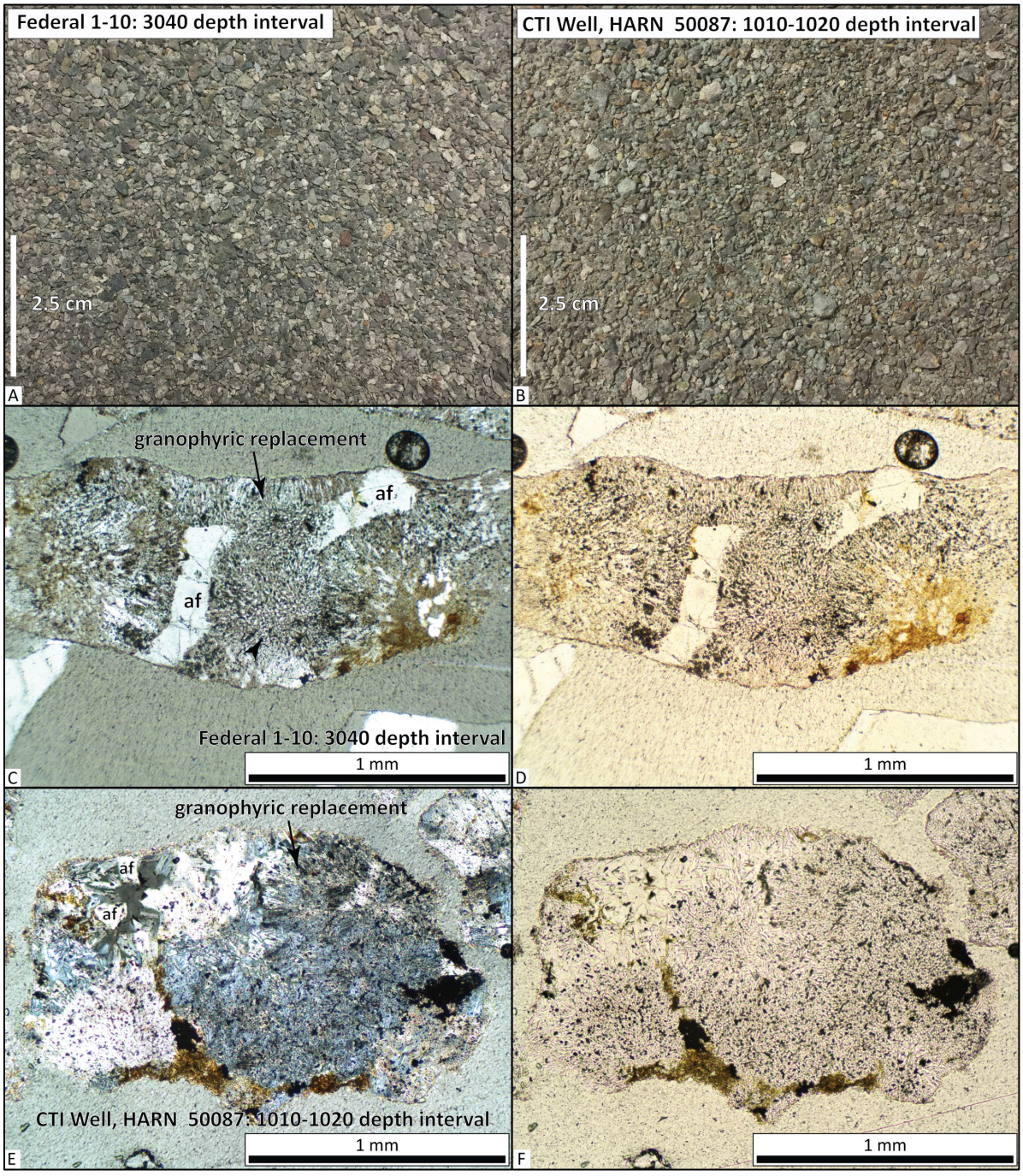

Tmtd **Devine Canyon Ash-flow Tuff (upper Miocene)**—Devitrified crystal-rich vitric tuff exposed in a south-dipping stratigraphic section, lying beneath the Prater Creek Ash-flow Tuff (**Tmtp**) and tuffaceous sedimentary rocks (**Tmst**) in the northern part of the Poison Creek 7.5′ quadrangle (**Figure 5-4**; Plate 1). The Devine Canyon Ash-flow Tuff (**Tmtd**) represents the oldest geologic unit exposed in the map area. The unit is not exposed south and east of the Silvies River in the Poison Creek 7.5′ quadrangle, projecting beneath land surface at that approximate latitude (43.67011^{0}N; Plate 1). Farther south, the Devine Canyon Ash-flow Tuff (**Tmtd**) is inferred to be present beneath the Harney Valley (Plate 2). We interpret the unit to be present at the 244 to 295 m (800 to 970 ft) depth interval of the Weed and Poteet #1 well on the basis of cuttings descriptions noting an "abundance of clear fine quartz crystals," "high quartz content," or "quartz embedded in clay" (Plate 2, cross sections A-A′ and B-B′; **Table 2-1**). The type section of the Devine Canyon Ash-flow Tuff (**Tmtd**) is defined by Greene (1973) and Walker (1979) along U.S. Highway 395, about 1 km (0.6 mi) north of the confluence of Poison Creek and Devine Canyon in the eastern part of the Poison Creek 7.5′ quadrangle (**Figure 5-4;** Plate 1; 43.700265, −119.019241 WGS84 geographic coordinates).

The Devine Canyon Ash-flow Tuff (**Tmtd**) forms distinctive cliffs and rimrock that can be easily traced in 1-m lidar DEMs and air photographs through the northern part of the Poison Creek 7.5' quadrangle (Plate 1; **Figure 5-4**). The tuff is generally massive to distinctly columnar jointed and strongly welded, exhibiting a eutaxitic fabric (**Figure 5-29a-b**). Strongly welded zones contain large (as much as 30 cm [12 in]) flattened glassy pumice exhibiting compaction ratios of 15:1. The unit contains occasional lithic fragments. A lithophysal section is recognizable in many outcrops of **Tmtd**, especially in the hoodoos of Devils Garden, where outcrops are marked by an abundance of flattened to oblate lithophysal cavities up to 20 cm (7.9 in) across (**Figure 5-29a**). The Devine Canyon Ash-flow Tuff (**Tmtd**) weathers to form a distinctive apron of very large (as much as 10 m [30 ft] diameter) boulders intermixed with alkali feldspar-rich sand (**Figure 5-30a**). The maximum exposed thickness of **Tmtd** in the map area is 73 m (242 ft).

Typical hand samples of the ash-flow tuff are light gray (N7 to N8) to greenish gray (5GY 5-6/1). Where outcrops are abundant in phenocrysts, the rock is medium to light gray (N5-N7) to pinkish, yellowish, and greenish gray (5 YR 8/1, 5Y 8/1, 5GY 6/1) with a streaked and mottled appearance (**Figure 5-30b**). Petrographically, the tuff contains as much as 30 percent crystals and crystal fragments of dominantly alkali feldspar (sanidine; Greene, 1973; Smith and MacKenzie, 1958), minor quartz, and rare pyroxene, ilmenite, and magnetite (**Figure 5-30c-d**). Alkali feldspar phenocrysts, recognized by cleavage and twinning, range from 30 to 35 percent by volume, whereas quartz content ranges from 0 to 7 percent (**Figure 5-30c-d**). Greene (1973) notes that alkali feldspar and quartz generally increase in abundance up section. Most of the phenocrysts are broken and exhibit rounding or embayment textures by resorption (**Figure 5-30c-d**). Rare pyroxene phenocrysts are green and yellow green (pleochroic). Samples obtained from this unit in the map area have a mildly peralkaline rhyolitic chemical composition with relatively invariable major element concentrations of 76.06 to 77.24 weight percent SiO_2, 10.92 to 11.75 weight percent Al_2O_3, 2.44 to 2.91 weight percent FeO*, 1.88 to 3.79 weight percent Na_2O, and 4.47 to 6.53 weight percent K_2O. The tuff has a wider range in trace element concentrations characterized by 603 to 1,328 ppm Zr, 46.3 to 95.1 ppm Nb, 22 to 166 ppm Y, 39 to 104 ppm La, and 156 to 202 ppm Ce (**Figure 5-6**, **Figure 5-7**, **Table 5-1**). Isom (2017) concludes from the wide compositional trace element ranges in zirconium, yttrium, and niobium that the tuff was erupted from a geochemically zoned magma chamber.

The Devine Canyon Ash-flow Tuff (**Tmtd**) is assigned a late Miocene age on the basis of stratigraphic position and $^{40}Ar/^{39}Ar$ ages of 9.74 ± 0.02 Ma (Jordan and others, 2004) and 9.63 ± 0.05 Ma (Ford and others, 2013). **Tmtd** outcrops cover an area >30,800 km^2 (>11,891 mi^2) (Isom, 2017), with an estimated erupted volume of ~250 to 300 km^3 (~60 to 72 mi^3) from a concealed source within the Harney Basin (Greene, 1973; Parker, 1974). Possible caldera or vent sources for the tuff, shown in **Figure 2-3,** are suggested to underly the Harney Basin, between Burns and Wright Point in the north-central to northwest part of the Harney Basin (Greene, 1973; Walker, 1974, 1979; Isom, 2017). Meigs and others (2009) and Ford and others (2013) showed a Devine Canyon Ash-flow Tuff eruptive center lying along the southeastern edge of Malheur Lake. Khatiwada and Keller (2015) inferred, through geophysical imaging, a possible eruptive source area for the Devine Canyon Ash-flow Tuff (Tmtp) in a similar location centered between Malheur Lake and Diamond Craters.

Informally named the welded tuff of Devine Canyon by Greene (1972) and Greene and others (1972); formally recognized as the Devine Canyon Ash-flow Tuff by Walker (1979). Partly equivalent to Td (Danforth Formation) of Piper and others (1939) and Tat (silicic ash-flow tuff) of Walker (1977).

Figure 5-29. Outcrops of Devine Canyon Ash-flow Tuff (Tmtd) in the Poison Creek 7.5' quadrangle (Plate 1). (A) Lithophysal section of Tmtd in outcrops forming the hoodoos of Devils Garden (43.74100, –119.09795 WGS84 geographic coordinates; 4845247mN, 331067mE WGS84 UTM Zone 11 coordinates). These outcrops are marked by an abundance of flattened to oblate lithophysal cavities up to 20 cm (7.9 in) across. View is looking northeast. (B) Columnar jointed Tmtd tuff exposed in Devine Canyon (43.70722, –119.01314 WGS84 geographic coordinates; 4841304mN, 337822mE WGS84 UTM Zone 11 coordinates). View is looking northwest. Photo credit: (A) Jason D. McClaughry, 2018; (B) Darrick Boschmann, 2018.

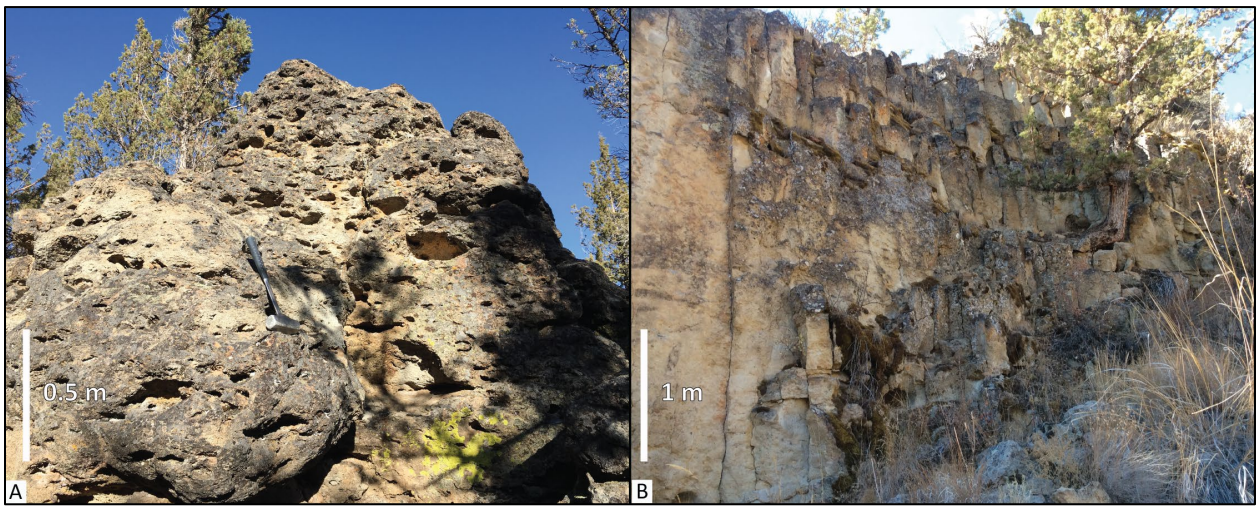

Figure 5-30. Hand sample and thin section photographs showing the Devine Canyon Ash-flow Tuff (Tmtd). (A) Crystal-rich sand eroding from outcrops of Tmtd. (B) Hand sample of strongly welded, devitrified, crystal-rich tuff. (C) Thin section under cross-polarized light. Subhedral to anhedral alkali feldspar and rounded quartz crystal phenocryst fragment distributed within a vitric groundmass of glass shards. Sample number HAH011-16. (D) Same view as (C), under plane-polarized light. Scale bar is 1 mm (0.04 in) in length. Abbreviations: af – alkali feldspar, qtz – quartz. Photo credit: (A-B) Jason D. McClaughry, 2018; (C-D) Robert A. Houston, 2017.

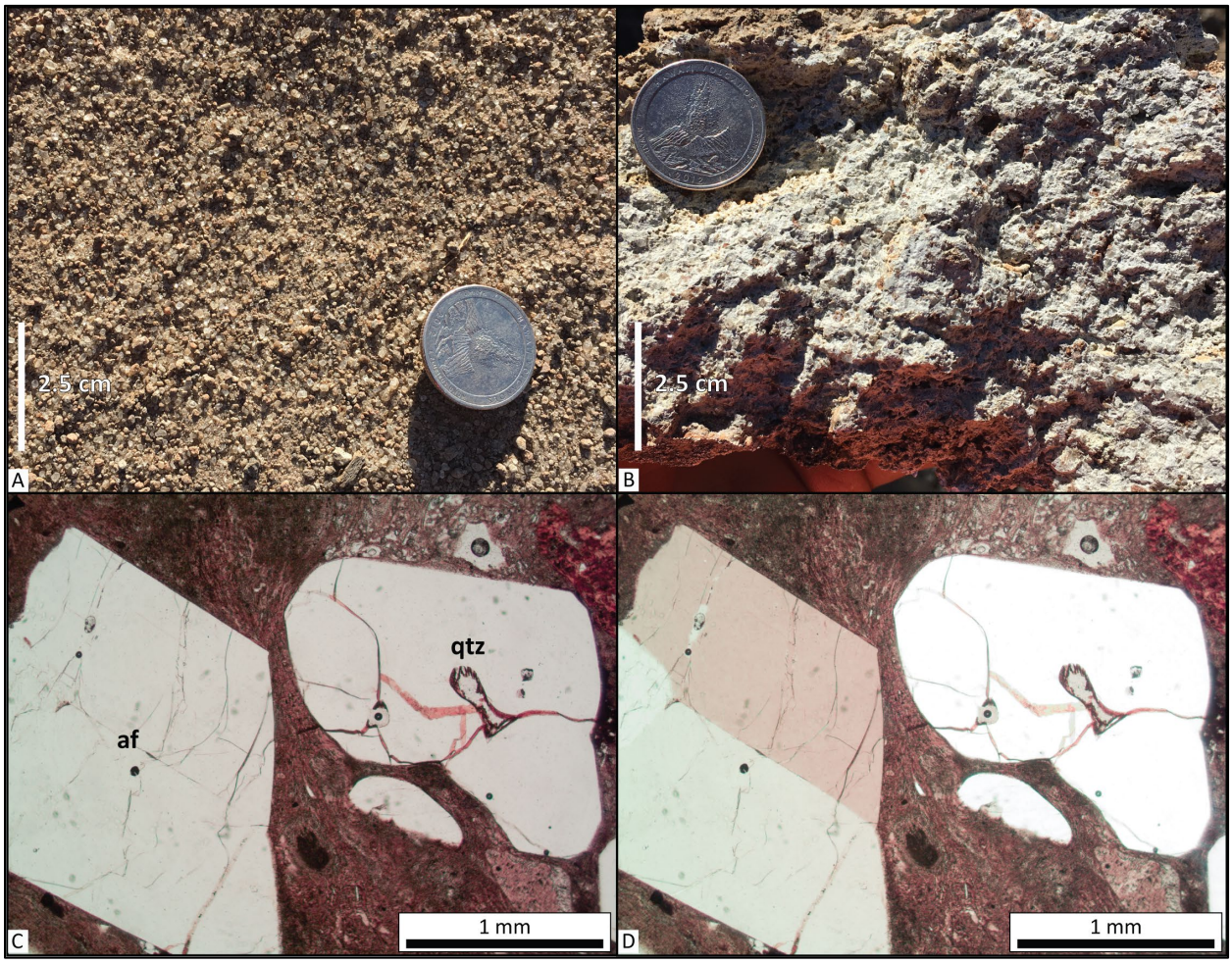

Tmst **tuffaceous sedimentary rocks (upper Miocene)**—Tuffaceous mudstone, siltstone, sandstone, conglomerate and fluvially reworked tuff beds, pumice tuff, and air-fall tuff interbedded with the Devine Canyon Ash-flow Tuff (**Tmtd**), Prater Creek Ash-flow Tuff (**Tmtp**), and the unit-capping Rattlesnake Tuff (**Tmtr**) (**Figure 5-4; Figure 5-31**). Fine- to coarse-grained, thinly bedded and well- to poorly-sorted sandstone layers contain ripple marks and trough cross-bedding. The unit is as much as 27 m (90 ft) thick in the map area, with the thickest exposed sections occurring between **Tmtd** and **Tmtp** along Mahogany Ridge in the northwest part of the Poison Creek 7.5′ quadrangle (Plate 1; cross section A-A′). The unit thins and thickens throughout much of the Poison Creek area and is largely absent from the interval between **Tmtp** and **Tmtr** across much of the northern part of the Poison Creek 7.5′ quadrangle (Plate 1). Thicker accumulations of **Tmst**

are found along this stratigraphic horizon in the southern part of the Poison Creek 7.5′ quadrangle (Plate 1) and into the northern part of the Burns 7.5′ quadrangle (Plate 2), suggesting thickening of the unit beneath the Harney Basin.

Samples of pumices obtained from this unit in the stratigraphic horizon above Devine Canyon Ash-flow Tuff (**Tmtd**) and below Prater Creek Ash-flow Tuff (**Tmtp**) have an altered rhyolitic chemical composition with very high loss on ignition (LOI) and low original analytical totals (Total_I). Trace-element concentrations from these pumices are comparable to Prater Creek Ash-flow Tuff (**Tmtp**) samples, with 469 to 492 ppm Zr and 33.3 to 38.3 ppm Nb (**Table 5-1**).

Tuffaceous sedimentary rocks (**Tmst**) are assigned a late Miocene age on the basis of stratigraphic position and bracketing by precisely dated tuff marker beds. Partly equivalent to Td (Danforth Formation) of Piper and others (1939), Tst (sedimentary rocks) of Greene (1972); sedimentary rocks overlying Tdv (welded tuff of Devine Canyon) of Greene (1972) and Greene and others (1972), Tst (tuffaceous sedimentary rocks and tuff) of Walker (1977), and Tmst-1, -2, and -3 (tuffaceous sedimentary rocks) of Brown and others (1980a).

Angular unconformity to disconformity

Figure 5-31. Outcrop of tuffaceous sedimentary rocks (Tmst) in the Poison Creek 7.5′ quadrangle (Plate 1; 43.64680, –119.07507 WGS84 geographic coordinates; 332646mE, 4834738mN WGS84 UTM Zone 11 coordinates). The section exposed here in a panoramic photograph shows several meters of massive, white (N9) air-fall tuff overlain by semi-consolidated grayish orange (10YR 7/4) tuffaceous claystone and siltstone containing obsidian and pumice fragments. A paleosol is present at the top of the Tmst section. The outcrop section is capped by the Rattlesnake Tuff (Tmtr). A normal fault cuts Tmst and Tmtr along the northern part of the outcrop, offsetting the units by ~ 0.5 m (~1.6 ft). U and D symbols are relative up and down along the fault, respectively. Scale bar is 2 m (6.6 ft) tall. View is looking northeast. Photo credit: Carlie J.M. Duda, 2019.

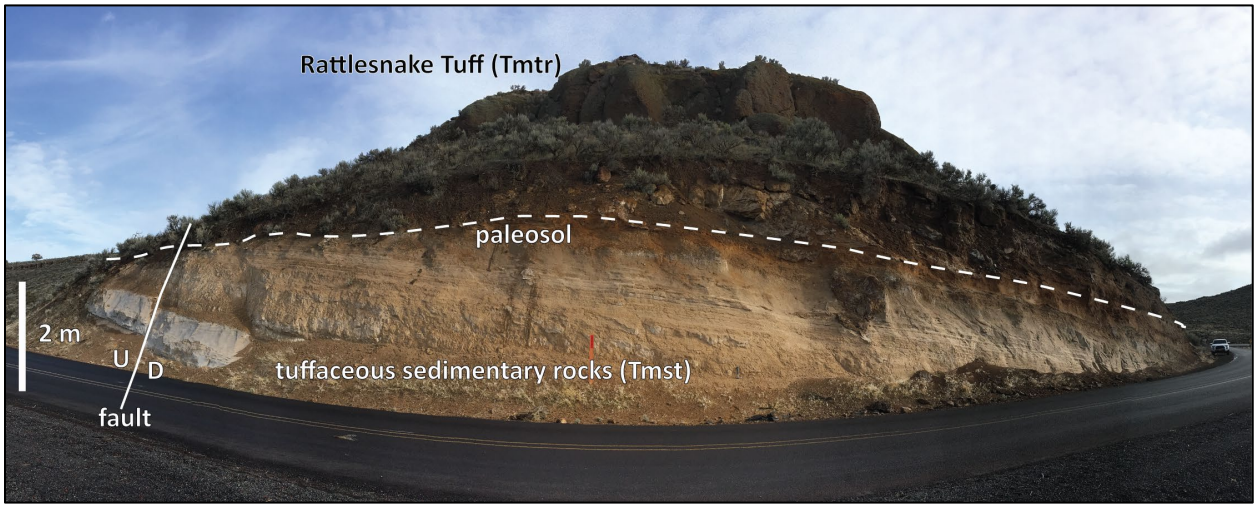

6.0 EXPLORATION WELLS

6.1 Introduction

Several deep wells have been drilled in the central and western parts of the Harney Basin, near the city of Burns, for the purposes of oil and gas exploration, geothermal testing, and groundwater monitoring (**Figure 6-1**, **Figure 6-2**). Cuttings retained for the Federal 1-10 and #1 Fay wells by DOGAMI and cuttings archived by OWRD for the CTI and HARN 52247 EOARC wells provide direct and detailed evidence about subsurface stratigraphic relationships in the Poison Creek and Burns 7.5′ quadrangles (**Figure 6-2**; Plates 1 and 2). Primary lithologic logs for other wells that do not have existing cuttings, like the Weed and Poteet #1 and Voglar #1 wells, can be reasonably although not unequivocally interpreted on the basis of knowledge of geologic relationships at the surface (**Figure 6-2**). **Table 2-1** shows a listing of exploration, test, and observation wells in this part of the Harney Basin. The following sections describe well history and stratigraphic interpretations of available data. Additional information on these wells is available from DOGAMI and OWRD, and specific web links are provided in individual well descriptions below.

Figure 6-1. Locations of deep exploration wells in the west-central Harney Basin. Yellow circles are located oil and gas exploration, geothermal test, and groundwater observation wells. TD is total depth of well in feet (ft) and meters (m). Solid white lines are the boundaries of the 7.5′ quadrangles mapped during this study. Dashed white line is the concealed eastern margin of the Silvies River caldera. Basemap is an oblique Google Earth™ landscape image. View of the image is looking due north.

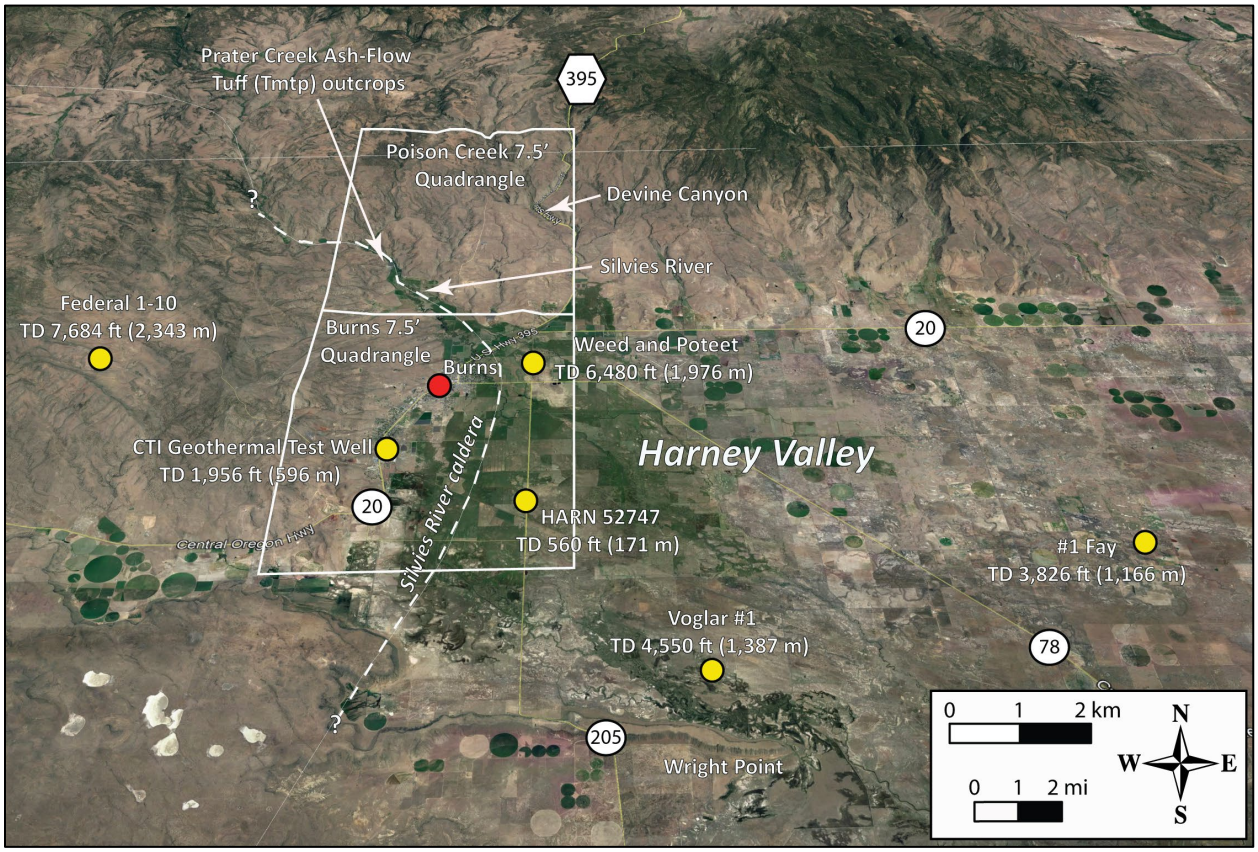

Figure 6-2. Interpreted stratigraphic logs for deep exploration wells in the west-central Harney Basin (next page). Vertical scale bars show true elevation and depth from collar of downhole intervals. Red-filled circles are stratigraphic horizons in exploration wells where XRF geochemical analyses have been obtained. Vertical red-dashed line separating the CTI and Weed and Poteet wells is the concealed eastern margin of the Silvies River caldera. The reader should note that in the absence of existing cuttings, units in the Weed and Poteet well are inferred on the basis of surrounding stratigraphic and lithologic relationships compared to primary lithologic mud logs recorded at the time of drilling. Unequivocal down-hole interpretations require direct examination of cuttings and subsequent geochemical analysis of primary volcanic units, as was completed during this study for the Federal 1-10, CTI, and Fay wells.

Figure 6-2. (Interpreted stratigraphic logs for deep exploration wells in the west-central Harney Basin – caption on previous page)

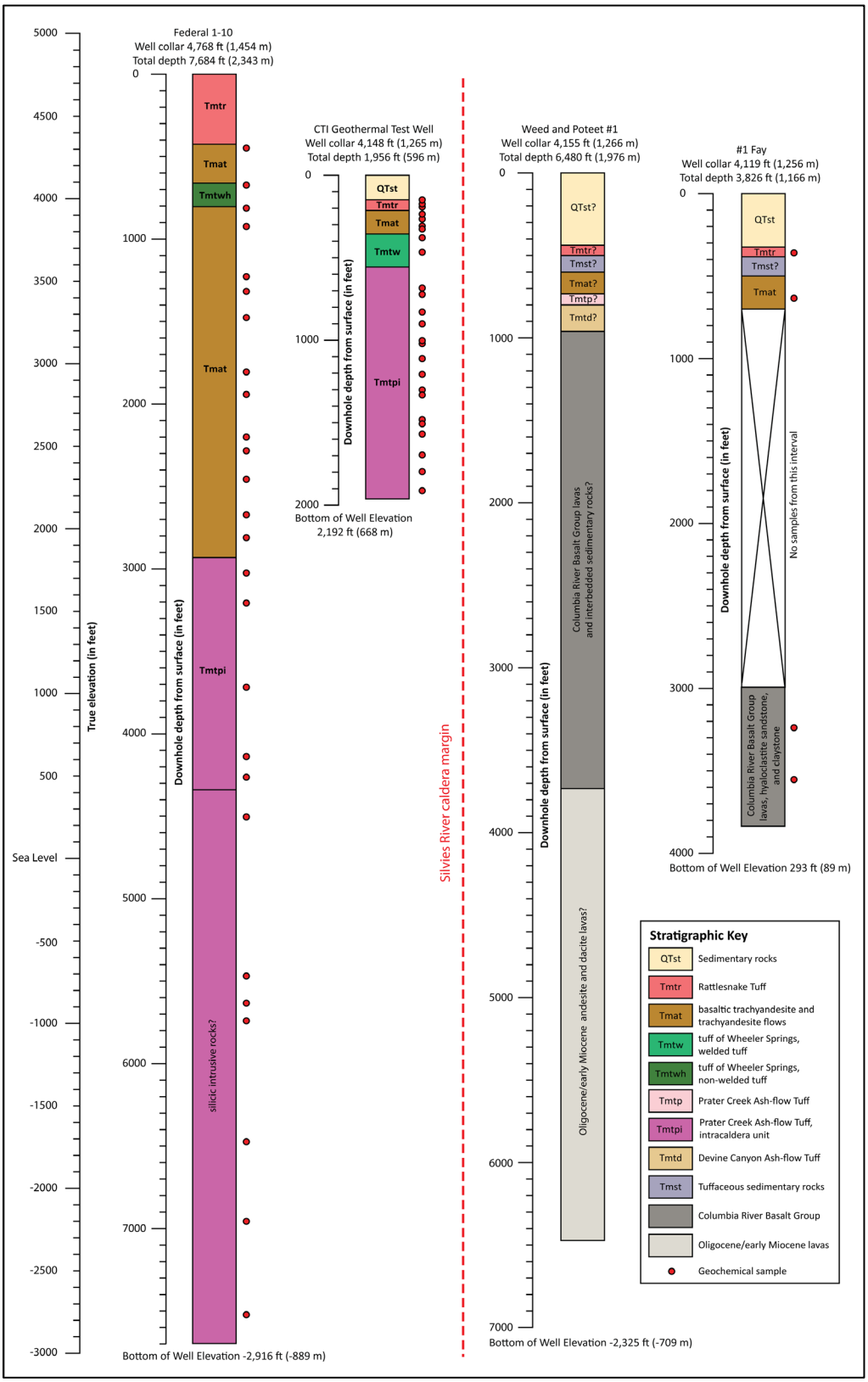

6.2 Michael T. Halbouty Federal 1-10 (HARN 52703)

The Michael T. Halbouty Federal 1-10 well was drilled by the Hunnicut and Camp Drilling Company ~13.5 km (~8.5 mi) west of Burns between June and September 1977 (Burns Butte 7.5′ quadrangle; **Table 2-1**; **Figure 2-3**, **Figure 6-1**, **Figure 6-2**). Total depth of the well is 2,343 m (7,684 ft). Elevation of the well collar is 1,454 m (4,768 ft, lidar). Cuttings in DOGAMI archives exist for the depth interval between 131 m (430 ft) and 2,326 m (7,630 ft) below land surface. Available data from DOGAMI and OWRD include the notice of intention to drill new well, drilling proposal, application for permit to drill new well or stratigraphic hole, plat of a survey for a proposed oil well drilling site, history of oil or gas well, log and core record of oil or gas well, mud log, dip meter log, temperature-depth log, sundry notices, spontaneous potential/conduction/resistivity logs, compensated neutron-formation density logs, and plugging record. Original log and core records report a section of undifferentiated Tertiary volcanics, including basalts, andesites, and tuffs. We reexamined the cuttings of the Federal 1-10 well and analyzed 26 stratigraphic intervals for major and trace element XRF geochemistry (**Figure 6-2**).

The Federal 1-10 well was spudded in Rattlesnake Tuff and penetrates 2,343 m (7,684 ft) of volcanic rock. Cuttings begin at a depth of 131 m (430 ft), where the borehole penetrated mafic lavas. The sequence from 131 m (430 ft) to 899 m (2,950 ft) penetrated a sequence of basaltic trachyandesite, trachyandesite, and trachydacite lavas, and an obsidian-clast vitric ash-flow tuff. Cuttings from 140 m (460 ft) are from a gray, aphyric basaltic trachyandesite that correlates with unit **Tmat.** An ~45 m (150 ft) thick, non-welded, obsidian-clast vitric ash-flow tuff underlies the basaltic trachyandesite at 204 m (670 ft) depth. Analyzed cuttings from the 204 to 213 m (670 to 700 ft) interval indicate the tuff is a peraluminous rhyolite correlative with the non-welded phase of the tuff of Wheeler Springs (**Tmtwh**), with 73.88 weight percent SiO_2, 227 ppm Zr, and 25.2 ppm Nb. At a depth of 250 m (820 ft), the Federal 1-10 borehole entered a series of interbedded basaltic trachyandesite and trachyandesite lavas, separated by thin tuffaceous and mafic scoria interbeds. Samples from 250 m (820 ft) and 287 m (940 ft) are basaltic trachyandesites that again resemble the basaltic andesites of unit **Tmat.** The more mafic flows overlie a thick sequence of trachyandesite lavas that extends over the depth interval of 366 to 518 m (1,200 to 1,700 ft). Cuttings from 543 m (1,780 ft) include tuff fragments. A porphyritic trachydacite lava extends from 552 to 662 m (1,810 to 2,170 ft). From 662 to 899 m (2,170 to 2,950 ft), porphyritic trachydacite is underlain by a section of interbedded basaltic trachyandesite, trachyandesite and trachydacite lavas. The complete section from the top of the logged hole at 126 to 899 m (414 to 2,950 ft) conspicuously lacks interbedded sedimentary rocks.

The interval from 899 to 1,326 m (2,950 to 4,350 ft) is interpreted to be rheomorphic, intracaldera ash-flow tuff (**Tmtpi**) within the Silvies River caldera, the top of which is defined by a banded rhyolite breccia. Five analyzed samples over an interval extending from 927 to 1,302 m (3,040 to 4,270 ft) indicate a single, remarkably monotonous and homogenous tuff unit characterized chemically by 75.44 to 78.00 weight percent SiO_2, 419 to 479 ppm Zr, and 36.0 to 42.0 ppm Nb. Major and trace element abundances closely resemble those obtained from the Prater Creek Ash-flow Tuff (**Tmtp**) exposed widely across the Harney Basin (**Table 5-1**; **Figure 2-3**, **Figure 5-7**). Like the CTI well, grain mount thin sections of cuttings from this interval display granophyric textures, indicative of a devitrified densely welded rheomorphic tuff (**Figure 5-28**). Cuttings from the underlying sequence that extends downward from 1,326 m (4,350 ft) display vitroclastic and lithophysal textures. An analyzed sample from the lower tuff contains 77.00 weight percent SiO_2, 190 ppm Zr, and 32.5 ppm Nb, more closely resembling the younger Rattlesnake Tuff (**Tmtr**). The remaining lower 854 m (2,800 ft) of cuttings in the Federal 1-10 well records a sequence of variably altered and compositionally diverse high-silica rhyolite that continues to the bottom of the hole

at 2,326 m (7,630 ft). A sample from near the bottom of the hole at 2,299 m (7,540 ft) contains 72.56 weight percent SiO_2; 107 ppm Zr, and 35.3 ppm Nb. Some of the cuttings from the lower part of the Federal 1-10 well contain muscovite and biotite in addition to quartz and alkali-feldspar.

Additional detailed information about this well is available from DOGAMI at https://www.oregongeology.org/mlrr/oilgas-logs.htm and from OWRD at https://apps.wrd.state.or.us/apps/gw/gw_info/gw_info_report/gw_details.aspx?gw_site_id=30493.

6.3 CTI Geothermal Test Well (HARN 50087)

The HARN 50087 CTI Geothermal Test well was drilled at the old Edward Hines Lumber Co. mill site at the south end of Hines between March and August 1996 (Burns 7.5′ quadrangle; Plate 2; **Table 2-1**; **Figure 2-3**, **Figure 6-1**, **Figure 6-2**). Total depth of the well is 596 m (1,956 ft). Elevation of the well collar is 1,265 m (4,148 ft, lidar). The primary purpose of the hole was exploration for geothermal water; it was situated to intersect a projected fault at depth. Cuttings for this well, at 3 m (10 ft) intervals, for well depth 43 to 596 m (140 to 1,956 ft) were provided to DOGAMI by OWRD. Available data from OWRD include the water supply well report, engineering schematics for the well, cuttings descriptions, and site photographs. We reexamined the cuttings of the CTI well and analyzed 25 stratigraphic intervals for major and trace element XRF geochemistry (**Figure 6-2**).

Cuttings begin at 43 m (140 ft), where the well penetrated a 6 m (20 ft) thick light brownish gray (5YR 6/1) welded ash-flow tuff with numerous lithic fragments and white feldspar crystals. A single geochemical analysis from this interval shows the rock is altered, with very high loss on ignition (LOI) and low original analytical totals (Total_I). Trace element concentrations in the sample from this interval are similar to the Rattlesnake Tuff (**Tmtr**), but with lower Zr (206 ppm) and Nb (19.8) (see geochemical data in geodatabase and appendix). Samples between the depth interval of 48 and 64 m (160 and 210 ft) consist of a mixture of pinkish gray (5YR 8/1) to white (N9) semi-consolidated tuff and very pale orange (10YR 8/2) pumice. Two geochemical analyses from this interval have very high loss on ignition (LOI) and low original analytical totals (Total_I) and are therefore interpreted to have altered major element concentrations. Trace element concentrations of samples from this interval are comparable to the Rattlesnake Tuff (**Tmtr**) with 260 to 281 ppm Zr and 27.6 to 29.0 ppm Nb. Samples between the depth interval of 64 and 107 m (210 and 350 ft) are yellowish gray (5Y 8/1), medium gray (N6), and moderate orange pink (10R 7/4) to light brownish gray (5YR 6/1) dense basaltic trachyandesite and interbedded cinders. Analyzed fresh cuttings from the this interval indicate a correlation with unit **Tmat** (basaltic trachyandesite and trachyandesite), with 56.37 to 57.10 weight percent SiO_2, 146 to 154 ppm Zr, and 10.3 to 10.7 ppm Nb (**Table 5-1**; **Figure 2-3**, **Figure 5-7**). At 106 to 158 m (350 to 550 ft) the well intersects a 61 m (200 ft) thick section of very light gray N8 to pinkish gray 5YR 8/12 strongly welded rheomorphic tuff with 73.47 to 75.25 weight percent SiO_2, 242 to 246 ppm Zr, and 27.3 to 29.8 ppm Nb (**Table 5-1**; **Figure 2-3**, **Figure 5-7**). Geochemical analyses from this interval are identical to the tuff of Wheeler Springs (**Tmtw**) (Plate 2, cross section B-B′). The interval from 168 to 596 m (550 to 1,956 ft) is lithologically homogeneous, but variably colored yellowish gray (5Y 8/1), pinkish gray (5YR 8/1), light brownish gray (5YR 6/1), medium light gray (N6), to dark gray (N3) rheomorphic ash-flow tuff. The tuff is grayish blue green (5BG 5/2) and dark reddish brown (10R 3/4) where altered. The top of the tuff is defined by a banded rhyolite breccia. Sixteen analyzed samples over this interval indicate a single, remarkably monotonous and homogenous unit with 75.37 to 77.40 weight percent SiO_2, 439 to 530 ppm Zr, and 35.8 to 44.0 ppm Nb. Major and trace element abundances closely resemble those in the Prater Creek Ash-flow Tuff exposed widely across the Harney Basin (**Table 5-1**; **Figure 2-3**, **Figure 5-7**). Grain

mount thin sections of cuttings from this interval display granophyric textures, indicative of a devitrified densely welded rheomorphic tuff (**Figure 5-28**). Three samples from the interval 515 to 591 m (1,690 to 1,940 ft) are lithologically identical and chemically similar to the above interval with 74.46 to 77.00 weight percent SiO_2 and 38.2 to 47.0 ppm Nb, but with slightly higher amounts of Zr (576 to 712 ppm). The interval is interpreted to be rheomorphic, intracaldera ash-flow tuff within the Silvies River caldera (**Tmtpi**). **Tmtpi** forms the base of the CTI well and may be of considerably greater thickness (**Figure 6-2**; Plate 2, cross section B-B′).

Additional detailed information about this well is available from OWRD at https://apps.wrd.state.or.us/apps/gw/gw_info/gw_info_report/gw_details.aspx?gw_site_id=12735.

6.4 United Company of Oregon, Inc., Weed and Poteet #1 (HARN 52707)

The Weed & Poteet Well #1 well was drilled ~3 km (~1.9 mi) east-northeast of Burns between January 1949 and November 1950 (Burns 7.5′ quadrangle; Plate 2; **Table 2-1**; **Figure 2-3**, **Figure 6-1**, **Figure 6-2**). Total depth of the well is 1,976 m (6,480 ft). Elevation of the well collar is 1,266 m (4,155 ft, lidar). No cuttings exist for this well in DOGAMI archives. Available data from DOGAMI and OWRD include well summary sheet, well summary report, log and core record, description of cuttings, composite log, log of the well, description of fluorescence samples, spontaneous potential/conduction/resistivity logs, casing record, bit record, drilling time, and history of oil or gas well. Original log and core records report a section of undifferentiated Tertiary volcanics and sedimentary rocks, including thick sections of shales, clay, sands, conglomerate, tuffs, ash, lavas, and agglomerate. Cuttings do not exist for direct analysis, but detailed lithologic logs (10 ft intervals) and a downhole resistivity log allow for interpretations of the stratigraphic sequence in the Weed and Poteet well. Interpretations are not unequivocal, but when compared with a detailed knowledge of the adjacent stratigraphic section reasonable inferences can be made about the downhole stratigraphy.

Projection of the south-dipping late Miocene section from the Poison Creek 7.5′ quadrangle, south through Weed and Poteet well to the HARN 52747 EOARC well, where the Rattlesnake Tuff (**Tmtr**) has been geochemically fingerprinted in the 159 to 168 m (520 to 550 ft depth interval), suggests flattening of the section to near horizontal beneath the Harney Valley. This stratigraphic projection suggests that the Rattlesnake Tuff (**Tmtr**) should be encountered at the 131 to 152 m (430 to 500 ft) depth interval of the Weed and Poteet well. The 131 m (430 ft) horizon of the Weed and Poteet well corresponds to an interval in the cuttings records where mud loggers describe a transition from “sand and gravel and tuffaceous shale and clay” to “soft white brown and coffee colored tuffaceous clay; conglomerate imbedded in clay.” Down to 152 m (500 ft) the section includes “soft white tan and coffee colored clay,” “hard light tan to yellow altered material,” “a little volcanic tuff,” and “more pure white clay (altered ash).” The section between the surface collar of the well down to 131 m (430 ft) is interpreted here as surficial sediments of the “Silvies River fan” (**Qfd**) overlying basin-fill sedimentary rocks (**QTst**). The underlying interval from 131 to 152 m (430 to 500 ft) is interpreted as the Rattlesnake Tuff (**Tmtr**). Between 152 and 183 m (500 and 600 ft) the cuttings log describes intervals of white to light yellow or salmon-colored clay and shales that may be correlative with tuffaceous sedimentary rocks of unit **Tmst**. Sedimentary rocks (**Tmst**) overlie an interval between 183 and 232 m (600 to 760 ft) described as vari-colored lavas with some brick red colored lavas and altered material. This interval we interpret as correlative with basaltic trachyandesite and trachyandesite lavas (**Tmat**) erupted from shield volcanoes forming the low hills west of the city of Burns. Cuttings described in the interval 232 and 244 m (760 and 800 ft) are described as “sandy conglomerate with fine clear quartz crystals,” “tuff and varicolored clay,” “clay,” and “clay with

leaflike material" interpreted as Prater Creek Ash-flow Tuff (**Tmtp**). Descriptions from the depth interval of 244 to 295 m (800 to 970 ft) note an "abundance of clear fine quartz crystals, "high quartz content," or "quartz embedded in clay." These descriptions resemble the highly porphyritic nature of the Devine Canyon Ash-flow Tuff (**Tmtd**), where hand samples contain as much as 30 percent crystals and crystal fragments of dominantly alkali feldspar and lesser quartz. Below 295 m (970 ft), cuttings descriptions describe many horizons of gray and grayish black lava, intermixed with variable amounts of sand, shale, agglomerate, and ash. These units are likely to be multiple thin mafic flows of Columbia River Basalt in a similar stratigraphic horizon to those exposed beneath the Devine Canyon Tuff (**Tmtd**) in the uplands of the northern Harney Basin (R. Houston and others [unpub. data, 2016]). At 366 m (1,200 ft) below land surface, mafic lavas are described to overlie an ~82 m (~270 ft) thick tuffaceous unit containing obsidian. Inferred stratigraphic position, suggests this tuffaceous section unit could be correlative with the Dinner Creek tuff, which contains abundant and conspicuous dark gray pumice fragments (R. Houston and others [unpub. data, 2016]). The obsidian clast unit overlies a glassy to grayish black lava that persists from 451 to 465 m (1,480 to 1,525 ft). Lost circulation zones separate the lava from a section that is described as very hard, grayish white, altered sediments that lie between 485 to 527 m (1,590 and 1,730 ft).

Although difficult to interpret, there appears to be a general transition from a sequence of light colored tuffaceous units to a darker shale-dominated sequence that resembles the 945 to 1,098 m (3,100 to 3,600 ft) interval in the #1 Fay well (**Table 2-1**; **Figure 2-3**). Well logs indicate that the transition occurs at about 688 m (2,255 ft) in the Weed and Poteet well. A sample taken from 716 m (2,350 ft) is described in the Weed and Poteet lithologic log as being similar to cuttings taken from the 915 m (3,000 ft) interval in the #1 Fay well. Intervals within the darker shale-dominated sequence at 715 m (2,345 ft) are described to contain black altered material, bentonitic clays, and occasional fish bones. Harder black "altered material" could be descriptive of thin olivine basalt flows similar to those analyzed and correlated with Columbia River Basalt in the #1 Fay well. The darker shale interval persists to a depth of 1,140 m (3,740 ft), where mud loggers describe a transition into a sequence dominated by lava flows. The lithologic log from 1,140 m (3,740 ft) to the bottom of the hole at 1,976 m (6,480 ft) describes generally grayish black lavas with shale and volcanic agglomerate interbeds. These units could be correlative with late Oligocene (ca. 24 to 22 Ma) andesites and dacites exposed in the highlands of the northern part of the Harney Basin (Niewendorp and others, 2018; Houston and others, 2018).

Additional detailed information about this well is available from DOGAMI at https://www.oregongeology.org/mlrr/oilgas-logs.htm and from OWRD at https://apps.wrd.state.or.us/apps/gw/gw_info/gw_info_report/gw_details.aspx?gw_site_id=30497.

6.5 EOARC Observation Well (HARN 52747)

The HARN 52747 EOARC (Eastern Oregon Agricultural Research Center) observation well was drilled ~7 km (~4.3 mi) southeast of Burns (Burns 7.5′ quadrangle; Plate 2) in September 2018 (**Table 2-1**; **Figure 2-3**, **Figure 6-1**, **Figure 6-2**). Total depth of the well is 171 m (560 ft). Elevation of the well collar is 1,261 m (4,135 ft, lidar). The primary use of the well is groundwater monitoring and observation in this part of the Harney Basin. Lithologic description of the upper 52 m (170 ft) of the well by OWRD reports a mixture of fine sand, dark clay, occasional thin coarse sand/gravel layers, and gray silt. These deposits are likely to be modern-fill basin sediments related to our marsh and alluvial deposit unit (**Qma**). The interval between 52 and 152 m (170 and 500 ft) is composed of "medium stiff" dark gray clay, medium to coarse sand, laminated silty clay, hard brittle dark gray to black siltstone, multi-colored silty clay, and thin horizons of white glassy ash layers. Medium stiffness or brittle character of these strata suggests

consolidation of older sediments, which are here interpreted as part of **QTst**. Ash-flow tuff cuttings from the 159 to 168 m (520 to 550 ft depth interval) have been analyzed and geochemically characterized by XRF. Trace element data from two samples correlate this horizon with the Rattlesnake Tuff (**Tmtr**) with 238 to 299 ppm Zr and 25.4 to 26.3 ppm Nb. Additional detailed information about this well is available from OWRD at https://apps.wrd.state.or.us/apps/gw/gw_info/gw_info_report/gw_details.aspx?gw_site_id=31110.

6.6 United Company of Oregon, Inc., #1 Fay

The United Company of Oregon, Inc., #1 Fay well was drilled ~25.5 km (~15.5 mi) southeast of Burns in February 1945 (Ninemile Slough 7.5′ quadrangle; **Table 2-1**; **Figure 2-3**, **Figure 6-1**, **Figure 6-2**). Total depth of the well is 1,166 m (3,826 ft). Elevation of the well collar is 1,256 m (4,119 ft, lidar). Cuttings in DOGAMI archives exist largely from an interval between 915 m (3,000 ft) and the bottom of the hole, which were originally believed to have indications of hydrocarbons. Core boxes included just two samples from above 915 m (3,000 ft); one sample is a zeolitized welded tuff at a depth of 108 m (355 ft) and the other is a sample of mafic lava recovered from a depth of 192 m (630 ft). Available data from DOGAMI are limited to a self-potential and resistivity log. We reexamined the available cuttings of the #1 Fay well and analyzed four stratigraphic intervals for major and trace element XRF geochemistry. The zeolitized welded tuff at a depth of 108 m (355 ft) has a high loss on ignition (LOI) and low original analytical total (Total_I) and is therefore interpreted to have altered major element concentrations. Trace element concentrations of this tuff interval are comparable to the Rattlesnake Tuff (**Tmtr**) with 248 ppm Zr and 23.0 ppm Nb. Mafic lava recovered from a depth of 192 m (630 ft) is a trachyandesite with a chemical composition comparable to unit **Tmat** (basaltic trachyandesite and trachyandesite flows and dikes) in the Burns area, with 57.77 weight percent SiO_2, 188 ppm Zr, and 14.5 ppm Nb. The well sequence below 915 m (3,000 ft) is predominately moderate brown (5YR 3/4) to moderate yellowish-brown (10YR 5/4), fine- to medium-grained hyaloclastite sandstone and claystone with thin interbedded olivine basalt lavas. Samples from 986 m (3,235 ft) and 1,085 m (3,560 ft) are olivine basalts with 51.31 to 52.62 weight percent SiO_2, 16.33 to 17.03 weight percent Al_2O_3, and 5.40 to 6.20 weight percent MgO. Major and trace element abundances closely resemble HAOT (high-alumina olivine tholeiites; Columbia River Basalt) collected at the surface beneath the Devine Canyon Tuff (**Tmtd**) in the uplands of the northeastern and eastern margins of the Harney Basin (R. Houston and others, unpub. data, 2016). Additional detailed information about this well is available from DOGAMI at https://www.oregongeology.org/mlrr/oilgas-logs.htm.

6.7 H.C. Voglar No. 1 (HARN 52706)

The H.C. Voglar No. 1 well was drilled by the I.W. Love Drilling Company ~18.5 km (~11.5 mi) south-southeast of the city of Burns near Wright Point in the Harney Basin between December 1949 and August of 1950 (Redress 7.5′ quadrangle; **Table 2-1**; **Figure 2-3**, **Figure 6-1**). Total depth of the well is 1,387 m (4,550 ft). Elevation of the well collar is 1,265 m (4,148 ft, lidar). No original cuttings from the well exist in DOGAMI's archives. Available data from DOGAMI and OWRD include the notice of intention to drill new well, well summary sheet, well summary report, log and core record of oil or gas well, and history of oil or gas well. The available driller log is not unequivocal, describing large intervals of sand interbedded with shale, sandy shale, hard lime, hard lime and chert, hard sand and shale, shale with streaks of sand, hard sand, lime, and streaks of volcanic ash, basalt (?), and sand. The well report summary sheet reports

geological markers encountered to include 1) Danforth Formation between depths of ±274 m and 488 m (±900 and 1,600 ft); 2) Steens basalt between 488 and 793 m (1,600 to 2,600 ft), 3) older silicic extrusions between 945 and 1,174 m (3,100 to 3,850 ft); 4) Pre-Tertiary sediments from 1,174 m (3,850 ft) to the bottom of the hole. The well summary report sheet indicates that geological markers were obtained by using formation thickness reported by Piper and others (1939) correlated with the well's electric log.

Additional detailed information about this well is available from DOGAMI at https://www.oregongeology.org/mlrr/oilgas-logs.htm and from OWRD at https://apps.wrd.state.or.us/apps/gw/gw_info/gw_info_report/gw_details.aspx?gw_site_id=30496.

6.8 Dog Mountain

The Central Oregon Oil and Gas Company Dog Mountain well was drilled ~12 km (~7.5 mi) south of the city of Burns starting in 1912 (Dog Mountain 7.5′ quadrangle; **Table 2-1**). Buwalda (1921) visited the site around that time and reported the hole had reached a depth of 1,147 m (3,763 ft). "The well was said to have given a little gas and to have shown a trace of oil" (Buwalda, 1921). Buwalda (1921) reported that the rocks into which the hole was being drilled included volcanic material composed of basic volcanic agglomerate, tuff and ash, and some basic lava. Detailed lithologic logs or archived cuttings do not exist for the Dog Mountain well.

7.0 STRUCTURE

7.1 Introduction

Geologic structures in the Poison Creek and Burns 7.5′quadrangles are recognized from offset between mapped geologic contacts, repeated sections, topographic lineaments (as observed in the field and in 1-m lidar DEMs, 10-m DEMs, and 2016 NAIP photographs), changes in bedding attitudes, alignment of springs, and subsurface lithologic data obtained from water and exploration wells (Plates 1 and 2; **Table 2-1**; **Figure 7-1**). Primary structural features (e.g., slickensides or fault breccia) are rarely observed in the field. Difficulties recognizing faults in the ash-flow tuffs and tuffaceous sedimentary rocks arise because 1) lateral facies changes in these rocks can be abrupt, including rapid depositional thickening and thinning as units are emplaced, 2) fault planes are not expected to be well preserved in moderately weakly indurated strata, 3) those faults observed often have small offsets (less than several centimeters to several meters in many cases), 4) separation of beds can be difficult to determine in the field, and 5) areas of distinctly contrasting lithology are rarely exposed.

Figure 7-1. Faulted cliff- and bench-forming Rattlesnake Tuff (Tmtr) in the Poison Creek 7.5′ quadrangle (Plate 1). (43.63529, −119.11974 WGS84 geographic coordinates; 4833550mN, 329011mE WGS84 UTM Zone 11 coordinates). The section exposed here is offset by several small-displacement, down-on-the-west normal fault strands (solid white lines). Dashed white lines are geologic contacts between unit Tmtr and Tmst. U and D symbols are relative up and down along normal fault strands. View is looking northeast. Photo credit: Jason D. McClaughry, 2018.

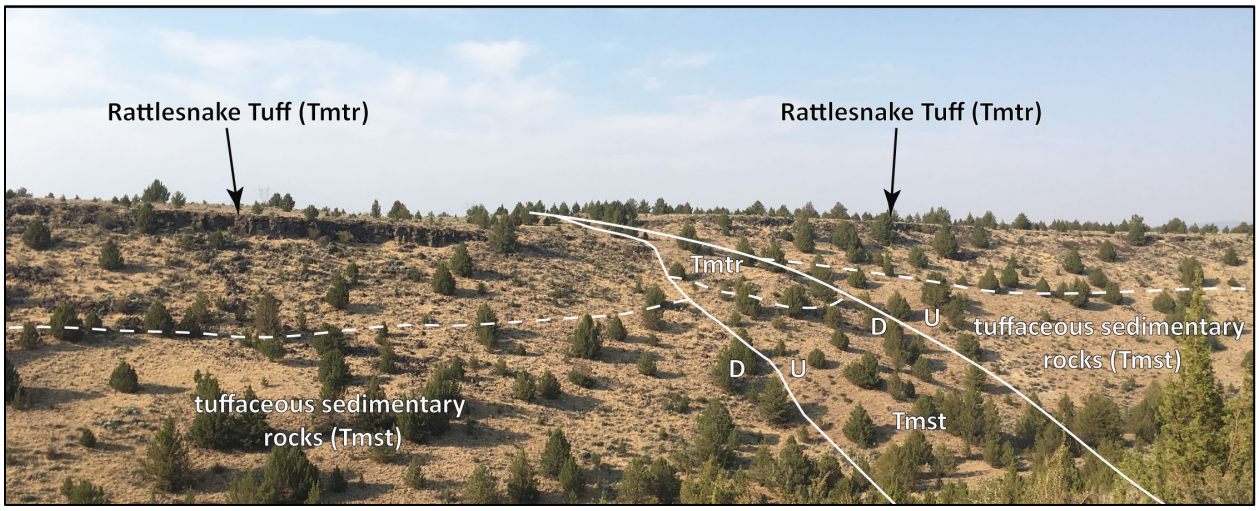

7.2 Faulting in the Poison Creek and Burns 7.5′ quadrangles

The Poison Creek and Burns 7.5′ quadrangles are underlain by a southerly dipping, stratigraphic section of three extensive late Miocene ash-flow tuffs (**Tmtr**, **Tmtp**, **Tmtd**) and interbedded tuffaceous sedimentary rocks (**Tmst**) (**Figure 1-1**; **Figure 2-2**; **Figure 2-3**; Plates 1 and 2). Older rocks, including early to middle Miocene tholeiitic lavas, late Oligocene to late Miocene calc-alkaline andesites and dacites, and pre-Cenozoic terranes are exposed beneath the ash-flow tuff sequence as the dip slope rises in highlands just to the north of the Poison Creek 7.5′ quadrangle. South into the Harney Basin, the south-dipping stratigraphic section flattens out across a broad monocline (Plates 1 and 2).

East of the Poison Creek and Burns 7.5′ quadrangles, in the Devine Ridge North and South 7.5′ quadrangles, the south-dipping section of ash-flow tuffs is cut by a predominant set of steeply dipping, north-striking dextral oblique strike-slip faults (Houston and others, 2018; Niewendorp and others, 2018). Houston and others (2018) and Niewendorp and others (2018) referred to these as the Trout Creek and Soldier Creek fault zones, respectively. Windows of older upper Oligocene stratigraphy in those areas, are surrounded by younger rocks, suggesting the development of a significant paleo-topography prior to the deposition of the late Miocene Devine Canyon Ash-flow Tuff (**Tmtd**), the oldest rock unit exposed in the Poison Creek 7.5′ quadrangle (Plate 1). Faults east of the study area cut Oligocene and Miocene aged rocks but are much less common in the late Miocene and younger rocks, suggesting that faulting may have been reactivated several times along selected structures through the late Miocene. West into the study area, few faults are identified cutting the southerly dipping late Miocene stratigraphic section. Those faults identified and mapped are confined to the western edges of both the Poison and Burns 7.5′ quadrangles (Plates 1 and 2). Faults, if present in the eastern half of the Burns 7.5′ quadrangle, are largely buried by Late Pleistocene and Holocene basin-fill sediments.

In the western part of Poison Creek and Burns 7.5′ quadrangles, west of the Silvies River, northwest-trending topographic lineaments are associated with recognizable offsets of cliff- and bench-forming ash-flow tuffs. These features are recognized both in the field and in 1-m lidar DEMs (**Figure 5-31**; **Figure 7-1**; Plates 1 and 2). Relative offsets of northwest-trending faults are in a normal sense, dropping discrete blocks down on the northeast or southwest, forming a number of mini northwest-trending grabens. Over the length of some longer faults in the Burns 7.5′ quadrangle, structures are recognized as scissors faults where direction of offset varies along the strike of the individual strand (Plate 2). Offsets along individual fault strands range from centimeters to tens of meters (**Figure 5-31**; **Figure 7-1**). Most faults cut and postdate emplacement of the 7.093 Ma Rattlesnake Tuff (**Tmtr**). The major scissors fault segment forming the eastern boundary of a mini graben northwest of the city of Burns is interpreted to cross cut younger rocks of unit **QTst**, and therefore displacement is latest Miocene to Quaternary in age (Plate 2).

7.3 Silvies River caldera

The Silvies River caldera, the source caldera for the 8.41 Ma Prater Creek Ash-flow Tuff (**Tmtp**), forms a concealed volcano-tectonic depression that lies buried at depth beneath the city of Burns, extending west into the Burns Butte area. The easternmost concealed ring-fracture zone of the caldera runs roughly north-northwest through the Burns and southwest part of the Poison Creek 7.5′ quadrangles (**Figure 6-1**; Plates 1 and 2). The location and distribution of the structure have been determined through a combination of surface mapping, lithologic investigation and geochemical characterization of numerous intervals from several deep exploration wells in the area, and from review and assessment of existing geophysical data (**Table 2-1**; **Figure 2-3**, **Figure 6-2**).

7.3.1 Evidence for the Silvies River caldera structure

- Monotonous, lithologically, petrographically, and geochemically identical sections of rhyolitic welded tuff are found in both the Federal 1-10 and CTI wells, exceeding 427 m (1,400 ft) in thickness (**Table 2-1**, **Table 5-1**; **Figure 2-3**, **Figure 5-6**, **Figure 5-7**, **Figure 5-28a-f, Figure 6-2**).
- Geochemical analyses compared between surface exposures of the Prater Creek Ash-flow Tuff (**Tmtp**) and thick rhyolitic tuff intervals (**Tmtpi**, intracaldera-fill tuff) in the Federal 1-10 and CTI wells are indistinguishable (**Table 2-1**, **Table 5-1**; **Figure 2-3**, **Figure 5-6**, **Figure 5-7**; **Figure 6-2**).
- Pervasive granophyric textures characterize rhyolitic tuff grains recovered from monotonous tuff intervals in both the Federal 1-10 and CTI wells (**Figure 5-28a-f**). Granophyric textures in tuffs are related to slow cooling and crystallization of formerly glassy components (glass shards and pumice) in the central parts of very thick (several tens to hundreds of meters) or densely welded ignimbrites (McPhie and others, 1993).
- The top of the Prater Creek Tuff caldera-fill sequence (**Tmtpi**) lies at an elevation of 561 m (1,840 ft) asl in the Federal 1-10 well and at 1,096 m (3,598 ft) asl in the CTI well (**Figure 6-1**, **Figure 6-2**; **Table 2-1**). The elevation of the top of the outflow Prater Creek Ash-flow Tuff (**Tmtp**) on the lower Silvies River, 12 km (7.3 mi) northeast of the Federal 1-10 well and 13.2 km (8.2 mi) north of the CTI well is at 1,320 m (4,330 ft) asl. There is 760 m (2,493 ft) of vertical offset between the top of unit **Tmtpi** in the Federal 1-10 well and top of Prater (**Tmtp)** outcrops on the Silvies River and 535 m (1,755 ft) of vertical offset between the top of **Tmtpi** in the Federal 1-10 well and top of **Tmtpi** in the CTI well. The area between the wells and Silvies River

outcrops is buried by post-caldera basaltic trachyandesite and trachyandesite flows (**Tmat)** and Rattlesnake Tuff (**Tmtr**); the two younger units are not cut or offset by any significant mapped surface faults. The lateral relationship between correlative deep well and surface stratigraphy is most simply and best explained by westward-deepening caldera collapse during formation of the Silvies River caldera at 8.41 Ma (**Figure 6-2**)

- There is an inferred stratigraphic discontinuity between the CTI well and the Weed and Poteet #1 well, located 6.9 km (4.3 mi) to the northeast of the city of Burns (**Figure 6-1**, **Figure 6-2;** Plate 2). In the CTI well, the **Tmtpi** rhyolitic tuff sequence is >429 m (>1,406 ft) thick and is directly overlain by ~58 m (190 ft) of silicic tuff correlated with the tuff of Wheeler Springs (**Tmtw**, **Tmtwh**) and farther upwards by ~43 m (~140 ft) of basaltic trachyandesite and trachyandesite, and minor dacite **(Tmat)**; the upper part of the CTI well sequence is capped by Rattlesnake Tuff (**Tmtr**) (**Figure 6-2**). Stratigraphy in the Weed and Poteet #1 is inferred on the basis of lithologic logs (no cuttings are available) to include from top to bottom the local Harney Basin stratigraphic sequence including sedimentary rocks (**QTst**), Rattlesnake Tuff (**Tmtr**), basaltic trachyandesite and andesite lava flows (**Tmat**), outflow Prater Creek Ash-flow Tuff (**Tmtp**), Devine Canyon Ash-flow Tuff (**Tmtd**), and tuffaceous sedimentary rocks (**Tmst**). These units overlie a >915 m (>3,000 ft) thick sequence of rocks presumed equivalent to the middle Miocene Columbia River Basalt, intercalated sedimentary rocks, and older Oligocene andesite and dacite. The inferred stratigraphic discontinuity between the two wells is interpreted to represent the easternmost caldera-bounding fault of the Silvies River caldera, juxtaposing caldera filling tuffs (**Tmtpi**) on the west against older late Oligocene to late Miocene strata on the east (**Figure 6-1**, **Figure 6-2**; Plates 1 and 2, cross sections).
- A bimodal suite of basaltic trachyandesite to trachyandesite lava flows and vent deposits (**Tmat**, **Tmvt**), rhyolitic tuffs (**Tmtw**, **Tmtwh**), and exogenous rhyolite domes and flows (**Tmrg**, **Tmrb**) form a narrow, post-caldera volcanic field above caldera-filling tuffs (**Tmtpi**), along the inferred eastern margin of the Silvies River caldera (**Figure 5-6**; **Figure 5-7**; Plates 1 and 2, cross sections).
- Basaltic trachyandesite and trachyandesite flow (**Tmat**) and vent deposits (**Tmvt**) are almost exclusively confined in their distribution to areas west and south of the Silvies River in the map area (Plates 1 and 2). The restricted distribution of these units is interpreted to be controlled by the low-lying topographic depression of the Silvies River caldera west of the Silvies River (**Figure 6-2**). It is also inferred that the main ring-fracture zone of the eastern part of the Silvies River caldera is a major volcanic-tectonic control determining the course of modern river entrenchment.
- Rheomorphic rhyolitic tuff and rhyolite xenoliths contained within basaltic trachyandesite and trachyandesite flow (**Tmat**) and vent deposits (**Tmvt**) in the area south and west of the Silvies River (Poison Creek 7.5′ quadrangle, Plate 2) are geochemically identical to chemical compositions defining the Prater Creek Ash-flow Tuff (**Tmtp**) across the Harney Basin and those obtained from thick, monotonous rhyolitic tuff intervals in the Federal 1-10 and CTI wells (**Table 5-1**; **Figure 2-3**, **Figure 5-6**, **Figure 5-7**, **Figure 5-14**, **Figure 5-18**, **Figure 5-19, Figure 6-2)**. The presence of the rheomorphic rhyolitic tuff and rhyolite xenoliths in late mafic sequences (**Tmat**, **Tmvt**) indicates cannibalizing of older rocks related to the caldera fill sequence underlying this area.
- Most low-temperature geothermal wells are clustered in the southwestern part of the Burns 7.5′ quadrangle (Plate 2). These wells are spatially associated with the concealed eastern ring-

fracture zone of the Silvies River caldera and late Miocene post-caldera bimodal basaltic trachyandesite and rhyolite volcanic vent complexes.

- West of the Poison Creek and Burns 7.5′ quadrangles (Plates 1 and 2), into the Burns Butte and Burns NW 7.5′ quadrangle, normal fault strands are portrayed by Brown (1982) as curvilinear structures transitioning from northwest-directed to west-northwest trends. The spatial transition of faults from linear northwest-directed features to more curvilinear west-northwest–directed traces corresponds with the interpreted location of the eastern part of the Silvies River caldera (Plates 1 and 2; **Figure 2-2**; **Figure 2-3**). Curvilinear faults shown by Brown (1982) offsetting Rattlesnake Tuff (**Tmtr**) in the Burns Butte and Burns NW 7.5′ quadrangle are likely older arcuate faults related to the underlying concealed Silvies River caldera, reactivated in post-Rattlesnake time (Post 7.1 Ma).
- Khatiwada and Keller (2015) show a seismic discontinuity at depth where we locate the buried eastern margin of the Silvies River caldera, just to the east of the city of Burns (**Figure 7-2**; Plate 2). Their figure 5F showing an east-west slice taken along 43.6^0 N latitude, passing close to the Weed & Poteet, CTI, and Federal 1-10 wells shows a discontinuity between the CTI and Weed & Poteet wells (**Figure 6-2**). A similar although less pronounced discontinuity shows up to the west, near Capehart Lake.
- Close proximity to other suggested possible caldera or vent sources for the Prater Creek Ash-flow Tuff (**Tmtp**), including Double O Ranch (Parker, 1974), the area lying along the northern edge of Wright Point (Meigs and others, 2009; Ford and others, 2013), and a vent area centered on Malheur Lake and Wright Point (northern caldera of Khatiwada and Keller, 2015) (**Figure 2-3**).
- Spatial association with the identified Rattlesnake Tuff (**Tmtr**) eruptive center, centered on Capehart Lake in the western Harney Basin (**Figure 2-3**).

Figure 7-2. Geophysical interpretation of the eastern margin of the Silvies River caldera. Map view of the Silvies River caldera and located deep exploration wells superimposed on a tomographic inversion velocity model taken along an east-west vertical slice at 43.6° N latitude. Vertical slice modified from Khatiwada and Keller (2015, figure 5F). Khatiwada and Keller (2015) imaged a subsurface feature here that appears to correspond to the eastern margin of the Silvies River caldera that we base on geologic mapping and lithologic and geochemical interpretation of deep exploration wells. White ellipses are deep exploration wells including the Federal 1-10 (F1-10), CTI (CTI), Weed and Poteet (WP), HARN 52747 EOARC (Obs), Voglar (VG), and #1 Fay (FAY) wells. Red solid line is the approximate location of the eastern margin of the Silvies River caldera.

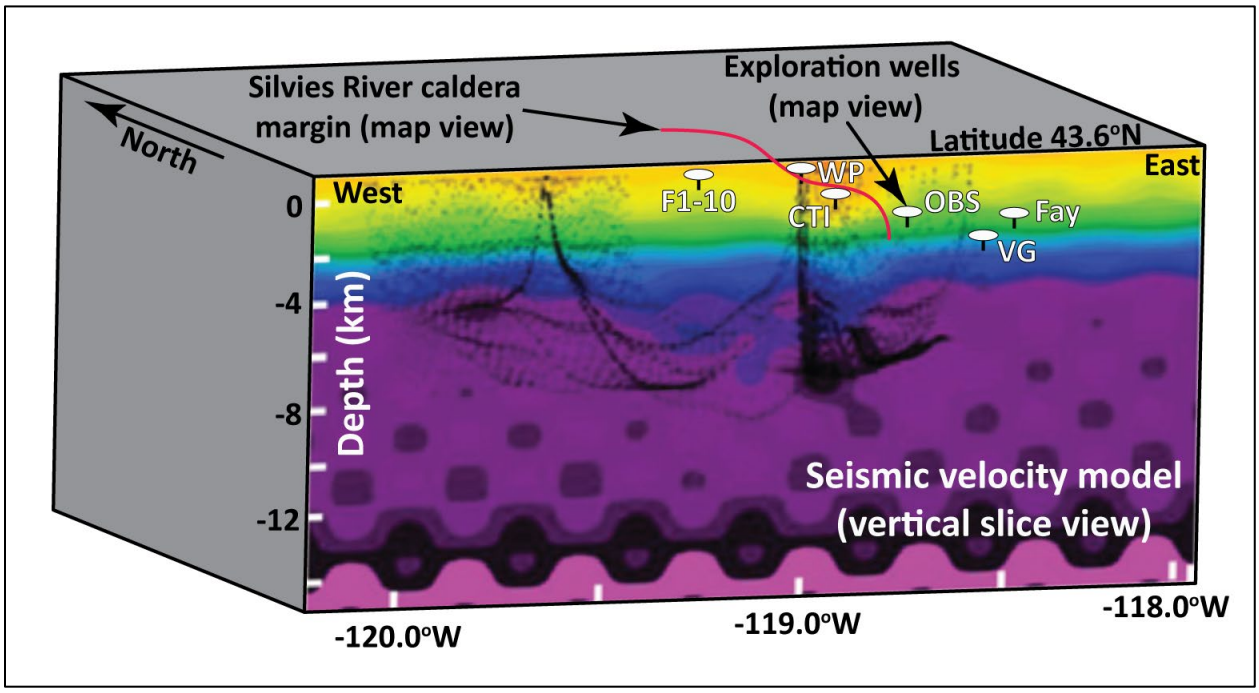

8.0 GEOLOGIC HISTORY

The "basement" rocks in the area include parts of the Olds Ferry and Izee terranes (Brooks and Vallier, 1978; Silberling and others, 1984; Ave'Lallemant, 1995). The Olds Ferry Terrane, the most inboard of the Blue Mountains terranes, is an island arc terrane composed of a wide range of arc rocks (basalts to rhyolites, predominantly andesites) and volcanogenic sedimentary rocks of Middle Triassic to Lower Jurassic ages. The Izee Terrane is a sedimentary cover sequence of Triassic/Jurassic flysch-like turbidites with ubiquitous volcanic flows in the lower part of the section. Pre-Cenozoic basement is overlain/intruded by a locally erupted late Oligocene (ca. 22 to 25 Ma) sequence of dacites, rhyolites, and andesites, and early to middle Miocene basalt flows, displaying similarities to Grande Ronde, Steens, and Picture Gorge basalts of the Columbia River Basalt Group (CRBG) (Niewendorp and others, 2018; Houston and others, 2018). Locally, in the northern Harney Basin, early to middle Miocene lavas are overlain by the ca. 16 Ma Dinner Creek Tuff.

8.1 Late Miocene (9.74 Ma to 7.093 Ma)

Three voluminous late Miocene ash-flow tuffs are widely exposed and recognized across the Harney Basin above the CRBG and older rocks. These tuffs, forming the oldest geologic units exposed in the Poison Creek

and Burns 7.5' quadrangles include 1) the 9.63/9.74 Ma Devine Canyon Ash-flow Tuff (**Tmtd**), 2) the 8.41 Ma Prater Creek Ash-flow Tuff (**Tmtp**), and 3) the 7.093 Ma Rattlesnake Tuff (**Tmtr**) (Walker, 1979; Streck, 1994; Streck and Grunder, 1995, 2008; Jordan and others, 2004; Ford and others, 2013; Isom, 2017). The three major late Miocene tuff units, each exceeding 200 km^3 (48 mi^3) in eruptive volume and covering areas ranging from ~9,615 km^2 (~3,713 mi^2) to > 35,000 km^2 (>13,500 mi^2) are presumed to have originated from caldera sources lying buried beneath the Harney Basin (**Figure 2-3**), including the Silvies River caldera. Rapidly moving incandescent pyroclastic flows emanating from these calderas completely inundated the landscape of the late Miocene Harney Basin, largely burying evidence of older late Miocene calderas. Tuffaceous sedimentary rocks preserved between ash-flow tuffs represent erosion, remobilization, transport, and deposition of abundant tuffaceous material in the intervals between caldera-forming eruptions. Some **Tmst** horizons include air-fall tuffs signaling continued regional eruptions and pumice and tuff beds formed during pre-cursor eruptions to caldera-forming ash-flow tuff events.

The Silvies River caldera formed in the area of the city of Burns and Burns Butte at 8.41 Ma, with the eruption of the Prater Creek Ash-flow tuff (**Tmtp**). Formation of the caldera resulted in the simultaneous eruption of ~200 km^3 (48 $mile^3$) of pyroclastic debris as ash flows that rapidly inundated more than 9,000 km^2 (>3,474 mi^2) of southeastern Oregon. Caldera-forming eruptions at the Silvies River caldera were followed by the emplacement of a bimodal suite of late Miocene (ca. 8.4 to 7.1 Ma) rhyolitic tuffs (tuff of Wheeler Springs, **Tmtw**, **Tmtwh**), 7.68 to 8.03 Ma exogenous rhyolite domes and flows (rhyolite of Golden Ranch **Tmrg**, rhyolite of Burns Butte **Tmrb**) and basaltic trachyandesite and trachyandesite flows, dikes, and vent deposits (**Tmat**, **Tmvt**), now forming the low hills west of Burns (Plate 2). These rocks define a narrow volcanic field of prominent silicic domes and mafic shield volcanoes that formed above caldera-filling tuffs following caldera formation (Plate 2, cross sections). At 7.093 Ma the Silvies River caldera and marginal volcanic fields were partially to completely buried by the Rattlesnake Tuff (**Tmtr**), one of the most far-traveled ash-flow tuffs known in the world (Streck and Grunder, 1995).

8.2 Late Miocene to Recent

Uplift of the Blue Mountains to the north and Steens Mountain to the south and downwarping of the Harney Valley into a broad synclinal trough occurred in post-Rattlesnake (**Tmtr**) time (Buwalda, 1921). Drainages in the northern Harney Basin entrenched themselves into the southerly tilted dip-slope, flowing into the valley forming the shallow Harney and Malheur lakes. These drainages carried locally derived detritus into the basin in the form of clay, sand, and gravel building up basin-fill deposits of considerable thickness in the central and marginal parts of the basin.

Late Miocene units in the central and marginal parts of the Harney Basin, including the Poison Creek and Burns 7.5′ quadrangles, are covered by sequences of late Pliocene to Quaternary sedimentary rocks (**QTst**). These rocks represent fluvial and lacustrine deposits that partially filled the Harney Basin and followed ancestral drainages 61 to 183 m (200 to 600 ft) above the modern valley floor. Neogene bedrock units in the area are locally covered by surficial units, including older fan deposits (**Qoaf**), colluvium (**Qc**), fan deposits (**Qaf**), stream channel alluvium (**Qa**), marsh and alluvial deposits (**Qma**), fan delta deposits (**Qfd**), and modern fill (**Qf**). Landslide deposits (**Qls**) are also present in some areas.

9.0 GEOLOGIC RESOURCES

9.1 Aggregate materials and industrial minerals

Aggregate in the form of crushed rock and gravel is the major mineral resource mined in the Harney Basin area. Niewendorp and Geitgey (2009) provided regional locations for aggregate and crushed rock resources (https://www.oregongeology.org/milo/index.htm). In the map area, sand and gravel quarries are sited mainly in sedimentary rocks (**QTst**). Those quarries developing crushed rock and cinders are sited in basaltic trachyandesite and trachyandesite flows (**Tmat**), basaltic trachyandesite and trachyandesite vent deposits (**Tmvt**), and rarely Rattlesnake Tuff (**Tmtr**). Industrial mineral sites hosting pumice and pumicite, and obsidian are found in the tuff of Wheeler Springs, non-welded lapilli tuff (**Tmtwh**). Obsidian and gemstone localities are also reported from unit **QTst** northwest of Burns. Presently, all quarries in the study area are small pit-run sources located on private lands and on lands administered by the Oregon Department of Transportation or the U.S. Forest Service. This material is used locally as pit-run resource for road construction and maintenance. However, certain localities may provide material suitable for decorative stone and for use as riprap for stabilization and erosion control purposes.

9.2 Energy resources

9.2.1 Geothermal

Brown and others (1980a), in a reconnaissance study, investigated the geothermal resource potential of the northern Harney Basin. Two low-temperature resource areas were identified: 1) the area near the Soldier Creek shear zone, northeast of the city of Burns, and 2) the area immediately south, west, and east of the city of Burns (Plate 2). The area surrounding the city of Burns is currently recognized as a Direct Use Geothermal Area, covering ~13,725 hectares (~33,917 acres) centered on the bimodal volcanic highlands southeast of Burns Butte (Niewendorp and others, 2007; https://www.oregongeology.org/gtilo/index.htm). Direct use areas are locations that, because of their geologic history, presence of thermal springs, wells, geohydrologic settings favorable for the recovery of thermal water, and similarity to areas with known geothermal/hydrothermal systems, are expected to contain geothermal resources suitable for direct heat applications (20°C and above) (Niewendorp and others, 2007).

Several warm springs are documented in the area along U.S. Highway 20 just south of Hines, including the Millpond well (26°C, 78.8°F maximum recorded temperature), unnamed (25°C, 77°F max recorded temperature), Goodman Spring (21°C, 71.6°F max recorded temperature), and Roadland Spring (22°C, 71.6°F max recorded temperature).

Fifty-two low-temperature geothermal wells are present in the study area. Low temperature wells are wells that have temperatures of 68°F (20°C) and above. The lower limit is based on a minimum temperature of 10°C above mean annual air temperature. Recorded maximum temperatures on these wells range between 18.3° and 35°C (64.9 to 95°F). Higher maximum temperatures of 58° and 71° (136.4° and 159.8° F) are reported, associated with the Weed and Poteet well and associated oil and gas test well, respectively. Most low-temperature geothermal wells in the study area are clustered in the southwestern part of the Burns 7.5′ quadrangle (Plate 2), associated with the eastern ring-fracture zone of the Silvies River caldera and late Miocene bimodal basaltic trachyandesite and rhyolite volcanic vent complexes forming the low hills west of Burns.

Six geothermal prospect wells have been drilled in the Burns 7.5′ quadrangle including the BN-12, BN-13, Weed and Poteet #1, Hotchkiss 1, Hines Mill No. 1, and Burns High School wells (Plate 1). These wells

were largely drilled in the 1970s and 1980s to gather temperature observation data. Data are contained in the unpublished permit files of the Oregon Department of Geology and Mineral Industries' Mineral Land Reclamation and Regulation program.

9.2.2 Oil and gas

Several oil and gas exploration wells were drilled in the central and western regions of the Harney Basin in the vicinity of the city of Burns starting around 1900 and then from the late 1940s into the late 1970s. Oil and gas well locations and drilling logs are available at https://www.oregongeology.org/mlrr/oilgas-logs.htm. Many of the wells reported shows of gas. A show is the appearance of oil and/or gas in cuttings, samples, or cores from drilling a well. Drilling records indicate that these wells were plugged and abandoned shortly after completion. This suggests that not all elements of a petroleum system for production of oil and/or gas are associated with the rocks within the Harney Basin, e.g., 1) a source rock for petroleum, 2) migration path(s), 3) reservoir rock, 4) seal, 5) trap, and 6) the geologic processes that form these elements. Therefore, the oil and gas potential for the area is none. **Table 2-1** shows a listing of Oil and Gas exploration wells in the Burns area and their history is described in preceding section 6.0, Exploration Wells.

9.3 Water resources

A full discussion of the geologic controls on surface and groundwater resources in the study is beyond the scope of this report. Field observations and preliminary findings on geologic parameters controlling water resources within the study area are briefly summarized below. The reader is referred to previous hydrogeologic investigations conducted by Piper and others (1939), Leonard (1970), Walker (1979), Whitehead (1994), and Gonthier (1985) for more in-depth discussions.

The Harney Basin is a dominantly agricultural area, with water resources allocated for a combination of domestic use, irrigated agriculture, livestock, and fish and wildlife needs. A database of 202 located wells accompanies the geodatabase for this report (see water well data in geodatabase and appendix). A majority of these wells are sited along the Silvies River Valley, Poison Creek, and the broad alluvial plain of the greater Harney Valley. A select number of other water wells are drilled in units **QTst** and **Tmtr**, and to a much lesser extent **Tmrb**, **Tmat**, and **Tmtwh**.

Unconsolidated to partly consolidated alluvial sand and gravel deposits preserved in terraces and floodplains (**Qa**, **Qma**, **Qfd**) and on alluvial and debris fans (**Qaf**) likely contain groundwater that typically saturates sediments just above the underlying bedrock platform and is usually in hydraulic connection with nearby streams (Plates 1 and 2; Piper and others, 1939; Leonard, 1970). The deposits are typically thin (<10 m [30 ft]) and likely sinuous but may be very permeable except where they contain large amounts of clay and silt (Piper and others, 1939; Leonard, 1970). Alluvial wells developed in higher-permeability sand and gravel intervals, with yields depending on annual precipitation, as compared to lower-permeability silt-rich sedimentary intervals, are likely favorable targets (Piper and others, 1939).

Other water-bearing horizons in the study area may generally be found at the basal contacts of **Tmtr**, **Tmtp**, and **Tmtd** rock types, although few wells are sited in these strata (Plates 1 and 2). These horizons serve as lateral pathways for groundwater flow. Tuffaceous sedimentary rocks (**Tmst**) between ash-flow tuffs appear to act as either confining units or porous media serving as a pathway for lateral transport of groundwater depending on percent clays.

10.0 GEOLOGIC HAZARDS

10.1 Landslide hazards

The downslope movement of rock and soil, in the form of landslides, rock falls, and debris flows, may present a geologic hazard to residents, infrastructure, and transportation corridors in the Poison Creek and Burns 7.5′ quadrangle.

10.1.1 Typical and colluvial landslides

Ninety landslide deposits (**Qls**) were recognized and mapped in the study area during the course of this study. Those landslide deposits (**Qls**) recognized cover ~0.003 percent of the map area and range from larger slides covering up to 19.5 hectares (48 acres) to the smallest mapped landslide deposit covering just 0.007 hectares (0.022 acres). A majority of mapped landslide deposits are simple rotational or translational slides or shallow-seated earthflow-type features occurring along all major drainages. Landslides typically originate on sparsely vegetated, moderate to steep slopes underlain by weakly consolidated tuffaceous sedimentary rocks (**Tmst**) forming interbeds between cliff- and bench-forming ash-flow tuffs (Plates 1 and 2). Many of these slides can be attributed to the combined influences of parallel topographic slope and faulting or bedding dip, undercutting by streams, intermittent heavy precipitation, groundwater conditions, and rock type. The generally weakly consolidated nature of the tuffaceous sedimentary rocks (**Tmst**) makes this unit especially prone to landslides on gently to steeply inclined slopes. Future landslides should be expected in **Tmst** particularly in areas of changing vegetation resulting from rangeland fires or changes in land use that may alter local groundwater conditions.

Unstable colluvium (**Qc**; wedges of soil and rock) mantles many slopes in the study area. These deposits typically form when weathered rock particles, ranging in size from clay to boulders, accumulate along a hillside. When the mass of the accumulated material reaches a critical size, a triggering event such as heavy rainfall or a seismogenic event may initiate the rapid downslope movement of this mass. Areas denuded by fire or other anthropogenic vegetative removal can especially be at risk from such events.

10.1.2 Rock fall

Rock fall and rockslide (**Qc**) hazards may be present in the study area where steep slopes and cliff exposures occur (Plates 1 and 2). Potential natural triggering mechanisms for rock fall events include freeze/thaw cycles, heavy rainfall, earthquakes, or extensive devegetation due to fire.

10.1.3 Alluvial fan deposits

Alluvial fan and debris fan (**Qaf**; **Qoaf**) deposits in the study area have been mapped along all drainages (Plates 1 and 2). Rapidly moving landslides in the form of debris flows may be expected on both alluvial and debris fans that lie at the mouths of steep-sided, colluvium-filled canyons and upland drainages. The potential for inundation of fan areas by rapidly moving debris flows increases during episodes of intense rainfall that occur after soils have been saturated by fall and early winter rainfall. Redirected drainage and poor construction practices are human activities that could initiate debris flows. Debris flows have the potential to threaten life and may cause extensive damage to property and transportation corridors.

10.2 Earthquake hazards

There has been little in the way of recorded historic (1896 to 2002) seismic activity in the Burns area (Niewendorp and Neuhaus, 2003). Three historic earthquake epicenters have been recorded in the greater area of Harney County, with events ranging in magnitude from M4.0 to M4.9 (Richter scale). Approximately 10 smaller events (<M4.0) have been documented in the southern part of the county in historical times (Niewendorp and Neuhaus, 2003). Weldon and others (2003), in their active fault map for central and eastern Oregon, show two fault strands in the Burns Butte 7.5' quadrangle (fault identification numbers 3797 and 1060), as well as a number of northwest-trending fault strands in the Brothers Fault Zone west of Wrights Point as possibly active during the Quaternary (2.58 Ma and younger). These workers also show a major north-south trending fault stand along the eastern edge of the Harney Valley (fault #1244), extending from Crane north through Buchanan, interpreted as active through the middle to late Quaternary (<0.78 Ma). In the northwest part of the Burns 7.5' quadrangle (Plate 2) we portray several northwest-trending fault strands to offset sedimentary rocks of unit **QTst**. Offset along these fault strands may range from late Miocene to sometime in the Quaternary. USGS probabilistic ground shaking estimates for the area range from 10 to 14 percent G for the peak ground acceleration with a 2 percent chance of exceedance in 50 years (USGS Earthquake Hazards Program, https://earthquake.usgs.gov/static/lfs/nshm/conterminous/2014/2014pga2pct.pdf).

11.0 ACKNOWLEDGMENTS

This project and publication were supported through the STATEMAP component of the National Cooperative Geologic Mapping Program under cooperative agreement number G18AC00136. Additional funds were provided by the State of Oregon. XRF geochemical analyses were prepared and analyzed by Dr. Ashley Steiner at the GeoAnalytical Lab at Washington State University, Pullman. The authors acknowledge several area landowners who provided local knowledge and graciously allowed access to private holdings within the study area. Cartography for the map plates was provided by Jon Franczyk. The authors sincerely appreciate field assistance and discussions with Darrick Boschmann about the geology of southeast Oregon and assistance from Jim O'Connor researching Late Pleistocene lake highstands. Critical and insightful reviews by Martin Streck, Josh Hackett, Clark Niewendorp, Ian Madin, Bob Houston, and Christina Appleby greatly enriched the final manuscript, geodatabase, and geologic maps.

12.0 REFERENCES

Ave'Lallemant, H. G., 1995, Pre-Cretaceous tectonic evolution of the Blue Mountains Province, Northeastern Oregon, *in* Vallier, T. C., and Brooks, H. C., eds., Geology of the Blue Mountains Region, U.S. Geological Survey Professional Paper 1438, p. 291–304.

Boschmann, D. E., 2012, Structural and volcanic evolution of the Glass Buttes area, High Lava Plains, Oregon: Corvallis, Oreg., Oregon State University, M.S. thesis, 100 p. https://ir.library.oregonstate.edu/concern/graduate_thesis_or_dissertations/47429d66f

Brooks, H. C., and Vallier, T. L., 1978, Mesozoic rocks and tectonic evolution of eastern Oregon and western Idaho, in Howell, D. G., and McDougall, K. A., eds., Mesozoic paleogeography of the western United States: Pacific Coast Paleogeography Symposium 2, Sacramento, Calif., Society of Economic Paleontologists and Mineralogists, Pacific Section, p. 133–136.

Brown, D. E., 1982, Map showing geology and geothermal resources of the southern half of the Burns 15-minute quadrangle, Oregon: Oregon Department of Geology and Mineral Industries Geological Map Series GMS-20, 1 pl., scale 1:24,000. https://www.oregongeology.org/pubs/gms/GMS-020.pdf

Brown, D. E., McLean, G. D., and Black, G. L., 1980a, Preliminary geology and geothermal resource potential of the northern Harney Basin, Oregon: Oregon Department of Geology and Mineral Industries Open-File Report 80-6, 52 p., 4 pl., scale 1:62,500. Zipped file: https://www.oregongeology.org/pubs/ofr/O-80-06.zip

Brown, D. E., McLean, G. D., and Black, G. L., 1980b, Preliminary geology and geothermal resource potential of the southern Harney Basin, Oregon: Oregon Department of Geology and Mineral Industries Open-File Report 80-7, 90 p. 8 pl. Zipped file: https://www.oregongeology.org/pubs/ofr/O-80-07.zip

Buwalda, J. P., 1921, Report on oil and gas possibilities of eastern Oregon: Oregon Bureau of Mines and Geology, Mineral Resources of Oregon, v. 3, no. 2, July 1921.

Cahoon, E. B., and Streck, M. J., 2017, Picture gorge basalt, eastern Oregon: Extended distribution and petrogenetic connections to Steens basalt and Strawberry Volcanics: Geological Society of America Abstracts with Programs, v. 49, no. 6. doi: 10.1130/abs/2017AM-304582. https://gsa.confex.com/gsa/2017AM/webprogram/Paper304582.html

Camp, V. E., Ross, M. E., and Hanson, W. E., 2003, Genesis of flood basalts and Basin and Range volcanic rocks from Steens Mountain to the Malheur River Gorge, Oregon: Geological Society of America Bulletin, v. 115, no. 1, p. 105–128. https://doi.org/10.1130/0016-7606(2003)115<0105:GOFBAB>2.0.CO;2

Camp, V. E., Ross, M. E., Duncan, R. A., Jarboe, N. A., Coe, R. S., Hanan, B. B., and Johnson, J. A., 2013, The Steens Basalt: Earliest lavas of the Columbia River Basalt Group, *in* Reidel, S. P., Camp, V. E., Ross, M. E., Wolff, J. A., Martin, B. S., Tolan, T. L., and Wells, R. E., The Columbia River Flood Basalt Province: Geological Society of America Special Paper 497, p. 87–116. https://doi.org/10.1130/2013.2497(04)

Cohen, K. M., Finney, S. C., Gibbard, P. L., and Fan, J.-X., 2013, The ICS International Chronostratigraphic Chart: Episodes, v. 36, no. 3, 199–204. Available at http://www.stratigraphy.org/ICSchart/Cohen2013_Episodes.pdf

Cox, C., 2011, A controlled-source seismic and gravity study of the High Lava Plains (HLP): Norman, Okla., University of Oklahoma, M.S. thesis, 110 p.

Cox, C., Keller, G. R., and Harder, S. H., 2013, A controlled-source seismic and gravity study of the High Lava Plains (HLP) of eastern Oregon: Geochemistry, Geophysics, Geosystems, v. 14, no. 12, p. 5208–5226. https://doi.org/10.1002/2013GC004870

Cox, K. G., Bell, J. D., and Pankhurst, R. J., 1979, The interpretation of igneous rocks: London, George Allen and Unwin, 450 p.

Deffontaines, B., and Chorowicz, J., 1991, Principles of drainage basin analysis from multisource data: Application to the structural analysis of the Zaire Basin, *in* Fourniguet, J., and Pierre, G., eds., Neotectonics: Tectonophysics, v. 194, no. 3, p. 237–263. https://doi.org/10.1016/0040-1951(91)90263-R

Donath, F. A., 1962, Analysis of basin-range structure, south-central Oregon: Geological Society of America Bulletin, v. 73, p. 1–16. https://doi.org/10.1130/0016-7606(1962)73[1:AOBSSO]2.0.CO;2

Dugas, D. P., 1998, Late Quaternary variations in the level of Paleo-Lake Malheur, eastern Oregon: Quaternary Research, v. 50, no. 3, p. 276–282. https://doi.org/10.1006/qres.1998.2005

Ferns, M. L., and McClaughry, J. D., 2013, Stratigraphy and volcanic evolution of the middle Miocene to Pliocene La Grande–Owyhee eruptive axis in eastern Oregon, *in* Reidel, S. P., Camp, V. E., Ross, M. E., Wolff, J. A., Martin, B. S., Tolan, T. L., and Wells, R. E., eds., The Columbia River Flood Basalt Province: Geological Society of America Special Paper 497, p. 401–427. https://doi.org/10.1130/2013.2497(16)

Fiebelkorn, R. B., Walker, G. W., MacLeod, N. S., McKee, E. H., and Smith, J. G., 1982, Index to K-Ar age determinations for the state of Oregon: U.S. Geological Survey Open File Report 82-596, 42 p. 1 plate.

Fiebelkorn, R. B., Walker, G. W., MacLeod, N. S., McKee, E. H., and Smith, J. G., 1983, Index to K-Ar age determinations for the state of Oregon: Isochron/West, no. 37, p. 3–60.

Ford, M. T., 2012, Rhyolitic magmatism of the High Lava Plains and adjacent northwest Basin and Range, Oregon: Implications for the evolution of continental crust: Corvallis, Oreg., Oregon State University, Ph.D. dissertation, 111 p. https://ir.library.oregonstate.edu/concern/graduate_thesis_or_dissertations/p5547t57d

Ford, M. T., Grunder, A. L., and Duncan, R. A., 2013, Bimodal volcanism of the High Lava Plains and northwestern Basin and Range of Oregon: Distribution and tectonic implications of age-progressive rhyolites: Geochemistry, Geophysics, Geosystems, v. 14, no. 8, p. 2837–2857. https://doi.org/10.1002/ggge.20175

Geological Society of America Rock-Color Chart Committee, 1991, Rock color chart, 7th printing: Boulder, Colo.

Gillespie, M. R., and Styles, M. T., 1999, BGS rock classification scheme, v. 1, Classification of igneous rocks: Keyworth, U.K., British Geological Survey Research Report RR 99-06 (reformatted), 52 p. http://nora.nerc.ac.uk/3223/1/RR99006.pdf

Gonthier, J. B., 1985, A description of aquifer units in eastern Oregon: U.S. Geological Survey Water-Resources Investigations Report 84-4095, 39 p., 4 pl., scale 1:500,000. https://doi.org/10.3133/wri844095

Gradstein, F. M., and others. 2004, A geologic time scale 2004: Cambridge University Press, 589 p.

Greene, R. C., 1972, Preliminary geologic map of the Burns and West Myrtle Butte 15-minute quadrangles, Oregon: U.S. Geological Survey Miscellaneous Field Studies Map MF-320, scale 1:62,500. https://ngmdb.usgs.gov/Prodesc/proddesc_2743.htm

Greene, R. C., 1973, Petrology of the welded tuff of Devine Canyon, southeast Oregon: U.S. Geological Survey Professional Paper 797, 26 p. https://doi.org/10.3133/pp797

Greene, R. C., Walker, G. W., and Corcoran, R. E., 1972, Geologic map of the Burns quadrangle, Oregon: U.S. Geological Survey Miscellaneous Geologic Investigations Map I-680, scale 1:250,000. https://ngmdb.usgs.gov/Prodesc/proddesc_9455.htm

Hallsworth, C. R., and Knox, R. W. O'B., 1999, BGS rock classification scheme, v. 3, Classification of sediments and sedimentary rocks: Keyworth, U.K., British Geological Survey Research Report RR 99-03, 44 p. http://nora.nerc.ac.uk/3227/1/RR99003.pdf

Houston, R. A., McClaughry, J. D., Duda, C. J. M., and Niewendorp, C. A., 2018, Geologic map of the Devine Ridge North 7.5′ quadrangle, Harney County, Oregon: Oregon Department of Geology and Mineral Industries Geologic Map Series GMS-121, 115 p., 1 pl., scale 1:24,000. https://www.oregongeology.org/pubs/gms/p-GMS-121.htm

Iademarco, M. J., 2009, Volcanism and faulting along the northern margin of Oregon's High Lava Plains: Hampton Butte to Dry Mountain: Corvallis, Oreg., Oregon State University, M.S. thesis, 158 p., 1 pl. https://ir.library.oregonstate.edu/concern/graduate_thesis_or_dissertations/t435gj391

Isom, S. L., 2017, Compositional and physical gradients in the magmas of the Devine Canyon Tuff, eastern Oregon: constraints for evolution models of voluminous high-silica rhyolites: Portland, Oreg., Portland State University, M.S. thesis, 147 p. https://pdxscholar.library.pdx.edu/open_access_etds/3885/

Johnson, D. M., Hooper, P. R., and Conrey, R. M., 1999, XRF analysis of rocks and minerals for major and trace elements on a single low dilution Li-tetraborate fused bead: Advances in X-ray Analysis, v. 41, p. 843–867. Available at: https://s3.wp.wsu.edu/uploads/sites/2191/2017/06/Johnson-Hooper-and-Conrey.pdf

Johnson, J. A., 1994, Geologic map of the Krumbo Reservoir quadrangle, Harney County, southeastern Oregon: U.S. Geological Survey Miscellaneous Field Studies Map MF-2267, 11 p., 1 pl., scale 1:24,000. https://pubs.er.usgs.gov/publication/mf2267

Johnson, J. A., 1996, Geologic map of the Page Springs quadrangle, Harney County, southeastern Oregon: U.S. Geological Survey Open-File Report OF-96-675, 1 pl., scale 1:24,000. https://ngmdb.usgs.gov/Prodesc/proddesc_18672.htm

Jordan, B.T., 2001, Basaltic volcanism and tectonics of the High Lava Plains, southeastern Oregon: Corvallis, Oreg., Oregon State University, Ph.D. dissertation, 218 p., https://ir.library.oregonstate.edu/concern/graduate_thesis_or_dissertations/nv935579s?locale=en

Jordan, B. T., Streck, M. J., and Grunder, A. L., 2002, Bimodal volcanism and tectonism of the High Lava Plains, Oregon, *in* Moore, G. W., ed., Field guide to geologic processes in Cascadia, Field trips to accompany the 98th Annual Meeting of the Cordilleran Section of the Geological Society of America, May 13–15, 2002, Corvallis, Oregon: Oregon Department of Geology and Mineral Industries Special Paper 36, p. 23–46. https://www.oregongeology.org/pubs/sp/SP-36.pdf

Jordan, B. T., Grunder, A. L., Duncan, R. A., and Deino, A. L., 2004, Geochronology of age-progressive volcanism of the Oregon High Lava Plains: implications for the plume interpretation of Yellowstone: Journal of Geophysical Research, v. 109, no. B10, B10202, 19 p. https://doi.org/10.1029/2003JB002776

Kasbohm, J., and Schoene, B., 2018, Rapid eruption of the Columbia River flood basalt and correlation with mid-Miocene climate optimum; Science Advances v. 4, no. 9. https://advances.sciencemag.org/content/4/9/eaat8223

Khatiwada, M., and Keller, G. R., 2015, An integrated geophysical imaging of the upper crustal features in the Harney Basin, southeast Oregon: Geosphere, v. 11, no. 1, p. 185–200. https://doi.org/10.1130/GES01046.1

Langer, V. W., 1991, Geology and petrologic evolution of the silicic to intermediate volcanic rocks underneath Steens Mountain basalt, SE Oregon: Corvallis, Oreg., Oregon State University, M.S. thesis, 109 p., 1 pl., scale 1:24,000. https://ir.library.oregonstate.edu/concern/graduate_thesis_or_dissertations/p8418q421

Lawrence, R. D., 1976, Strike-slip faulting terminates the Basin and Range province in Oregon: Geological Society of America Bulletin, v. 87, no. 6, p. 846–850. https://doi.org/10.1130/0016-7606(1976)87<846:SFTTBA>2.0.CO;2

Le Bas, M. J., and Streckeisen, A. L., 1991, The IUGS systematics of igneous rocks: Journal of the Geological Society, v. 148, no. 5, p. 825–833. https://doi.org/10.1144/gsjgs.148.5.0825

Le Bas, M. J., Le Maitre, R. W., Streckeisen, A., and Zanettin, B., 1986, A chemical classification of volcanic rocks based on the total alkali-silica diagram: Journal of Petrology, v. 27, no. 3, p. 745–750. https://doi.org/10.1093/petrology/27.3.745

Le Maitre, R. W., and others, 1989, A classification of igneous rocks and glossary of terms: Recommendations of the International Union of Geological Sciences Subcommission on the Systematics of Igneous Rocks: Oxford, Blackwell, 193 p.

Le Maitre, R. W. (ed.), and others, 2004, Igneous rocks: a classification and glossary of terms: recommendations of the International Union of Geological Sciences, Subcommission on the Systematics of Igneous Rocks: Cambridge, Cambridge University Press, 236 p.

Leonard, A. R., 1970, Ground-water resources in Harney Valley, Harney County, Oregon: Salem, Oreg., Oregon Water Resources Department, Ground Water Report 16, 65 p., 3 pl., scale 1:125,000. https://www.oregon.gov/owrd/wrdreports/gw_report_16_harney.pdf

Mackenzie, W. S., Donaldson, C. H., and Guilford, C., 1997, Atlas of igneous rocks and their textures (7th ed.): Addison Wesley Longman, 148 p.

McGrane, D. J., 1985, Geology of the Idol City area: a volcanic-hosted, disseminated precious-metal occurrence in east-central Oregon: Missoula, Mont., University of Montana, M.S. thesis, 88 p. https://scholarworks.umt.edu/etd/7536

MacLean, J. W., 1994, Geology and geochemistry of Juniper Ridge, Horsehead Mountain, and Burns Butte: implications for the petrogenesis of silicic magma on the high lava plains, southeastern Oregon: Corvallis, Oreg., Oregon State University, M.S. thesis, 141 p. https://ir.library.oregonstate.edu/concern/graduate_thesis_or_dissertations/zp38wf64g?locale=en

MacLeod, N. S., Walker, G. W., and McKee, E. H., 1976, Geothermal significance of eastward increase in age of upper Cenozoic rhyolitic domes in southeastern Oregon, *in* Second United Nations Symposium on the Development and Use of Geothermal Resources, v. 1: Washington D.C., Government Printing Office, p. 465–474.

McPhie, J., Doyle, M., Allen, R. L., and Allen, R., 1993, Volcanic textures: A guide to the interpretation of textures in volcanic rocks: Centre for Ore Deposit and Exploration Studies, University of Tasmania, 198 p.

Meigs, A., Scarberry, K., Grunder, A., Carlson, R., Ford, M. T., Fouch, M., Grove, T., Hart, W. K., Iademarco, M., Jordan, B., and Milliard, J., 2009, Geological and geophysical perspectives on the magmatic and tectonic development, High Lava Plains and northwest Basin and Range, *in* O'Connor, J. E., Dorsey, R. J., and Madin, I. P., GSA Field Guide 15, Volcanoes to Vineyards: Boulder, Colo., Geological Society of America. https://doi.org/10.1130/2009.fld015(21)

Milliard, J. B., 2010, Two-stage opening of the northwestern Basin and Range in eastern Oregon: Evidence from the Miocene Crane Basin: Corvallis, Oreg., Oregon State University, M.S. thesis, 82 p. https://ir.library.oregonstate.edu/concern/graduate_thesis_or_dissertations/fn107319d

NCGMP (USGS National Cooperative Geologic Mapping Program), 2010, NCGMP09—Draft standard format for digital publication of geologic maps, version 1.1, *in* Soller, D. R., ed., Digital Mapping Techniques '09—Workshop Proceedings: U.S. Geological Survey Open-File Report 2010–1335, p. 93–146. https://pubs.usgs.gov/of/2010/1335/pdf/usgs_of2010-1335.pdf

NCGMP (USGS National Cooperative Geologic Mapping Program), 2018, GeMS (Geologic Map Schema)—a standard format for digital publication of geologic maps: U.S. Geological Survey, version 2, draft 7, 78 p. https://ngmdb.usgs.gov/Info/standards/GeMS/docs/GeMSv2_draft7g_ProvisionalRelease.pdf

Niem, A. R., 1974, Wright's Point, Harney County, Oregon: an example of inverted topography: Ore Bin, v. 36, no. 3, 33–49. https://www.oregongeology.org/pubs/OG/OBv36n03.pdf

Niewendorp, C. A., and Geitgey, R. P., 2009, Mineral information layer for Oregon (MILO), release 2, GIS files. https://www.oregongeology.org/milo/index.htm

Niewendorp, C. A., and Neuhaus, M. E., 2003, Map of selected earthquakes for Oregon, 1841 through 2002: Oregon Department of Geology and Mineral Industries Open-File Report O-03-02, 1 pl. http://www.oregongeology.org/pubs/ofr/p-OFR.htm

Niewendorp, C. A., Schueller, D. A., and Welch, T. J., 2007, Geothermal Information Layer for Oregon [GTILO], release 1: Oregon Department of Geology and Mineral Industries Digital Data Series, GIS files, 1:100,000-scale. https://www.oregongeology.org/gtilo/index.htm.

Niewendorp, C. A., Duda, C. J. M., Houston, R. A., and McClaughry, J. D., 2018, Geologic map of the Devine Ridge South 7.5′ quadrangle, Harney County, Oregon: Oregon Department of Geology and Mineral Industries Geologic Map Series GMS-120, 65 p., 1 pl., scale 1:24,000. https://www.oregongeology.org/pubs/gms/p-GMS-120.htm

Ogg, J. G., Ogg, G., and Gradstein, F. M., 2008, The concise geologic time scale: Cambridge University Press, 150 p.

Parker, D. J., 1974, Petrology of selected volcanic rocks of the Harney Basin, Oregon: Corvallis, Oreg., Oregon State University, Ph.D. dissertation, 153 p., 1 pl. https://ir.library.oregonstate.edu/concern/graduate_thesis_or_dissertations/r494vn606

Piper, A. M., Robinson, T. W., and Park C. F., 1939, Geology and ground-water resources of the Harney Basin, Oregon: U.S. Geological Survey Water Supply Paper 841, 189 p., 1 pl., scale 1:125,000. https://pubs.er.usgs.gov/publication/wsp841

Robertson, S., 1999, BGS rock classification scheme, v. 2, Classification of metamorphic rocks: Keyworth, U.K., British Geological Survey Research Report RR 99-02, 24 p. http://nora.nerc.ac.uk/id/eprint/3226/1/RR99002.pdf

Russell, I. C., 1884, A geological reconnaissance in southern Oregon: U.S. Geological Survey Annual Report 4 (1882-1883), p. 431–464. https://doi.org/10.3133/ar4

Scarberry, K., Meigs, A., and Grunder, A., 2009, Faulting in a propagating continental rift: Insight from the late Miocene structural development of the Abert Rim fault, southern Oregon, USA: Tectonophysics, v. 488, no. 1–4, p. 71–86. https://doi.org/10.1016/j.tecto.2009.09.025

Sheppard, R. A., 1994, Zeolitic diagenesis of tuffs in Miocene lacustrine rocks near Harney Lake, Harney County, Oregon: U.S. Geological Survey Bulletin 2108, 28 p. https://pubs.usgs.gov/bul/2108/report.pdf

Sherrod, D. R., and Johnson, J. A., 1994, Geologic map of the Irish Lake quadrangle, Harney County, south-central Oregon: U.S. Geological Survey Miscellaneous Field Studies Map MF-2256, 1 sheet, scale 1:24,000. https://ngmdb.usgs.gov/Prodesc/proddesc_5877.htm

Silberling, N. J., Jones, D. L., and Blake, M. C., Jr., 1984, Lithotectonic terrane map of the conterminous western United States, Pt C *of* Silberling, N. J., and Jones D. L., eds., Lithotectonic terrane maps of northern Cordillera: U.S. Geological Survey Open-File Report 84-523, 43 p. https://doi.org/10.3133/ofr84523

Smith, G. A., 1986a, Stratigraphy, sedimentology, and petrology of Neogene rocks in the Deschutes Basin, central Oregon: a record of continental margin volcanism and its influence on fluvial sedimentation in an arc-adjacent basin: Corvallis, Oreg., Oregon State University, Ph.D. dissertation, 467 p, 3 pl., scale 1:24,000. https://ir.library.oregonstate.edu/concern/graduate_thesis_or_dissertations/c247dw09t

Smith, G. A., 1986b, Stratigraphy, sedimentology, and the petrology of Neogene rocks in the Deschutes Basin, central Oregon: A record of continental-margin volcanism and its influence on fluvial sedimentation in an arc-adjacent basin: Richland, Wash., U.S. Department of Energy Basalt Waste Isolation Project, Rockwell Hanford Operations Publication RHO-BW-SA-555-P, 1 pl., scale 1:24,000.

Smith, J. V., and MacKenzie, W. S., 1958, The cooling history of high-temperature sodium-rich feldspars, pt. 4 *of* The alkali feldspars: Am. Mineralogist, v. 43, no. 9-10, p. 872–889. http://www.minsocam.org/ammin/am44/am44_1169.pdf

Smith, R. L., and Roe, W. P., 2015, Oregon geologic data compilation [OGDC], release 6 (statewide): Oregon Department of Geology and Mineral Industries Digital Data Series OGDC-6, geodatabase. https://www.oregongeology.org/pubs/dds/p-OGDC-6.htm

Streck, M. J., 1994, Volcanology and petrology of the Rattlesnake Ash-flow Tuff, eastern Oregon: Corvallis, Oreg., Oregon State University, Ph.D. dissertation, 184 p. https://ir.library.oregonstate.edu/concern/graduate_thesis_or_dissertations/kh04ds239

Streck, M., and Ferns, M. L., 2004, The Rattlesnake Tuff and other Miocene silicic volcanism in eastern Oregon, chap. 1 *of* Haller, K. M., and Wood, S. H., Geological field trips in southern Idaho, eastern Oregon, and northern Nevada: U.S. Geological Survey Open-File Report 2004-1222, p. 4–19. https://pubs.usgs.gov/of/2004/1222/

Streck, M. J., and Grunder, A. L., 1995, Crystallization and welding variations in a widespread ignimbrite sheet; the Rattlesnake Tuff, eastern Oregon, USA: Bulletin of Volcanology, v. 57, no. 3, p. 151–169. https://doi.org/10.1007/BF00265035

Streck, M. J., and Grunder, A. L., 2008, Phenocryst-poor rhyolites of bimodal, tholeiitic provinces: The Rattlesnake Tuff and implications for mush extraction models: Bulletin of Volcanology, v. 70, no. 3, p. 385–401. https://doi.org/10.1007/s00445-007-0144-3

Streck, M. J., Johnson, J. A., and Grunder, A. L., 1999, Field guide to the Rattlesnake Tuff and High Lava Plains near Burns, Oregon: Ore Bin, v. 61, no. 3, 64–76. https://www.oregongeology.org/pubs/og/OGv61n03.pdf

Streck, M. J., Ferns, M. L., and McIntosh, W., 2015, Large, persistent rhyolitic magma reservoirs above Columbia River Basalt storage sites: The Dinner Creek Tuff Eruptive Center, eastern Oregon: Geological Society of America, Geosphere, v. 11, no. 2, 226–235. https://doi.org/10.1130/GES01086.1

Thompson, G. A., and Burke, D. B., 1974, Regional geophysics of the Basin and Range province: Ann. Rev. Earth Planet. Sci., v. 2, 213-238. https://doi.org/10.1146/annurev.ea.02.050174.001241

Thormahlen, D. J., 1984, Geology of the northwest one-quarter of the Prineville quadrangle, central Oregon: Corvallis, Oreg., Oregon State University, M.S. thesis, 106 p. 1 pl., scale 1:24,000.

Trench, D., 2008, The termination of the Basin and Range Province into a clockwise rotating region of transtension and volcanism, central Oregon: Corvallis, Oreg., Oregon State University, M.S. thesis, 64 p. https://ir.library.oregonstate.edu/concern/graduate_thesis_or_dissertations/qr46r331w

Walker, G. W., 1970, Cenozoic ash-flow tuffs of Oregon: Ore Bin, v. 32, no. 6, 97–115. https://www.oregongeology.org/pubs/OG/OBv32n06.pdf

Walker, G. W., 1974, Some implications of Late Cenozoic volcanism to geothermal potential in the High Lava Plains of south-central Oregon: Ore Bin, v. 36, no. 7, p. 109–119. https://www.oregongeology.org/pubs/og/OBv36n07.pdf

Walker, G. W., 1977, Geologic map of Oregon east of the 121st meridian: U.S. Geological Survey Miscellaneous Investigations Map I-902, 2 sheets, scale 1:500,000. https://ngmdb.usgs.gov/Prodesc/proddesc_9795.htm

Walker, G. W., 1979, Revisions to the Cenozoic stratigraphy of Harney Basin, southeastern Oregon: U.S. Geological Survey Bulletin 1475, 35 p., 1 pl. https://doi.org/10.3133/b1475

Walker, G. W., and MacLeod, N. S., 1991, Geologic map of Oregon: U.S. Geological Survey, scale 1:500,000. https://ngmdb.usgs.gov/Prodesc/proddesc_16259.htm

Walker, G. W., and Nolf, B., 1981, High Lava Plains, Brothers fault zone to Harney Basin, Oregon, *in* Johnson, D.A., and Donnelly-Nolan, J., eds., Guides to Some Volcanic Terranes in Washington, Idaho, Oregon, and Northern California: U.S. Geological Survey Circular 838, p. 105–111. https://doi.org/10.3133/cir838

Weldon, R. J., II, Fletcher, D. K., Weldon, E. M., Scharer, K. M., and McCrory, P. A., 2003, An update of Quaternary faults of central and eastern Oregon: U.S. Geological Survey Open-File Report 02-301. http://pubs.usgs.gov/of/2002/of02-301/

Wentworth, C. K., 1922, A scale of grade and class terms of clastic sediments: Journal of Geology, v. 30, no. 5, p. 377–392. https://www.jstor.org/stable/30063207

Whitehead, R. L., 1994, Ground water atlas of the United States: Segment 7, Idaho, Oregon, Washington: U.S. Geological Survey Hydrologic Atlas 730-H, 31 p. https://doi.org/10.3133/ha730H

Zakšek, K., Oštir, K., and Kokalj, Ž., 2011, Sky-view factor as a relief visualization technique: Remote Sensing, v. 3, no. 2, p. 398–415. https://doi.org/10.3390/rs3020398

13.0 APPENDIX

This appendix contains a summary of the geodatabase along with a description of analytical and field methods and the list of attribute fields for spreadsheets (see page 5 of this report). The appendix is divided into two sections:

- Section 13.1 describes the digital databases included with this publication.
- Section 13.2 contains a summary of analytical and field methods. Accompanying tables explain the fields listed in various spreadsheets.

13.1 Geographic Information Systems (GIS) database

Geodatabase specifications

Digital data created for the Poison Creek and Burns 7.5′ quadrangles are stored in an Esri format geodatabase. The geodatabase structure follows that outlined by the U.S. Geological Survey (USGS) Geologic Map Schema (GeMS), version 2.7 (USGS National Cooperative Geologic Mapping Program, 2018). The following information describes the overall database structure, the feature classes, and supplemental tables (**Figure 13-1**, **Figure 13-2**, **Figure 13-3**, **Table 13-1**, and **Table 13-2**).

The data are stored in a file geodatabase feature dataset (GeologicMap). Accessory file geodatabase tables (DataSources, DescriptionOfMapUnits, GeoMaterialDict, and Glossary) were created by using ArcGIS version 10.6 (SP 1). The GeologicMap feature dataset contains all the spatially oriented data (feature classes) created for the Poison Creek and Burns 7.5′ quadrangles. The file geodatabase tables are used to hold additional geologic attributes. Additional information and complete descriptions of the "GeMS" — Geologic Map Schema (formerly "NCGMP09") can be found at https://ngmdb.usgs.gov/Info/standards/GeMS/#docs.

Figure 13-1. Poison Creek and Burns 7.5′ quadrangle geodatabase feature dataset and data tables.

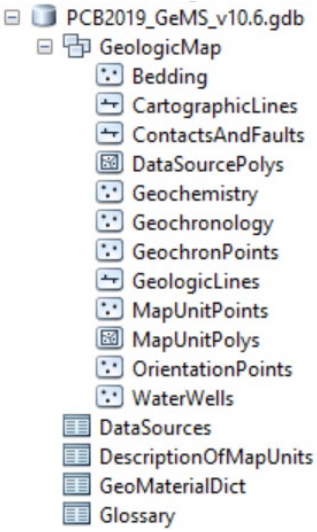

Geodatabase feature class specifications

Each feature class within the GeologicMap feature dataset in the geodatabase contains detailed metadata. Please see the embedded metadata for detailed information such as process descriptions, accuracy specifications, and entity attribute descriptions.

Figure 13-2. Poison Creek and Burns 7.5' quadrangles geodatabase feature classes and descriptions.

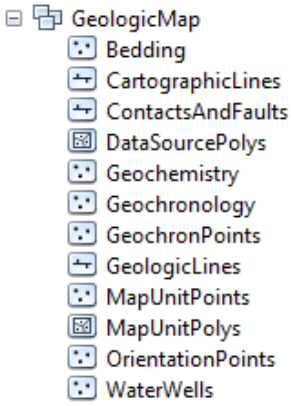

Table 13-1. Feature class description.

Name	Description
Bedding	This feature class represents point locations in the quadrangle where bedding measurements were made or were compiled from previous studies. These data are also contained in the bedding (strike and dip) spreadsheet described in more detail below.
CartographicLines	Vector lines that have no real-world physical existence and do not participate in map-unit topology. The feature class includes cross section lines used for cartography for the quadrangle.
ContactsAndFaults	The vector lines in this feature class contain geologic content including contacts and fault locations used to create the map unit polygon boundaries. The existence and location confidence values for the contacts and faults are provided in the feature class attribute table.
DataSourcePolys	This feature class contains polygons that delineate data sources for all parts of the geologic map. These sources may be a previously published map, new mapping, or mapping with a certain technique. For a map with one data source, for example all new mapping, this feature class contains one polygon that encompasses the map area.
Geochemistry	This feature class represents point locations where whole-rock samples have been analyzed by X-ray fluorescence (XRF) techniques in the quadrangle. Includes data collected by the authors during this study or compiled from previous studies. These data are also contained in the geochemistry spreadsheet described in more detail below.
Geochronology	This feature class represents point locations where 40Ar/39Ar isotopic ages have been obtained for rock samples in the quadrangle. Data collected by the authors during the course of this study. These data are also contained in the geochronology spreadsheet described in more detail below.
GeochronPoints	This feature class represents point locations where 40Ar/39Ar isotopic ages have been obtained for rock samples in the quadrangle. Complete analytical data are shown in the analysis-specific table Geochronology.
GeologicLines	These vector lines represent known fold axis locations in the quadrangle. The existence and location confidence for the fold axes are provided in the feature class attribute table.
MapUnitPoints	This feature class represents points used to generate the MapUnitPolys feature class from the ContactsAndFaults feature class.
MapUnitPolys	This polygon feature class represents the geologic map units as defined by the authors.
OrientationPoints	This feature class represents point locations in the quadrangle where bedding measurements were made or were compiled from previous studies. These data are also contained in the bedding (strike and dip) spreadsheet described in more detail below.
WaterWells	This feature class represents point locations of water wells in the quadrangle. Includes data obtained by the authors from the Oregon Department of Water Resources (OWRD). These data are also contained in the WaterWells spreadsheet described in more detail below.

Geodatabase table specifications

Figure 13-3. Poison Creek and Burns 7.5' quadrangles geodatabase data tables.

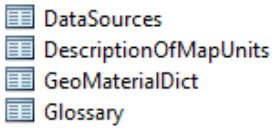

Table 13-2. Geodatabase tables.

Name	Description
DataSources	Data table that contains information about data sources used to compile the geology of the area.
DescriptionOfMapUnits	Data table that captures the content of the Description of Map Units (DMU), or equivalent List of Map Units and associated pamphlet text, included in a geologic map.
GeoMaterialDict	Data table providing definitions and hierarchy for GeoMaterial names prescribed by the GeMS database schema.
Glossary	Data table that contains information about the definitions of terms used in the geodatabase.

Geodatabase projection specifications

All spatial data are stored in the Oregon Statewide Lambert Conformal Conic projection. The datum is NAD83 HARN. The linear unit is international feet. See detailed projection parameters below:

Projection: Lambert_Conformal_Conic
False_Easting: 1312335.958005
False_Northing: 0.0
Central_Meridian: -120.5
Standard_Parallel_1: 43.0
Standard_Parallel_2: 45.5
Latitude_Of_Origin: 41.75
Linear Unit: Foot (0.3048)

Geographic Coordinate System: GCS_North_American_1983_HARN
Angular Unit: Degree (0.0174532925199433)
Prime Meridian: Greenwich (0.0)
Datum: D_North_American_1983_HARN
Spheroid: GRS_1980
Semimajor Axis: 6378137.0
Semiminor Axis: 6356752.314140356
Inverse Flattening: 298.257222101

Geologic map

This report is accompanied by a two map plates displaying the surficial and bedrock geology at a scale of 1:24,000 and geologic cross sections (see Plate 1 and 2 facsimiles below) for the Poison Creek and Burns 7.5’ quadrangles. The map plate was generated from detailed geologic data (scale of 1:8,000 or better) contained in the accompanying Esri format geodatabase. Both bedrock and surficial geologic interpretations can be recovered from the geodatabase and can be used to create a variety of additional thematic maps.

Plate 1. Reproduction of the geologic map of the Poison Creek 7.5’ quadrangle, Harney County, Oregon (Plate 1). Plate dimensions are 34 by 48 inches, scale 1;24,000. See digital folder for map plate.

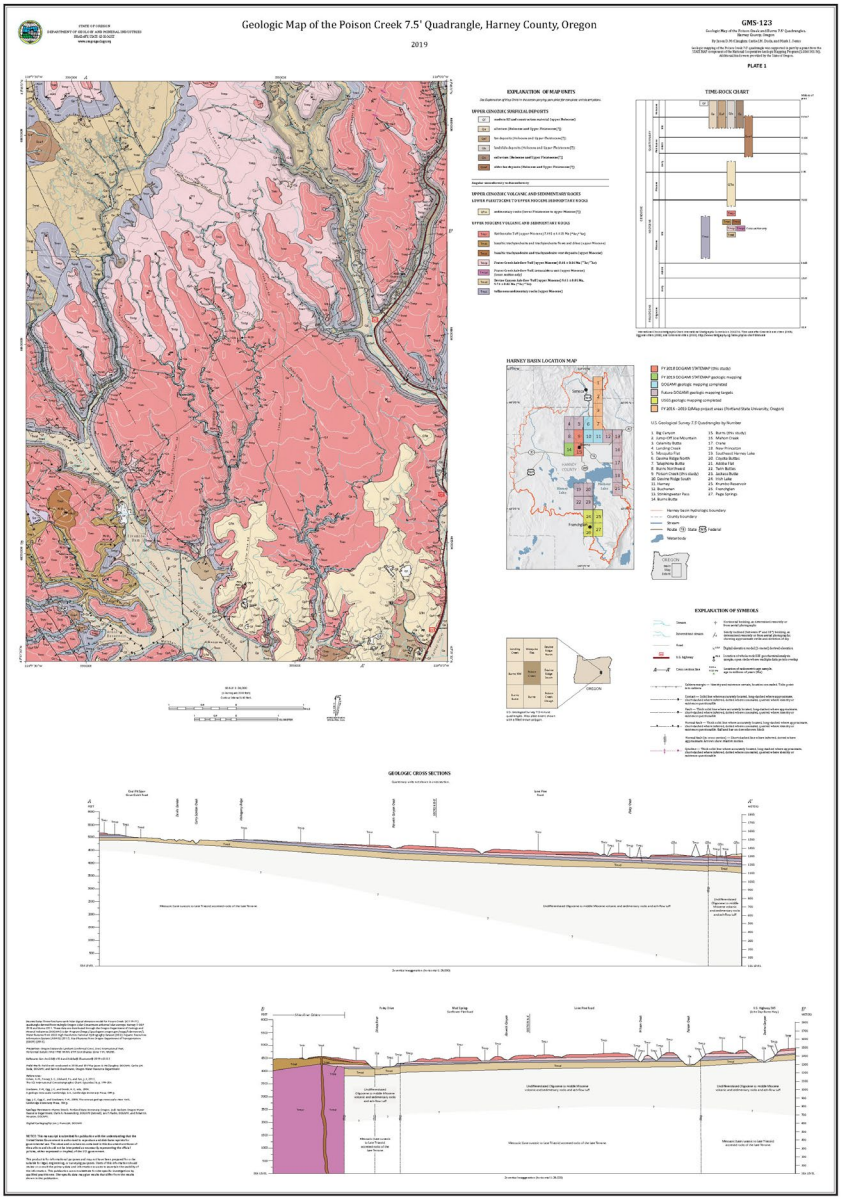

Plate 2. Reproduction of the geologic map of the Burns 7.5’ quadrangle, Harney County, Oregon (Plate 2). Plate dimensions are 34 by 46 inches, scale 1;24,000. See digital folder for map plate.

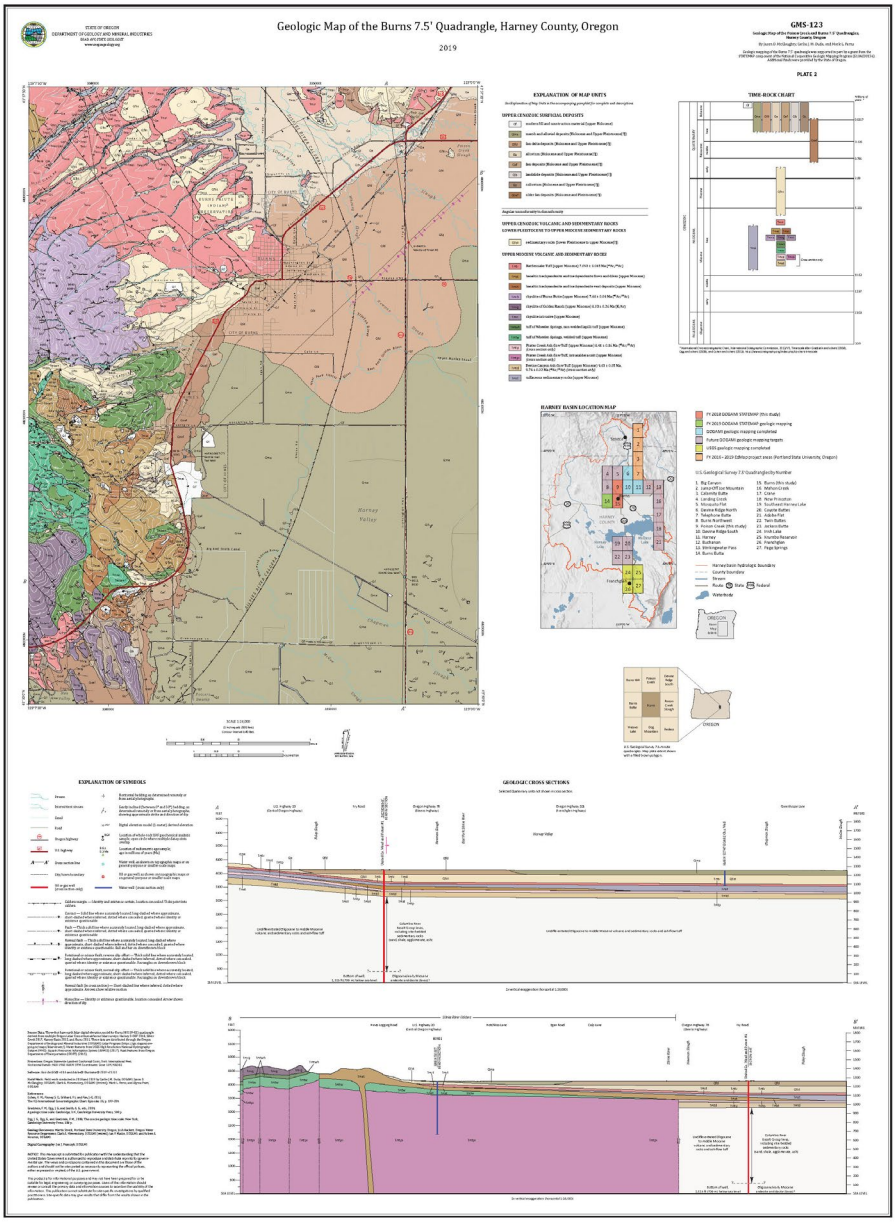

13.2 Methods

Geochemical analytical methods

Geologic mapping in the Poison Creek and Burns 7.5′ quadrangles was supported by numerous new and compiled X-ray fluorescence (XRF) geochemical analyses of whole-rock samples. Descriptive rock unit names for igneous rocks are based on normalized major element analyses plotted on the total alkalis ($Na_2O + K_2O$) versus silica (SiO_2) diagram (TAS) of Le Bas and others (1986), Le Bas and Streckeisen (1991), and Le Maitre and others (1989, 2004). New and compiled XRF-geochemical analyses are included in the geodatabase, in a separate shapefile named PCB2019_Geochemistry, and in Microsoft Excel® workbook PCB2019_DATA.xls (sheet PCB2019_Geochemistry). **Table 13-3** describes the fields listed in the spreadsheet. The locations of all geochemical samples are given in five coordinate systems: UTM Zone 11 (datum = NAD 27, NAD 83, units = meters), Geographic (datum = NAD 27, NAD 83, units = decimal degrees), and Oregon Lambert (datum = NAD 83, HARN, units = international feet).

Samples denoted by lab abbreviation WSU were analyzed by XRF at the Washington State University GeoAnalytical Lab, Pullman, Washington. Analytical procedures for the Washington State University GeoAnalytical Lab are described by Johnson and others (1999) and can be obtained online at https://s3.wp.wsu.edu/uploads/sites/2191/2017/06/Johnson-Hooper-and-Conrey.pdf. The location of each sample is given in five coordinate systems: UTM Zone 11 (datum = NAD 27, NAD 83, units = meters), Geographic (datum = NAD 27, NAD 83, units = decimal degrees), and Oregon Lambert (datum = NAD 83, HARN, units = international feet). Notes for spreadsheet: -9 equals no data for numerical fields for analytical data; nd equals no data in text fields; na equals information not applicable for text fields; samples shown with an “R” (e.g., HARN 50087 170-180R) are a repeat analysis of a single sample.

Table 13-3. Geochemistry spreadsheet field names and descriptions.

Field	Description
SAMPLE_NO	A unique number identifying the sample – e.g., 18 PCBJ 18.
WELL ID	Well log number for wells. Wells in Wasco County preceded by acronym HARN – e.g., HARN 53799.
MAP_NO	A unique number identifying the sample on the map plates – e.g., PG21.
QUADRANGLE	The USGS 7.5' quadrangle in which the sample is located – e.g., Burns.
ELEV_FT	Elevation of sample location in feet – e.g., 4141.
UTMN_NAD27	Meters north in NAD 27 UTM projection, zone 11.
UTME_NAD27	Meters east in NAD 27 UTM projection, zone 11.
LAT_NAD27	Latitude in NAD 27 geographic coordinates.
LONG_NAD27	Longitude in NAD 27 geographic coordinates.
UTMN_NAD83	Meters north in NAD 83 UTM projection, zone 11.
UTME_NAD83	Meters east in NAD 83 UTM projection, zone 11.
LAT_NAD83	Latitude in NAD 83 geographic coordinates.
LONG_NAD83	Longitude in NAD 83 geographic coordinates.
N_83HARN	Feet north in Oregon Lambert NAD 83, HARN, international feet.
E_83HARN	Feet east in Oregon Lambert NAD 83, HARN, international feet.
TERRANE_GR	Geologic group that the sample is assigned to. See GeologicMap, MapUnitPolys in the geodatabase – e.g., Harney Basin Volcanic Field. See pamphlet and DescriptionOfMapUnits table in the geodatabase.
FORMATION	Geologic formation that the sample is assigned to. See GeologicMap, MapUnitPolys in the geodatabase – e.g., Rattlesnake Tuff. See pamphlet and DescriptionOfMapUnits table in the geodatabase.
MEMBER	Geologic member that the sample is assigned to. See GeologicMap, MapUnitPolys in the geodatabase – e.g., Silvies River caldera. See pamphlet and DescriptionOfMapUnits table in the geodatabase.
MAP_UNIT_N	Geologic unit that the sample is assigned to. See GeologicMap, MapUnitPolys in the geodatabase – e.g., Rattlesnake Tuff. See pamphlet and DescriptionOfMapUnits table in the geodatabase.
MAP_UNIT_L	Unique label identifying the geologic unit that the sample is assigned to. See GeologicMap, MapUnitPolys in the geodatabase – e.g., Tmtr. See pamphlet and DescriptionOfMapUnits table in the geodatabase.
VOLCANIC_FIELD	Volcanic field that the unit is assigned to. In igneous provinces, a well-defined area covered with volcanic rocks with a common geologic history.
TAS_LITH	Rock name assigned based on the total alkalis ($Na_2O + K_2O$) versus silica (SiO_2) diagram (TAS) of Le Bas and others (1986), Le Bas and Streckeisen (1991), and Le Maitre and others (1989) – e.g., basalt, rhyolite.
MAJOR ELEMENTS	SiO_2, Al_2O_3, TiO_2, FeO*, MnO, CaO, MgO, K_2O, Na_2O, P_2O_5. In wt. percent.
TRACE ELEMENTS	Ni, Cr, Sc, V, Ba, Rb, Sr, Zr, Y, Nb, Ga, Cu, Zn, Pb, La, Ce, Th, Nd, U, Co, Hf, Sm, Eu, Yb, Lu. In ppm.
Total_I	Original analytical total as reported by the lab.
LOI	Value for loss on ignition as reported by the laboratory.
FE2O3	Iron (III) oxide or ferric oxide reported in original analysis.
FeO	Iron (II) oxide or ferrous oxide reported in original analysis.
REFERENCE	Publication reference, keyed to the reference list in this report.
METHOD	Analytical method used by laboratory that analyzed the sample – e.g., XRF.
LABORATORY	Analytical laboratory that analyzed the sample – e.g., WSU.
NOTES	Special information about certain samples – e.g., alteration.

Geochronology analytical methods

Seven K/Ar and $^{40}Ar/^{39}Ar$ isotopic ages were compiled for this study. No new samples were analyzed for radiometric ages. Geochronological data are included in the geodatabase, in a separate shapefile named PCB2019_Geochronology, and in Microsoft Excel® workbook PCB2019_DATA.xls (sheet PCB2019_Geochronology). **Table 13-4** describes the fields listed in the spreadsheet. The location of each radiometric age is given in five coordinate systems: UTM Zone 11 (datum = NAD 27, NAD 83, units = meters), Geographic (datum = NAD 27, NAD 83, units = decimal degrees), and Oregon Lambert (datum = NAD 83, HARN, units = international feet). Notes for spreadsheet: -9 equals no data for numerical fields for analytical data; nd equals no data in text fields; na equals information not applicable for text fields.

Table 13-4. Geochronology spreadsheet field names and descriptions.

Field	Description
SAMPLE_NO	A unique number identifying the sample – e.g., 18 PCBJ 18.
QUADRANGLE	The USGS 7.5' quadrangle in which the sample is located – e.g., Burns.
ELEV_FT	Elevation of sample location in feet – e.g., 4141.
UTMN_NAD27	Meters north in NAD 27 UTM projection, zone 11.
UTME_NAD27	Meters east in NAD 27 UTM projection, zone 11.
LAT_NAD27	Latitude in NAD 27 geographic coordinates.
LONG_NAD27	Longitude in NAD 27 geographic coordinates.
UTMN_NAD83	Meters north in NAD 83 UTM projection, zone 11.
UTME_NAD83	Meters east in NAD 83 UTM projection, zone 11.
LAT_NAD83	Latitude in NAD 83 geographic coordinates.
LONG_NAD83	Longitude in NAD 83 geographic coordinates.
N_83HARN	Feet north in Oregon Lambert NAD 83, HARN, international feet.
E_83HARN	Feet east in Oregon Lambert NAD 83, HARN, international feet.
TERRANE_GR	Geologic group that the sample is assigned to. See GeologicMap, MapUnitPolys in the geodatabase – e.g., Harney Basin Volcanic Field. See pamphlet and DescriptionOfMapUnits table in the geodatabase.
FORMATION	Geologic formation that the sample is assigned to. See GeologicMap, MapUnitPolys in the geodatabase – e.g., Rattlesnake Tuff. See pamphlet and DescriptionOfMapUnits table in the geodatabase.
MEMBER	Geologic member that the sample is assigned to. See GeologicMap, MapUnitPolys in the geodatabase – e.g., Silvies River caldera. See pamphlet and DescriptionOfMapUnits table in the geodatabase.
MAP_UNIT_N	Geologic unit that the sample is assigned to. See GeologicMap, MapUnitPolys in the geodatabase – e.g., Rattlesnake Tuff. See pamphlet and DescriptionOfMapUnits table in the geodatabase.
MAP_UNIT_L	Unique label identifying the geologic unit that the sample is assigned to. See GeologicMap, MapUnitPolys in the geodatabase – e.g., Tmtr. See pamphlet and DescriptionOfMapUnits table in the geodatabase.
VOLCANIC_FIELD	Volcanic field that the unit is assigned to. In igneous provinces, a well-defined area covered with volcanic rocks with a common geologic history.
LITHOLOGY	Rock type analyzed – e.g., basalt, dacite, rhyolite.
POLARITY	Natural remanent magnetization of sample as determined from a portable fluxgate magnetometer. N (normal), R (reversed), I (indeterminate).
AGE_KA	Age determined for the sample in thousands of years.
ERROR_KA	Error in age determination in thousands of years.
AGE_MA	Age determined for the sample in millions of years.
ERROR_MA	Error in age determination in millions of years.
METHOD	Analytical method used by laboratory that analyzed the sample – e.g., $^{40}Ar/^{39}Ar$.
MATERIAL_DATED	Type of material analyzed – e.g., amphiboles, plagioclase.
REFERENCE	Publication reference, keyed to the reference list in this report.
LABORATORY	Analytical laboratory that analyzed the sample – e.g., BCG.
NOTES	Special information about certain samples – e.g., alteration.

Bedding (strike and dip)

Strike and dip measurements of inclined bedding were taken in the Poison Creek and Burns area during the course of this study by traditional compass and clinometer methods. Additional bedding measurements were determined from interpretation of lidar imagery. DOGAMI has developed a routine and model in Esri ArcGIS™ Model Builder to calculate three-point solutions for lidar-derived bedding. The modeling process incorporates the use of 1) a 1-m lidar-derived DEM (digital elevation model); 2) the registration of three non-collinear points picked along the trace of a geological plane or contact discernable from a 1-m lidar DEM; 3) updating these points with their lidar-derived elevation values; and 4) creating a TIN (triangular irregular network) facet of the three points. The aspect of the TIN facet is equivalent to the dip direction, and the slope corresponds to the dip (0 to 90 degrees). The strike is then determined from the dip direction, subtracting or adding 90 degrees on the basis of the right-hand rule (described in below).

The factors influencing the certainty of lidar-derived bedding are the subjectivity of the digitizer and the clarity of the feature presumed to be indicative of bedding. To improve the clarity of lidar visualization, lidar-derived bedding was compiled using both a hillshade and slopeshade image, each at 50 percent transparency, draped over a Sky-View Factor (SVF) image. Sky-View Factor images are enhanced 1-m lidar DEMs, processed using the Sky-View Factor computation tool. The Sky-View Factor computation tool is part of the Relief Visualization Toolbox (RVT), open-source processing software produced by the Institute of Anthropological and Spatial Studies (http://iaps.zrc-sazu.si/en) at the Research Centre of the Slovenian Academy of Sciences and Arts (ZRCSAZU), to help visualize raster elevation model datasets. Sky-View visualizes hillshade models using diffuse illumination, overcoming the common problem of direct illumination, which can obscure linear objects that lie parallel to the direction of the light source and saturation of shadow areas. This brings improvements in detection of linear structures because the method exposes edges and holes (Zakšek and others, 2011). DOGAMI's visualization routine, combining a lidar-derived hillshade, slopeshade, and SVF imagery, helps illuminate shadows and amplifies the edges/ridges related to bedding features. Where possible, aerial photography, combined with a contextual knowledge of the geology of the area, was used to verify bedding features interpreted from lidar.

Strikes and dips are reported in both quadrant format (e.g., N. 30° W., 15° NE.) and azimuthal format using the right-hand rule (e.g., 330°, 15° NE., American convention). Field-measured bedding is coded by its appropriate Federal Geographic Data Committee (FGDC) reference number for geologic map symbolization. The measured point data are included in the geodatabase, in a separate shapefile named PCB2019_Bedding, and in Microsoft Excel® workbook PCB2019_DATA.xls (sheet PCB2019_ Bedding). **Table 13-5** describes the fields listed in the spreadsheet. The locations of these point data are given in five coordinate systems: UTM Zone 10 (datum = NAD 27, NAD 83, units = meters), Geographic (datum = NAD 27, NAD 83, units = decimal degrees), and Oregon Lambert (datum = NAD 83, HARN, units = international feet). Strike and dip symbols can be properly drawn by the Esri ArcMap product by opening the layer properties, categorizing by type, choosing the appropriate symbol, and rotating the symbol based on the "Strike_Azi" field. (The Advanced button allows you to select the rotation field.) The rotation style should be set to geographic in order to maintain the right-hand rule property. Azimuths are given in true north; an additional clockwise correction of about 1.6 degrees is needed to plot strikes and dips properly on the Oregon Lambert conformal conic projection in this area. Notes for spreadsheet: nd, no data.

Table 13-5. Bedding (strike and dip) spreadsheet field names and descriptions.

Field	Description
STRUCTURE	Type of geologic structure from which feature was determined. E.g., Inclined bedding.
FGDC_REF	An attribute code assigned to each feature, derived from the Federal Geographic Data Committee (FGDC) digital standard for geologic map symbolization. E.g., 6.2.
QUADRANGLE	The USGS 7.5' quadrangle in which the sample is located. E.g., Devine Ridge North.
ELEV_FT	Elevation of data location in feet. E.g., 22.
UTMN_NAD27	Meters north in NAD 27 UTM projection, zone 11.
UTME_NAD27	Meters east in NAD 27 UTM projection, zone 11.
LAT_NAD27	Latitude in NAD 27 geographic coordinates.
LONG_NAD27	Longitude in NAD 27 geographic coordinates.
UTMN_NAD83	Meters north in NAD 83 UTM projection, zone 11.
UTME_NAD83	Meters east in NAD 83 UTM projection, zone 11.
LAT_NAD83	Latitude in NAD 83 geographic coordinates.
LONG_NAD83	Longitude in NAD 83 geographic coordinates.
N_83HARN	Feet north in Oregon Lambert NAD 83, HARN, international feet.
E_83HARN	Feet east in Oregon Lambert NAD 83, HARN, international feet.
TERRANE_GR	Geologic group that the sample is assigned to. See GeologicMap, MapUnitPolys in the geodatabase. E.g., Columbia River Basalt Group.
FORMATION	Geologic formation that the sample is assigned to. See GeologicMap, MapUnitPolys in the geodatabase. E.g., Rattlesnake Tuff Formation.
MEMBER	Geologic member that the sample is assigned to. See GeologicMap, MapUnitPolys in the geodatabase.
MAP_UNIT_N	Geologic unit that the sample is assigned to. See GeologicMap, MapUnitPolys in the geodatabase. E.g., dacite.
MAP_UNIT_L	Unique label identifying the geologic unit that the sample is assigned to. See GeologicMap, MapUnitPolys in the geodatabase. E.g., Toda.
STRIKE_QUAD	Strike direction of the inclined plane, stated in a north-directed quadrant format. E.g., N35E.
DIP	Amount of dip, degrees from horizontal, with direction. E.g., 45SE.
STRIKE_AZI	Strike direction of the inclined plane, as determined by employing the right-hand rule (American convention). E.g., 035.
DIP_AZIMUTH	Azimuthal direction of dip. E.g., 125.
DIP_AMOUNT	Amount of dip, degrees from horizontal. E.g., 45.
REFERENCE	Publication reference, keyed to the reference list in this report.
Notes	Special information (e.g., lidar derived)

Water well logs

The well log spreadsheet is derived from written drillers' logs provided by Oregon Department of Water Resources (OWRD). Well logs vary greatly in completeness and accuracy, so the utility of subsurface interpretations based upon these data can be limited. Water well logs compiled and used for interpretation during this study were not field located. The approximate locations were estimated using tax lot maps, street addresses (coordinates obtained from Google Earth™), and aerial photographs to plot locations on the map. The accuracy of the locations ranges widely, from errors of one-half mile possible for wells located only by section and plotted at the section centroid to a few tens of feet for wells located by address or tax lot number on a city lot with bearing and distance from a corner. At each mapped location the number of the well log is indicated. This number can be combined with the first four letters of the county name (e.g., HARN 5473), to retrieve an image of the well log from the OWRD website.

Point data are included in the geodatabase, as a separate shapefile named DRN2018_WaterWells.shp, and as a Microsoft Excel spreadsheet named DRN2018_WaterWells.xlsx.

Table 13-6 describes the fields listed in the spreadsheet. The locations of water well point data are given in six coordinate systems: UTM Zone 11 (datum = WGS 84, NAD 27, NAD 83, units = meters), Geographic (datum = NAD 27, NAD 83, units = decimal degrees), and Oregon Lambert (datum = NAD 83, HARN, units = international feet).

Lithologies in well intervals listed in the well log spreadsheet can alternate between consolidated and unconsolidated and may be listed as alternating between bedrock and surficial geologic units. This may occur where bedrock units are soft, where paleosols or weak zones lie within bedrock, or where cemented or partly cemented zones alternate with unconsolidated zones in surficial deposits.

Lithologic abbreviations (alphabetical by group)

UNCONSOLIDATED SURFICIAL UNITS	
Abbreviation	**Description**
bd	boulders
c	clay
ch	clay, hard (often logged as claystone but probably not bedrock)
g	gravel
gc	cemented gravel
gs	gravel and sand (also sandy gravel)
m	mud
s	sand
sg	sand and gravel (also gravelly sand)
st	silt
Rock, sedimentary	
bc	breccia
cg	conglomerate
cs	claystone
sh	shale
ss	sandstone
Rock, igneous	
an	andesite
b	basalt
cd	cinders
pu	pumice
gr	granite
l	lava
r	rhyolite
sc	scoria
t	tuff
v	volcanic, undivided
vb	volcanic breccia
Other	
af	artificial fill
cl	coal (lignite)
dg	decomposed granite
o	other (drillers unit listed in notes column of spreadsheet)
rk	rock
sl	soil
u	unknown (typically used where a well has been deepened)

Table 13-6. Water well log spreadsheet field names and descriptions.

Field	*Description and Example
TRS	Two digits for township, two digits for range, and two for section; negative if township is south of Willamette baseline. Exception for township and range if they contain a decimal. E.g., −2132.503.
COUNTY	Harney County. e.g., HARN.
GRID	Well log number for wells. Wells in Harney County preceded by acronym HARN (e.g., HARN 53799). e.g., 53779.
WELL_EL_FT	Wellhead elevation in feet as given by Google Earth™ at corresponding WGS 84 location. e.g., 1978.
LOCATED_BY	Google Earth™ elevation for cursor location at a given address. e.g., Google. Google Earth™ elevation at house in vicinity of given address. e.g., House. Pad identifying approximate well location, visible in air photo. e.g., Pad. Approximate taxlot centroid or other best guess for well location using a combination of taxlot maps and aerial photographs. e.g., Taxlot. Owner name. e.g., Owner. Address of well listed on Oregon Water Resources Department (OWRD) Startcard. Wells located by Oregon Water Resources Department (OWRD) using handheld GPS. e.g., OWRD. GPS coordinates of wellhead included with well log. e.g., GPS. Approximate quarter-quarter-quarter section centroid. e.g., QQQ. Approximate quarter-quarter-section centroid. e.g., QQ. Approximate quarter-section centroid. e.g., Q. Approximate fit to sketch map included with well log. e.g., map.
LITHOLOGY	Best interpretation of driller's log using abbreviations above. e.g., g.
BASE_FT	Record base of driller's interval or, if lithology abbreviation would not change, similar intervals, in feet below wellhead. e.g., 17.
TOP_FT	Calculated top of driller's interval or similar intervals, in feet below wellhead. e.g., 14.
TOP_EL_FT	Calculated elevation at top of driller's interval, or similar intervals, in feet above sea level. e.g., 86.
BASE_EL_FT	Calculated elevation at base of driller's interval, or similar intervals, in feet above sea level. e.g., 83.
BEDRK_LITH	Lists bedrock lithologies, when encountered, abbreviations listed above. e.g., b.
BEDRK_ELEV	Calculated elevation at which bedrock or soil over bedrock was first encountered, in feet above sea level. e.g., 1924.
TAX_LOT	Taxlot number. Where it is determined that a taxlot number is used more than once in the section then the appropriate subdivision of the section is indicated in the notes field. e.g., 800.
COLOR	Color of interval as reported by the well driller. e.g., green.
NOTES	Notes about the stratigraphic interval as originally described by the well driller.
MAP_LABEL	Geologic unit interpreted in subsurface based on drillers log and designated by map unit label used in accompanying geodatabase. Intervals labeled "suna" (surface unit not applicable) are those where the lithology as interpreted by the original drillers' log do not correspond; also denotes intervals in the subsurface where a precise unit label cannot be applied. e.g., Tb.
QUADRANGLE	The USGS 7.5' quadrangle in which the sample is located. e.g., Poison Creek.
UTMN_WGS84	Meters north in WGS84 UTM projection, zone 11.
UTME_WGS84	Meters east in WGS84 UTM projection, zone 11.
UTMN_NAD27	Meters north in NAD 27 UTM projection, zone 11.
UTME_NAD27	Meters east in NAD 27 UTM projection, zone 11.
LAT_NAD27	Latitude in NAD 27 geographic coordinates.
LONG_NAD27	Longitude in NAD 27 geographic coordinates.
UTMN_NAD83	Meters north in NAD 83 UTM projection, zone 11.
UTME_NAD83	Meters east in NAD 83 UTM projection, zone 11.
LAT_NAD83	Latitude in NAD 83 geographic coordinates.
LONG_NAD83	Longitude in NAD 83 geographic coordinates.
N_83HARN	Feet north in Oregon Lambert NAD 83, HARN, international feet.
E_83HARN	Feet east in Oregon Lambert NAD 83, HARN, international feet.

*Well location given in six coordinate systems calculated by reprojecting original WGS 84 UTM, zone 11 locations.

CTI Geothermal Test Well – cuttings and log

The following section 1) shows cuttings samples from the HARN 50087 CTI Geothermal Test Well in Hines, 2) provides tabulated geochemical data for samples obtained from the well (**Table 13-7**), and 3) provides detailed descriptions/interpretations of cuttings by J.D. McClaughry (**Table 13-8**).

Name of Well: HARN 50087 - CTI Geothermal Test Well **Year well drilled**: 1996
Location of Well: Hines, Oregon **Latitude, Longitude (NAD83)**: 43.55013, -119.08158
Elevation of well collar: 1264 (4148 ft) asl
Total depth drilled: 596 m (1956 ft), depth intervals of retrieved cuttings shown in feet (e.g., 140-150).

Cuttings shown are from depth intervals 140 to 340 ft.

Name of Well: HARN 50087 - CTI Geothermal Test Well **Year well drilled**: 1996
Location of Well: Hines, Oregon **Latitude, Longitude (NAD83)**: 43.55013, -119.08158
Elevation of well collar: 1264 (4148 ft) asl
Total depth drilled: 596 m (1956 ft), depth intervals of retrieved cuttings shown in feet (e.g., 140-150).

Cuttings shown are from depth intervals 340 to 500 ft.

Name of Well: HARN 50087 - CTI Geothermal Test Well **Year well drilled**: 1996
Location of Well: Hines, Oregon **Latitude, Longitude (NAD83)**: 43.55013, -119.08158
Elevation of well collar: 1264 (4148 ft) asl
Total depth drilled: 596 m (1956 ft), depth intervals of retrieved cuttings shown in feet (e.g., 140-150).

Cuttings shown are from depth intervals 500 to 700 ft.

Name of Well: HARN 50087 - CTI Geothermal Test Well **Year well drilled**: 1996
Location of Well: Hines, Oregon **Latitude, Longitude (NAD83)**: 43.55013, -119.08158
Elevation of well collar: 1264 (4148 ft) asl
Total depth drilled: 596 m (1956 ft), depth intervals of retrieved cuttings shown in feet (e.g., 140-150).

Cuttings shown are from depth intervals 700 to 900 ft.

Name of Well: HARN 50087 - CTI Geothermal Test Well **Year well drilled**: 1996
Location of Well: Hines, Oregon **Latitude, Longitude (NAD83)**: 43.55013, -119.08158
Elevation of well collar: 1264 (4148 ft) asl
Total depth drilled: 596 m (1956 ft), depth intervals of retrieved cuttings shown in feet (e.g., 140-150).
Cuttings shown are from depth intervals 900 to 1100 ft; no returns for interval 970 to 1000.

Name of Well: HARN 50087 - CTI Geothermal Test Well **Year well drilled**: 1996
Location of Well: Hines, Oregon **Latitude, Longitude (NAD83)**: 43.55013, -119.08158
Elevation of well collar: 1264 (4148 ft) asl
Total depth drilled: 596 m (1956 ft), depth intervals of retrieved cuttings shown in feet (e.g., 140-150).

Cuttings shown are from depth intervals 1100 to 1300 ft.

5 cm

Name of Well: HARN 50087 - CTI Geothermal Test Well **Year well drilled**: 1996
Location of Well: Hines, Oregon **Latitude, Longitude (NAD83)**: 43.55013, -119.08158
Elevation of well collar: 1264 (4148 ft) asl
Total depth drilled: 596 m (1956 ft), depth intervals of retrieved cuttings shown in feet (e.g., 140-150).

Cuttings shown are from depth intervals 1335 to 1500 ft.

5 cm

Name of Well: HARN 50087 - CTI Geothermal Test Well **Year well drilled**: 1996
Location of Well: Hines, Oregon **Latitude, Longitude (NAD83)**: 43.55013, -119.08158
Elevation of well collar: 1264 (4148 ft) asl
Total depth drilled: 596 m (1956 ft), depth intervals of retrieved cuttings shown in feet (e.g., 140-150).

Cuttings shown are from depth intervals 1500 to 1700 ft.

Name of Well: HARN 50087 - CTI Geothermal Test Well **Year well drilled**: 1996
Location of Well: Hines, Oregon **Latitude, Longitude (NAD83)**: 43.55013, -119.08158
Elevation of well collar: 1264 (4148 ft) asl
Total depth drilled: 596 m (1956 ft), depth intervals of retrieved cuttings shown in feet (e.g., 140-150).

Cuttings shown are from depth intervals 1700 to 1900 ft.

5 cm

Name of Well: HARN 50087 - CTI Geothermal Test Well **Year well drilled**: 1996
Location of Well: Hines, Oregon **Latitude, Longitude (NAD83)**: 43.55013, -119.08158
Elevation of well collar: 1264 (4148 ft) asl
Total depth drilled: 596 m (1956 ft), depth intervals of retrieved cuttings shown in feet (e.g., 140-150).
Cuttings shown are from depth intervals 1900 to 1956 ft.

5 cm

Table 13-7. Geochemical analyses obtained from cuttings from the HARN 50087 CTI Geothermal Test Well (2 tables). "R" sample numbers indicate repeat analyses.

Sample No. with Depth Interval (ft)	HARN 50087 140-160	HARN 50087 170-180	HARN 50087 170-180R	HARN 50087 190-200	HARN 50087 220-250	HARN 50087 260-270	HARN 50087 290-330	HARN 50087 330-340	HARN 50087 360-400	HARN 50087 440-490	HARN 50087 670-680	HARN 50087 720-810
Geographic Area	Hines	Hines	Hines	Hines	Hines	Hines	Hines	Hines	Hines	Hines	Hines	Hines
MAP_UNIT_N	Sed. rocks	Rattlesnake Tuff	Rattlesnake Tuff	Rattlesnake Tuff	basaltic trachyand./ trachyand. flows	basaltic trachyand./ trachyand. flows	basaltic trachyand./ trachyand. flows	basaltic trachyand./ trachyand. flows	tuff of Wheeler Springs, welded tuff	tuff of Wheeler Springs, welded tuff	Prater Creek Ash-flow Tuff, intra-caldera unit	Prater Creek Ash-flow Tuff, intra-caldera unit
MAP_UNIT_L	QTst	Tmtr	Tmtr	Tmtr	Tmat	Tmat	Tmat	Tmat	Tmtw	Tmtw	Tmtpi	Tmtpi
UTM_N (NAD 83)	4824014	4824014	4824014	4824014	4824014	4824014	4824014	4824014	4824014	4824014	4824014	4824014
UTM_E (NAD 83)	331853	331853	331853	331853	331853	331853	331853	331853	331853	331853	331853	331853
Age (Ma)	nd	nd	nd	nd	nd	nd	nd	nd	nd	nd	nd	nd
Map No.	BG16	BG17	BG18	BG19	BG20	BG21	BG22	BG23	BG24	BG25	BG26	BG27
Oxides, weight percent												
SiO_2	80.65	68.71	68.73	69.15	61.04	56.37	64.26	57.10	73.47	75.25	76.47	75.37
Al_2O_3	10.37	18.62	18.56	18.11	15.75	17.53	14.42	17.49	14.15	13.21	12.27	12.40
TiO_2	0.16	0.29	0.29	0.25	1.06	1.06	0.96	1.15	0.23	0.22	0.12	0.14
FeO*	1.27	2.41	2.48	2.04	8.70	7.53	6.83	8.21	1.67	1.50	1.77	2.05
MnO	0.02	0.06	0.06	0.06	0.12	0.14	0.14	0.13	0.04	0.03	0.03	0.05
CaO	0.56	2.85	2.84	2.66	5.52	7.46	5.25	7.99	1.03	0.71	0.25	0.42
MgO	0.16	5.95	5.95	5.11	4.31	3.97	4.96	3.20	0.38	0.31	0.10	0.14
K_2O	3.88	0.56	0.55	1.33	1.65	1.85	2.06	1.16	5.02	4.93	4.95	5.09
Na_2O	2.91	0.52	0.50	1.27	1.62	3.63	0.63	2.87	3.97	3.80	4.01	4.20
P_2O_5	0.03	0.03	0.03	0.03	0.23	0.46	0.49	0.70	0.04	0.04	0.02	0.15
LOI	1.81	19.56	19.56	16.87	12.47	0.95	15.44	6.92	3.74	1.11	1.22	1.34
Total_I	97.57	80.00	80.20	82.48	86.78	98.48	84.15	92.59	95.83	98.42	98.48	98.37
Trace Elements, parts per million												
Ni	7	7	3	7	29	37	21	35	4	5	4	5
Cr	4	4	5	4	41	52	26	64	4	4	3	5
Sc	2	5	5	5	17	20	16	21	3	3	0	0
V	14	40	42	43	75	165	46	113	11	12	8	10
Ba	477	125	128	208	2087	788	563	714	695	549	228	212
Rb	91	19	19	31	104	30	105	32	101	108	109	121
Sr	33	82	83	81	424	527	477	550	63	43	46	17
Zr	206	276	281	260	134	154	128	146	242	246	501	530
Y	29	40	41	40	17	23	20	23	40	42	65	80
Nb	19.8	27.6	28.3	29.0	8.9	10.3	9.5	10.7	27.3	29.8	42.8	44.0
Ga	13	18	17	18	15	19	14	17	17	17	22	23
Cu	6	29	28	15	77	69	36	73	5	5	7	9
Zn	23	69	69	56	68	79	58	82	36	29	95	118
Pb	10	20	21	20	7	7	6	7	19	13	35	18
La	30	49	49	45	21	20	18	25	40	38	58	61
Ce	55	93	90	99	34	47	37	46	71	73	92	116
Th	7	10	10	11	2	3	2	2	10	9	9	9
Nd	22	37	37	35	19	26	21	22	29	30	37	54
U	2	0	1	1	1	1	3	2	3	3	4	3

Major element determinations have been normalized to a 100-percent total on a volatile-free basis and recalculated with total iron expressed as FeO*; nd - no data or element not analyzed; na - not applicable or no information. LOI, Loss on Ignition; Total_I, original analytical total.

Table 13-7, continued. Geochemical analyses obtained from cuttings from the HARN 50087 CTI Geothermal Test Well.

Sample No. with Depth Interval (ft)	**HARN 50087 830-900**	**HARN 50087 900-970**	**HARN 50087 1000-1010**	**HARN 50087 1010-1100**	**HARN 50087 1100-1200**	**HARN 50087 1200-1300**	**HARN 50087 1300-1340**	**HARN 50087 1335-1380**	**HARN 50087 1470-1500**	**HARN 50087 1500-1560**	**HARN 50087 1560-1600**	**HARN 50087 1690-1710**	**HARN 50087 1780-1810**	**HARN 50087 1900-1940**
Geographic Area	Hines	Hines	Hines	Hines	Hines	Hines	Hines	Hines	Hines	Hines	Hines	Hines	Hines	Hines
MAP_UNIT_N	Prater Creek Ash-flow Tuff, intra-caldera unit	Prater Creek Ash-flow Tuff, intra-caldera unit	Prater Creek Ash-flow Tuff, intra-caldera unit	Prater Creek Ash-flow Tuff, intra-caldera unit	Prater Creek Ash-flow Tuff, intra-caldera unit	Prater Creek Ash-flow Tuff, intra-caldera unit	Prater Creek Ash-flow Tuff, intra-caldera unit	Prater Creek Ash-flow Tuff, intra-caldera unit	Prater Creek Ash-flow Tuff, intra-caldera unit	Prater Creek Ash-flow Tuff, intra-caldera unit	Prater Creek Ash-flow Tuff, intra-caldera unit	Prater Creek Ash-flow Tuff, intra-caldera unit	Prater Creek Ash-flow Tuff, intra-caldera unit	Prater Creek Ash-flow Tuff, intra-caldera unit
MAP_UNIT_L	Tmtpi	Tmtpi	Tmtpi	Tmtpi	Tmtpi	Tmtpi	Tmtpi	Tmtpi	Tmtpi	Tmtpi	Tmtpi	Tmtpi	Tmtpi	Tmtpi
UTM_N (NAD 83)	4824014	4824014	4824014	4824014	4824014	4824014	4824014	4824014	4824014	4824014	4824014	4824014	4824014	4824014
UTM_E (NAD 83)	331853	331853	331853	331853	331853	331853	331853	331853	331853	331853	331853	331853	331853	331853
Age (Ma)	nd	Age (Ma)	nd	nd	nd	8.41	8.41	nd	nd	nd	nd	nd	nd	nd
Map No.	BG28	BG29	BG30	BG31	BG32	BG33	BG34	BG35	BG36	BG37	BG38	BG39	BG40	BG41
Oxides, weight percent														
SiO_2	77.29	77.40	77.28	76.38	77.12	76.85	76.98	76.82	76.76	77.04	76.72	74.46	77.00	76.78
Al_2O_3	11.60	11.52	11.73	11.40	11.60	11.64	11.66	12.08	11.57	11.48	11.92	12.23	11.17	11.18
TiO_2	0.13	0.13	0.12	0.12	0.12	0.12	0.12	0.12	0.11	0.12	0.13	0.17	0.16	0.15
FeO*	2.04	2.08	1.74	1.87	1.91	2.19	2.24	1.92	2.65	2.17	2.11	3.14	2.70	3.12
MnO	0.04	0.04	0.03	0.03	0.04	0.11	0.03	0.03	0.05	0.03	0.05	0.08	0.05	0.08
CaO	0.18	0.18	0.40	1.77	0.61	0.28	0.18	0.13	0.10	0.48	0.37	0.31	0.31	0.20
MgO	0.07	0.06	0.03	0.07	0.06	0.07	0.06	0.08	0.08	0.08	0.04	0.12	0.17	0.09
K_2O	4.77	4.75	4.81	4.67	4.67	4.70	4.69	4.82	4.72	4.81	4.55	5.86	4.70	4.63
Na_2O	3.86	3.82	3.85	3.66	3.85	3.97	4.01	3.99	3.93	3.78	4.11	3.61	3.72	3.74
P_2O_5	0.03	0.03	0.02	0.02	0.02	0.05	0.03	0.02	0.02	0.02	0.01	0.02	0.02	0.02
LOI	0.80	0.67	0.52	1.99	1.20	0.93	0.68	0.81	0.76	1.12	3.42	1.94	1.31	1.43
Total_I	98.72	98.74	99.26	97.57	98.13	98.71	98.82	98.51	99.04	98.32	96.17	97.63	98.45	98.29
Trace Elements, parts per million														
Ni	8	8	2	4	8	10	10	9	9	6	4	4	6	5
Cr	35	23	3	16	20	19	12	28	14	8	5	5	7	14
Sc	1	0	0	0	1	2	1	1	1	0	1	1	2	0
V	11	8	6	7	5	4	5	3	5	3	1	12	4	8
Ba	182	181	177	187	173	177	167	169	163	171	194	106	48	64
Rb	112	107	110	105	107	109	110	117	118	111	112	119	105	104
Sr	15	15	12	21	16	16	12	13	12	15	12	21	13	19
Zr	487	486	483	448	461	442	444	439	488	498	497	712	640	576
Y	72	71	70	66	67	65	61	61	59	64	73	68	81	75
Nb	41.6	41.7	40.9	37.4	38.3	39.4	37.3	35.8	39.7	38.8	41.1	47.5	37.9	38.2
Ga	21	21	21	20	20	21	21	21	21	20	21	22	20	22
Cu	10	11	7	12	10	16	17	84	14	20	13	7	43	17
Zn	97	95	149	119	123	107	97	158	103	116	103	141	124	122
Pb	19	18	17	27	28	38	16	42	18	20	24	24	24	24
La	63	57	54	55	55	53	56	50	50	50	56	66	61	58
Ce	113	115	100	106	109	107	110	103	98	98	110	131	125	127
Th	9	8	9	8	8	8	8	7	9	7	9	9	8	8
Nd	51	52	44	49	51	49	51	48	44	46	52	60	57	53
U	1	1	3	3	3	2	3	3	3	3	3	5	4	1

Major element determinations have been normalized to a 100-percent total on a volatile-free basis and recalculated with total iron expressed as FeO*; nd - no data or element not analyzed; na - not applicable or no information. LOI, Loss on Ignition; Total_I, original analytical total.

Table 13-8. Descriptions and interpretations of downhole lithologies from HARN 50087 CTI Geothermal Test Well cuttings. Cuttings described and interpreted by J.D. McClaughry during 2018 to 2019.

Depth Interval (ft)		Elevation Interval (ft)		Geochemical Sample ID	Color	Interval Description	Map Unit
0	23	4148	4125		Brown	Sand.	Qoaf
23	36	4125	4112		Blue	Clay.	Qoaf
36	102	4112	4046		Brown	Clay.	Qoaf
102	126	4046	4022		Brown	Clay/sand.	QTst
126	134	4022	4014		Brown/red	Cinders.	QTst
134	140	4014	4008		Gray	Volcanic rock.	QTst
140	150	4008	3998		Light brownish gray (5YR 6/1)	Welded tuff, numerous lithic fragments and white feldspar crystals.	QTst
150	160	3998	3988	**HARN 50087 140-160**	Light brownish gray (5YR 6/1)	Welded tuff, numerous lithic fragments and white feldspar crystals.	QTst
160	170	3988	3978		Pinkish gray (5YR 8/1)	Semi-consolidated tuff.	Tmtr
170	180	3978	3968	**HARN 50087 170-180**	White (N9)	Semi-consolidated tuff.	Tmtr
180	190	3968	3958		Very pale orange (10YR 8/2)	Highly expanded pumice.	Tmtr
190	200	3958	3948	**HARN 50087 190-200**	White (N9)	Semi-consolidated tuff.	Tmtr
200	210	3948	3938		Yellowish gray (5Y 8/1)	Semi-consolidated tuff.	Tmtr
210	220	3938	3928		Medium gray (N5)	Vesicular trachyandesite with microlite plagioclase.	Tmat
220	230	3928	3918	**HARN 50087 220-250**	Medium gray (N5) to White (N9)	Mixed vesiculated trachyandesite and crystal tuff. Bleached white, hydrothermally altered.	Tmat
230	240	3918	3908		Medium gray (N5)	Vesicular trachyandesite. Bleached white, hydrothermally altered.	Tmat
240	250	3908	3898		Medium gray (N5)	Vesicular trachyandesite. Bleached white, hydrothermally altered.	Tmat
250	260	3898	3888		Moderate reddish brown (10R 3/4)	Vesicular, microcrystalline cinders.	Tmat
260	270	3888	3878	**HARN 50087 260-270**	Moderate orange pink (10R 7/4) to Light brownish gray (5YR 6/1)	Vesicular to dense trachyandesite. Silica, botryoidal zeolite.	Tmat
270	280	3878	3868		Moderate orange pink (10R 7/4) to White (N9)	Vesicular to dense trachyandesite. Silica, botryoidal zeolite.	Tmat
280	290	3868	3858		Yellowish gray (5Y 8/1)	Crystal tuff, clear blocky feldspar, ash shards. Zeolite.	Tmat
290	300	3858	3848	**HARN 50087 290-330**	Yellowish gray (5Y 8/1)	Crystal tuff, clear blocky feldspar, ash shards. Zeolite.	Tmat
300	310	3848	3838		Yellowish gray (5Y 8/1)	Crystal tuff, clear blocky feldspar, ash shards. Zeolite.	Tmat
310	320	3838	3828		Yellowish gray (5Y 8/1)	Crystal tuff, clear blocky feldspar, ash shards.	Tmat
320	330	3828	3818		Yellowish gray (5Y 8/1)	Crystal tuff, abundant clear blocky feldspar, prismatic black pyroxene, ash shards.	Tmat
330	340	3818	3808	**HARN 50087 330-340**	Brownish gray (5YR 4/1) to White (N9)	Microcrystalline cinders. Bleached white where altered. Bladed zeolite.	Tmat
340	350	3808	3798		Medium gray (N6) to White (N9)	Vesicular to dense trachyandesite. Fragments of bleached white, crystal-rich volcaniclastic sandstone. Zeolite.	Tmat
350	360	3798	3788		Light gray N7 to Medium dark gray (N4)	Mixed crystalline welded tuff, microcrystalline trachyandesite. Zeolite.	Tmtw
360	370	3788	3778	**HARN 50087 360-400**	Clear to Very light gray (N8)	Perlitic, very sparsely pyroxene microphyric obsidian.	Tmtw
370	380	3778	3768		Clear to Very light gray (N8)	Perlitic, very sparsely pyroxene microphyric obsidian.	Tmtw
380	390	3768	3758		Clear to Very light gray (N8)	Perlitic, very sparsely pyroxene microphyric obsidian.	Tmtw
390	400	3758	3748		Clear to Very light gray (N8) to Pinkish gray (5YR 8/1)	Perlitic, very sparsely pyroxene microphyric obsidian, crystalline rhyolite fragments.	Tmtw

Depth Interval (ft)	Elevation Interval (ft)	Geochemical Sample ID	Color	Interval Description	Map Unit
400 410	3748 3738		Very light gray (N8) to Pinkish gray (5YR 8/2)	Crystal tuff, sparse blocky clear feldspar and black pyroxene microphenocrysts, perlitic obsidian fragments.	Tmtw
410 420	3738 3728		Very light gray (N8) to Pinkish gray (5YR 8/2)	Crystal tuff, sparse blocky clear feldspar and black pyroxene microphenocrysts, perlitic obsidian fragments.	Tmtw
420 430	3728 3718		Very light gray (N8) to Pinkish gray (5YR 8/2)	Crystal tuff, sparse blocky clear feldspar and black pyroxene microphenocrysts, perlitic obsidian fragments.	Tmtw
430 440	3718 3708		Very light gray (N8) to Pinkish gray (5YR 8/2)	Crystal tuff, sparse blocky clear feldspar and black pyroxene microphenocrysts, perlitic obsidian fragments.	Tmtw
440 450	3708 3698	**HARN 50087 440-490**	Very light gray (N8) to Pinkish gray (5YR 8/2)	Crystal tuff, sparse blocky clear feldspar and black pyroxene microphenocrysts, perlitic obsidian fragments.	Tmtw
450 460	3698 3688		Very light gray (N8) to Pinkish gray (5YR 8/2)	Crystal tuff, sparse blocky clear feldspar and black pyroxene microphenocrysts, perlitic obsidian fragments.	Tmtw
460 470	3688 3678		Very light gray (N8) to Pinkish gray (5YR 8/2)	Crystal tuff, sparse blocky clear feldspar and black pyroxene microphenocrysts, perlitic obsidian fragments.	Tmtw
470 480	3678 3668		Very light gray (N8) to Pinkish gray (5YR 8/2)	Crystal tuff, sparse blocky clear feldspar and black pyroxene microphenocrysts, perlitic obsidian fragments.	Tmtw
480 490	3668 3658		Very light gray (N8) to Pinkish gray (5YR 8/2)	Crystal tuff, sparse blocky clear feldspar and black pyroxene microphenocrysts, perlitic obsidian fragments.	Tmtw
490 500	3658 3648		Very light gray (N8) to Pinkish gray (5YR 8/2)	Crystal tuff, sparse blocky clear feldspar and black pyroxene microphenocrysts, perlitic obsidian fragments.	Tmtw
500 510	3648 3638		Very light gray (N8) to Pinkish gray (5YR 8/2)	Crystal tuff, sparse blocky clear feldspar and black pyroxene microphenocrysts, perlitic obsidian fragments.	Tmtw
510 520	3638 3628		Medium light gray (N6)	Crystal tuff, sparse blocky clear feldspar and black pyroxene microphenocrysts, perlitic obsidian fragments.	Tmtw
520 530	3628 3618		Medium light gray (N6)	Crystal tuff, sparse blocky clear feldspar and black pyroxene microphenocrysts, perlitic obsidian fragments.	Tmtw
530 540	3618 3608		Medium light gray (N6) to Light brownish gray (5YR 6/1) to White (N9)	Crystal tuff. Sparse blocky clear feldspar and black pyroxene microphenocrysts. Eutaxitic texture.	Tmtw
540 550	3608 3598		Medium light gray (N6) to Light brownish gray (5YR 6/1) to White (N9)	Crystal tuff. Sparse blocky clear feldspar and black pyroxene microphenocrysts. Eutaxitic texture.	Tmtw
550 560	3598 3588		White (N9) to yellowish gray (5Y 8/1) to moderate reddish brown (10R 3/4)	Mixed crystal tuff, feldspar and pyroxene microphenocrysts. Red iron staining on fragments.	Tmtpi
560 570	3588 3578		White (N9) to yellowish gray (5Y 8/1) to moderate reddish brown (10R 3/4)	Mixed crystal tuff, feldspar and pyroxene microphenocrysts. Red iron staining on fragments.	Tmtpi
570 580	3578 3568		White (N9) to yellowish gray (5Y 8/1) to moderate reddish brown (10R 3/4)	Mixed crystal tuff, feldspar and pyroxene microphenocrysts. Red iron staining on fragments.	Tmtpi
580 590	3568 3558		White (N9) to yellowish gray (5Y 8/1) to moderate reddish brown (10R 3/4)	Mixed crystal tuff, feldspar and pyroxene microphenocrysts. Red iron staining on fragments.	Tmtpi
590 600	3558 3548		White (N9) to Yellowish gray (5Y 8/1)	Aphyric crystal tuff.	Tmtpi
600 610	3548 3538		White (N9) to Yellowish gray (5Y 8/1)	Aphyric crystal tuff, scattered mafic lithics.	Tmtpi

Depth Interval (ft)	Elevation Interval (ft)	Geochemical Sample ID	Color	Interval Description	Map Unit
610 620	3538 3528		White (N9) to Yellowish gray (5Y 8/2) to Light gray (N7)	Aphyric crystal tuff.	Tmtpi
620 630	3528 3518		White (N9) to Yellowish gray (5Y 8/2) to Light gray (N7)	Aphyric crystal tuff.	Tmtpi
630 640	3518 3508		White (N9) to Yellowish gray (5Y 8/1)	Aphyric crystal tuff, sparse blocky clear feldspar and prismatic pyroxene microphenocrysts.	Tmtpi
640 650	3508 3498		White (N9) to Yellowish gray (5Y 8/2) to Greenish gray (5GY 4/1)	Mixed crystal tuff and perlitic obsidian fragments.	Tmtpi
650 660	3498 3488		White (N9) to Yellowish gray (5Y 8/2) to Greenish gray (5GY 4/1)	Mixed crystal tuff and perlitic obsidian fragments.	Tmtpi
660 670	3488 3478		White (N9) to Yellowish gray (5Y 8/2) to Greenish gray (5GY 4/1)	Mixed crystal tuff and perlitic obsidian fragments. Pink spherulites common.	Tmtpi
670 680	3478 3468	**HARN 50087 670-680**	Medium light gray (N6) to Light brownish gray (5YR 6/1)	Spherulitic to lithophysal welded tuff. Very sparse fragments with 1 to 2 mm blocky clear feldspar crystals.	Tmtpi
680 690	3468 3458		Medium light gray (N6) to Light brownish gray (5YR 6/1)	Spherulitic to lithophysal welded tuff. Very sparse fragments with 1 to 2 mm blocky clear feldspar crystals.	Tmtpi
690 700	3458 3448		Medium light gray (N6) to Light brownish gray (5YR 6/1)	Spherulitic to lithophysal welded tuff. Very sparse fragments with 1 to 2 mm blocky clear feldspar crystals.	Tmtpi
700 710	3448 3438		White (N9)	Crystal tuff, very sparsely microphyric, < 1 percent blocky clear alkali feldspar 1 to 2 mm. Variably lithophysal.	Tmtpi
710 720	3438 3428		White (N9)	Crystal tuff, very sparsely microphyric, < 1 percent blocky clear alkali feldspar 1 to 2 mm. Variably lithophysal.	Tmtpi
720 730	3428 3418	**HARN 50087 720-810**	White (N9)	Crystal tuff, very sparsely microphyric, < 1 percent blocky clear alkali feldspar 1 to 2 mm. Variably lithophysal.	Tmtpi
730 740	3418 3408		White (N9)	Crystal tuff, very sparsely microphyric, < 1 percent blocky clear alkali feldspar 1 to 2 mm. Variably lithophysal.	Tmtpi
740 750	3408 3398		White (N9)	Crystal tuff, very sparsely microphyric, < 1 percent blocky clear alkali feldspar 1 to 2 mm. Variably lithophysal.	Tmtpi
750 760	3398 3388		White (N9)	Crystal tuff, very sparsely microphyric, < 1 percent blocky clear alkali feldspar 1 to 2 mm. Variably lithophysal.	Tmtpi
760 770	3388 3378		White (N9)	Crystal tuff, very sparsely microphyric, < 1 percent blocky clear alkali feldspar 1 to 2 mm. Variably lithophysal.	Tmtpi
770 780	3378 3368		White (N9)	Crystal tuff, very sparsely microphyric, < 1 percent blocky clear alkali feldspar 1 to 2 mm. Variably lithophysal.	Tmtpi
780 790	3368 3358		White (N9)	Crystal tuff, very sparsely microphyric, < 1 percent blocky clear alkali feldspar 1 to 2 mm. Variably lithophysal.	Tmtpi
790 800	3358 3348		White (N9)	Crystal tuff, very sparsely microphyric, < 1 percent blocky clear alkali feldspar 1 to 2 mm. Variably lithophysal.	Tmtpi
800 810	3348 3338		White (N9)	Crystal tuff, very sparsely microphyric, < 1 percent blocky clear alkali feldspar 1 to 2 mm. Variably lithophysal.	Tmtpi
810 820	3338 3328		White (N9)	Crystal tuff, very sparsely microphyric, < 1 percent blocky clear alkali feldspar 1 to 2 mm. Variably lithophysal.	Tmtpi

Depth Interval (ft)	Elevation Interval (ft)	Geochemical Sample ID	Color	Interval Description	Map Unit
820 830	3328 3318		White (N9)	Crystal tuff, very sparsely microphyric, < 1 percent blocky clear alkali feldspar 1 to 2 mm. Variably lithophysal.	Tmtpi
830 840	3318 3308	**HARN 50087 830-900**	White (N9)	Crystal tuff, very sparsely microphyric, < 1 percent blocky clear alkali feldspar 1 to 2 mm. Variably lithophysal.	Tmtpi
840 850	3308 3298		White (N9) to medium light gray (N6)	Crystal tuff, very sparsely microphyric, < 1 percent blocky clear alkali feldspar 1 to 2 mm. Variably lithophysal.	Tmtpi
850 860	3298 3288		White (N9) to medium light gray (N6)	Crystal tuff, very sparsely microphyric, < 1 percent blocky clear alkali feldspar 1 to 2 mm. Variably lithophysal.	Tmtpi
860 870	3288 3278		White (N9) to medium light gray (N6)	Crystal tuff, very sparsely microphyric, < 1 percent blocky clear alkali feldspar 1 to 2 mm. Variably lithophysal.	Tmtpi
870 880	3278 3268		White (N9) to medium light gray (N6)	Crystal tuff, very sparsely microphyric, < 1 percent blocky clear alkali feldspar 1 to 2 mm. Variably lithophysal.	Tmtpi
880 890	3268 3258		White (N9) to medium light gray (N6)	Crystal tuff, very sparsely microphyric, < 1 percent blocky clear alkali feldspar 1 to 2 mm. Variably lithophysal.	Tmtpi
890 900	3258 3248		White (N9)	Xeolitized crystal tuff, very sparsely microphyric < 1 percent blocky clear alkali feldspar 1 to 2 mm. Variably lithophysal.	Tmtpi
900 910	3248 3238	**HARN 50087 900-970**	White (N9) to medium light gray (N6)	Xeolitized crystal tuff, very sparsely microphyric < 1 percent blocky clear alkali feldspar 1 to 2 mm. Variably lithophysal.	Tmtpi
910 920	3238 3228		White (N9) to medium light gray (N6)	Xeolitized crystal tuff, very sparsely microphyric < 1 percent blocky clear alkali feldspar 1 to 2 mm. Variably lithophysal.	Tmtpi
920 930	3228 3218		White (N9) to medium light gray (N6)	Xeolitized crystal tuff, very sparsely microphyric < 1 percent blocky clear alkali feldspar 1 to 2 mm. Variably lithophysal.	Tmtpi
930 940	3218 3208		White (N9) to medium light gray (N6)	Xeolitized crystal tuff, very sparsely microphyric < 1 percent blocky clear alkali feldspar 1 to 2 mm. Variably lithophysal.	Tmtpi
940 950	3208 3198		White (N9) to medium light gray (N6)	Xeolitized crystal tuff, very sparsely microphyric < 1 percent blocky clear alkali feldspar 1 to 2 mm. Variably lithophysal.	Tmtpi
950 960	3198 3188		White (N9) to medium light gray (N6)	Xeolitized crystal tuff, very sparsely microphyric 1 to 2 percent blocky clear alkali feldspar 1 to 2 mm. Variably lithophysal.	Tmtpi
960 970	3188 3178		White (N9) to medium light gray (N6)	Xeolitized crystal tuff, very sparsely microphyric < 1 percent blocky clear alkali feldspar 1 to 2 mm. Variably lithophysal.	Tmtpi
970 980	3178 3168		No sample	No sample	No sample
980 990	3168 3158		No sample	No sample	No sample
990 1000	3158 3148		No sample	No sample	No sample
1000 1010	3148 3138	**HARN 50087 1000-1010**	White (N9) to Medium light gray (N6)	Xeolitized crystal tuff, very sparsely microphyric < 1 percent blocky clear alkali feldspar 1 to 2 mm. Variably lithophysal.	Tmtpi
1010 1020	3138 3128	**HARN 50087 1010-1100**	White (N9) to Medium light gray (N6)	Xeolitized crystal tuff, very sparsely microphyric < 1 percent blocky clear alkali feldspar 1 to 2 mm. Variably lithophysal.	Tmtpi
1020 1030	3128 3118		White (N9) to Medium light gray (N6)	Xeolitized crystal tuff, very sparsely microphyric < 1 percent blocky clear alkali feldspar 1 to 2 mm. Variably lithophysal.	Tmtpi
1030 1040	3118 3108		White (N9) to Medium light gray (N6)	Xeolitized crystal tuff, very sparsely microphyric < 1 percent blocky clear alkali feldspar 1 to 2 mm. Variably lithophysal.	Tmtpi

Depth Interval (ft)	Elevation Interval (ft)	Geochemical Sample ID	Color	Interval Description	Map Unit
1040 1050	3108 3098		White (N9) to Medium light gray (N6)	Silicified variably xeolitized crystal tuff, very sparsely microphyric < 1 percent blocky, clear alkali feldspar 1 to 2 mm.	Tmtpi
1050 1060	3098 3088		White (N9) to Medium light gray (N6)	Silicified variably xeolitized crystal tuff, very sparsely microphyric < 1 percent blocky, clear alkali feldspar 1 to 2 mm.	Tmtpi
1060 1070	3088 3078		White (N9) to Medium light gray (N6)	Silicified variably xeolitized crystal tuff, very sparsely microphyric < 1 percent blocky, clear alkali feldspar 1 to 2 mm.	Tmtpi
1070 1080	3078 3068		White (N9) to Medium light gray (N6)	Silicified variably xeolitized crystal tuff, very sparsely microphyric < 1 percent blocky, clear alkali feldspar 1 to 2 mm.	Tmtpi
1080 1090	3068 3058		White (N9) to Medium light gray (N6)	Silicified variably xeolitized crystal tuff, very sparsely microphyric < 1 percent blocky, clear alkali feldspar 1 to 2 mm.	Tmtpi
1090 1100	3058 3048		White (N9) to Medium light gray (N6)	Silicified variably xeolitized crystal tuff, very sparsely microphyric < 1 percent blocky, clear alkali feldspar 1 to 2 mm.	Tmtpi
1100 1110	3048 3038	**HARN 50087 1100-1200**	Medium light gray (N6)	Silicified variably xeolitized crystal tuff, very sparsely microphyric < 1 percent blocky, clear alkali feldspar 1 to 2 mm.	Tmtpi
1110 1120	3038 3028		Medium light gray (N6)	Silicified variably xeolitized crystal tuff, very sparsely microphyric < 1 percent blocky, clear alkali feldspar 1 to 2 mm.	Tmtpi
1120 1130	3028 3018		Medium light gray (N6)	Silicified variably xeolitized crystal tuff, sparsely microphyric < 1 percent blocky, clear alkali feldspar 1 to 2 mm.	Tmtpi
1130 1140	3018 3008		Medium light gray (N6)	Silicified variably xeolitized crystal tuff, very sparsely microphyric < 1 percent blocky, clear alkali feldspar 1 to 2 mm.	Tmtpi
1140 1150	3008 2998		Medium light gray (N6)	Silicified variably xeolitized crystal tuff, very sparsely microphyric < 1 percent blocky, clear alkali feldspar 1 to 2 mm.	Tmtpi
1150 1160	2998 2988		Medium light gray (N6)	Silicified variably xeolitized crystal tuff, very sparsely microphyric < 1 percent blocky, clear alkali feldspar 1 to 2 mm.	Tmtpi
1160 1170	2988 2978		Medium light gray (N6)	Silicified variably xeolitized crystal tuff, sparsely microphyric < 1 percent blocky, clear alkali feldspar 1 to 2 mm.	Tmtpi
1170 1180	2978 2968		Medium light gray (N6)	Silicified variably xeolitized crystal tuff, very sparsely microphyric < 1 percent blocky, clear alkali feldspar 1 to 2 mm.	Tmtpi
1180 1190	2968 2958		Medium light gray (N6)	Silicified variably xeolitized crystal tuff, very sparsely microphyric < 1 percent blocky, clear alkali feldspar 1 to 2 mm.	Tmtpi
1190 1200	2958 2948		Medium light gray (N6)	Silicified variably xeolitized crystal tuff, very sparsely microphyric < 1 percent blocky, clear alkali feldspar 1 to 2 mm.	Tmtpi
1200 1210	2948 2938	**HARN 50087 1200-1300**	Medium light gray (N6)	Silicified variably xeolitized crystal tuff, very sparsely microphyric < 1 percent blocky, clear alkali feldspar 1 to 2 mm.	Tmtpi
1210 1220	2938 2928		Medium light gray (N6)	Silicified variably xeolitized crystal tuff, very sparsely microphyric < 1 percent blocky, clear alkali feldspar 1 to 2 mm.	Tmtpi
1220 1230	2928 2918		Medium light gray (N6)	Silicified variably xeolitized crystal tuff, very sparsely microphyric < 1 percent blocky, clear alkali feldspar 1 to 2 mm.	Tmtpi
1230 1240	2918 2908		Medium light gray (N6)	Silicified variably xeolitized crystal tuff, very sparsely microphyric < 1 percent blocky, clear alkali feldspar 1 to 2 mm.	Tmtpi
1240 1250	2908 2898		Medium light gray (N6)	Silicified variably xeolitized crystal tuff, very sparsely microphyric < 1 percent blocky, clear alkali feldspar 1 to 2 mm.	Tmtpi

Depth Interval (ft)	Elevation Interval (ft)	Geochemical Sample ID	Color	Interval Description	Map Unit
1250 1260	2898 2888		Medium light gray (N6)	Silicified variably xeolitized crystal tuff, very sparsely microphyric < 1 percent blocky, clear alkali feldspar 1 to 2 mm.	Tmtpi
1260 1270	2888 2878		Medium light gray (N6)	Silicified variably xeolitized crystal tuff, very sparsely microphyric < 1 percent blocky, clear alkali feldspar 1 to 2 mm.	Tmtpi
1270 1280	2878 2868		Medium light gray (N6)	Silicified variably xeolitized crystal tuff, very sparsely microphyric < 1 percent blocky, clear alkali feldspar 1 to 2 mm.	Tmtpi
1280 1290	2868 2858		Medium light gray (N6)	Silicified variably xeolitized crystal tuff, very sparsely microphyric < 1 percent blocky, clear alkali feldspar 1 to 2 mm.	Tmtpi
1290 1300	2858 2848		Medium light gray (N6)	Silicified variably xeolitized crystal tuff, very sparsely microphyric < 1 percent blocky, clear alkali feldspar 1 to 2 mm.	Tmtpi
1300 1310	2848 2838	**HARN 50087 1300-1340**	Medium light gray (N6)	Silicified variably xeolitized crystal tuff, aphyric.	Tmtpi
1310 1320	2838 2828		Medium light gray (N6)	Silicified variably xeolitized crystal tuff, aphyric.	Tmtpi
1320 1330	2828 2818		Medium light gray (N6)	Silicified variably xeolitized crystal tuff, aphyric.	Tmtpi
1330 1340	2818 2808	**HARN 50087 1335-1380**	Medium light gray (N6)	Silicified variably xeolitized crystal tuff, aphyric.	Tmtpi
1340 1350	2808 2798		Medium light gray (N6)	Silicified variably xeolitized crystal tuff, aphyric.	Tmtpi
1350 1360	2798 2788		Medium light gray (N6)	Silicified variably xeolitized crystal tuff, rare blocky subhedral, clear alkali feldspar.	Tmtpi
1360 1370	2788 2778		Medium light gray (N6)	Silicified variably xeolitized crystal tuff, aphyric.	Tmtpi
1370 1380	2778 2768		Medium light gray (N6)	Silicified variably xeolitized crystal tuff, aphyric.	Tmtpi
1380 1390	2768 2758		Medium gray (N5)	Crystal tuff, very sparsely microphyric < 1 percent blocky, clear alkali feldspar 1 to 2 mm. Variably lithophysal.	Tmtpi
1390 1400	2758 2748		Medium gray (N5)	Silicified crystal tuff, aphyric.	Tmtpi
1400 1410	2748 2738		Medium gray (N5)	Silicified crystal tuff, aphyric.	Tmtpi
1410 1420	2738 2728		Medium gray (N5)	Silicified crystal tuff, aphyric.	Tmtpi
1420 1430	2728 2718		Medium gray (N5)	Silicified crystal tuff, aphyric.	Tmtpi
1430 1440	2718 2708		Medium gray (N5)	Silicified crystal tuff, aphyric.	Tmtpi
1440 1450	2708 2698		Medium gray (N5)	Silicified crystal tuff, aphyric. Abundant iron staining on fragments.	Tmtpi
1450 1460	2698 2688		Medium gray (N5)	Silicified crystal tuff, aphyric. Abundant iron staining on fragments.	Tmtpi
1460 1470	2688 2678		Medium gray (N5)	Silicified crystal tuff, aphyric. Abundant iron staining on fragments.	Tmtpi
1470 1480	2678 2668	**HARN 50087 1470-1500**	Medium gray (N5)	Silicified crystal tuff, aphyric. Abundant iron staining on fragments.	Tmtpi
1480 1490	2668 2658		Medium gray (N5)	Silicified crystal tuff, aphyric. Abundant iron staining on fragments.	Tmtpi
1490 1500	2658 2648		Medium gray (N5)	Silicified crystal tuff, aphyric. Abundant iron staining on fragments.	Tmtpi
1500 1510	2648 2638	**HARN 50087 1500-1560**	Medium gray (N5)	Silicified variably xeolitized crystal tuff, aphyric.	Tmtpi
1510 1520	2638 2628		Medium gray (N5)	Silicified variably xeolitized crystal tuff, aphyric.	Tmtpi
1520 1530	2628 2618		Medium gray (N5)	Silicified variably xeolitized crystal tuff, aphyric.	Tmtpi
1530 1540	2618 2608		Medium gray (N5)	Silicified crystal tuff, aphyric. Abundant iron staining on fragments.	Tmtpi
1540 1550	2608 2598		Medium gray (N5)	Silicified crystal tuff, aphyric. Flow banded. Abundant iron staining on fragments.	Tmtpi
1550 1560	2598 2588		Medium gray (N5)	Crystal tuff, very sparsely microphyric < 1 percent blocky, clear alkali feldspar 1 to 2 mm. Variably lithophysal. Flow banded.	Tmtpi
1560 1570	2588 2578	**HARN 50087 1560-1600**	Pale pink (5RP 8/2) to Grayish black (N2)	Silicified aphyric tuff mixed with fresh perlitic obsidian.	Tmtpi
1570 1580	2578 2568		Grayish black (N2)	Perlitic obsidian.	Tmtpi
1580 1590	2568 2558		Grayish black (N2)	Perlitic obsidian.	Tmtpi
1590 1600	2558 2548		Grayish black (N2)	Perlitic obsidian.	Tmtpi

Depth Interval (ft)	Elevation Interval (ft)	Geochemical Sample ID	Color	Interval Description	Map Unit
1600 1610	2548 2538		Grayish black (N2)	Perlitic obsidian.	Tmtpi
1610 1620	2538 2528		Very pale green (10G 8/2)	Xeolitized aphyric crystal tuff mixed with fresh perlitic obsidian.	Tmtpi
1620 1630	2528 2518		Very pale green (10G 8/2)	Xeolitized aphyric crystal tuff mixed with fresh perlitic obsidian.	Tmtpi
1630 1640	2518 2508		Very pale green (10G 8/2)	Xeolitized aphyric crystal tuff mixed with fresh perlitic obsidian.	Tmtpi
1640 1650	2508 2498		Very pale green (10G 8/2)	Xeolitized aphyric crystal tuff mixed with fresh perlitic obsidian.	Tmtpi
1650 1660	2498 2488		Very pale green (10G 8/2)	Xeolitized aphyric crystal tuff mixed with fresh perlitic obsidian.	Tmtpi
1660 1670	2488 2478		Very pale green (10G 8/2)	Xeolitized aphyric crystal tuff mixed with fresh perlitic obsidian.	Tmtpi
1670 1680	2478 2468		Very pale green (10G 8/2)	Xeolitized aphyric crystal tuff mixed with fresh perlitic obsidian.	Tmtpi
1680 1690	2468 2458		Very pale green (10G 8/2)	Xeolitized aphyric crystal tuff mixed with fresh perlitic obsidian.	Tmtpi
1690 1700	2458 2448	**HARN 50087 1690-1710**	Yellowish gray (5Y 8/1)	Xeolitized aphyric crystal tuff pink rhyolite lithics.	Tmtpi
1700 1710	2448 2438		Yellowish gray (5Y 8/1)	Xeolitized aphyric crystal tuff pink rhyolite lithics.	Tmtpi
1710 1720	2438 2428		Medium gray (N5)	Xeolitized variably silicified crystal tuff, aphyric.	Tmtpi
1720 1730	2428 2418		Medium gray (N5)	Xeolitized variably silicified crystal tuff, aphyric.	Tmtpi
1730 1740	2418 2408		Medium gray (N5)	Xeolitized variably silicified crystal tuff, aphyric.	Tmtpi
1740 1750	2408 2398		Medium gray (N5)	Xeolitized variably silicified crystal tuff, aphyric.	Tmtpi
1750 1760	2398 2388		Medium gray (N5)	Xeolitized variably silicified crystal tuff, aphyric.	Tmtpi
1760 1770	2388 2378		Medium gray (N5)	Xeolitized to variably silicified crystal tuff, aphyric. Abundant iron staining on fragments.	Tmtpi
1770 1780	2378 2368		Medium gray (N5)	Xeolitized to variably silicified crystal tuff, aphyric.	Tmtpi
1780 1790	2368 2358	**HARN 50087 1780-1810**	Medium gray (N5)	Xeolitized to variably silicified crystal tuff, aphyric.	Tmtpi
1790 1800	2358 2348		Medium gray (N5)	Xeolitized to variably silicified crystal tuff, aphyric.	Tmtpi
1800 1810	2348 2338		Medium light gray (N6)	Xeolitized to variably silicified crystal tuff, aphyric.	Tmtpi
1810 1820	2338 2328		Medium light gray (N6)	Xeolitized to variably silicified crystal tuff, aphyric. Abundant iron staining on fragments.	Tmtpi
1820 1830	2328 2318		Medium light gray (N6)	Xeolitized to variably silicified crystal tuff, aphyric.	Tmtpi
1830 1840	2318 2308		Medium light gray (N6)	Xeolitized to variably silicified crystal tuff, aphyric. Iron staining on fragments.	Tmtpi
1840 1850	2308 2298		Medium light gray (N6)	Xeolitized to variably silicified crystal tuff, aphyric.	Tmtpi
1850 1860	2298 2288		Medium light gray (N6)	Xeolitized to variably silicified crystal tuff, aphyric.	Tmtpi
1860 1870	2288 2278		Medium light gray (N6)	Xeolitized to variably silicified crystal tuff, aphyric. Abundant iron staining on fragments.	Tmtpi
1870 1880	2278 2268		Medium light gray (N6)	Xeolitized to variably silicified crystal tuff, aphyric.	Tmtpi
1880 1890	2268 2258		Medium light gray (N6)	Xeolitized to variably silicified crystal tuff, aphyric. Abundant iron staining on fragments.	Tmtpi
1890 1900	2258 2248		Medium light gray (N6)	Xeolitized to variably silicified crystal tuff, aphyric. Abundant iron staining on fragments.	Tmtpi
1900 1910	2248 2238	**HARN 50087 1900-1940**	Medium light gray (N6)	Xeolitized crystal tuff, aphyric.	Tmtpi
1910 1920	2238 2228		Medium light gray (N6)	Xeolitized crystal tuff, aphyric.	Tmtpi
1920 1930	2228 2218		Medium light gray (N6)	Xeolitized crystal tuff, aphyric.	Tmtpi
1930 1940	2218 2208		Medium light gray (N6)	Xeolitized crystal tuff, aphyric.	Tmtpi
1940 1950	2208 2198		Medium light gray (N6)	Xeolitized crystal tuff, aphyric. Abundant iron staining on fragments.	Tmtpi
1950 1956	2198 2192		Medium light gray (N6)	Xeolitized crystal tuff, aphyric.	Tmtpi